Fall 1-31-2002

Simultaneous removal of ortho-dichlorobenzene and ethanol vapors in a biotrickling filter : experimental results and process modeling

Suchismita Bhattacharya
New Jersey Institute of Technology

ABSTRACT

SIMULTANEOUS REMOVAL OF ortho-DICHLOROBENZENE AND ETHANOL VAPORS IN A BIOTRICKLING FILTER: EXPERIMENTAL RESULTS AND PROCESS MODELING

by
Suchismita Bhattacharya

This study investigated the possibility of simultaneous removal of vapors of dissimilar volatile organic compounds from air streams in a biotrickling filter (BTF). Using a microbial consortium known to utilize ortho-dichlorobenzene (o-DCB) as sole carbon and energy source, a culture was developed on o-DCB/ethanol mixtures and a BTF unit was developed and operated with air streams carrying o-DCB and ethanol vapors. Simultaneous removal of the two compounds was observed in experiments that span a period of over three years.

Experiments were performed at air residence times ranging from 4 to 6.5 min, liquid flow rates from 3.6 to 9 Lh^{-1}, and inlet air concentrations from 0.85 to 4.5 gm^{-3} and 0.95 to 11 gm^{-3} for o-DCB and ethanol, respectively. The maximum removal rate was 40 and 150 gm^{-3} packing h^{-1} for o-DCB and ethanol, respectively. It was possible to duplicate results in experiments performed under a given set of operating conditions at time intervals as far as 9 months apart from one another.

The presence of the readily degradable ethanol at relatively high concentrations led to the formation of significant amounts of biomass in the liquid recirculating through the BTF resulting in the removal of o-DCB and ethanol both in the liquid phase and the biomass attached to the packing material. The readily biodegradable ethanol led to better coverage of the packing with biofilm, resulting in a positive effect on the removal of

o-DCB vapor. However, every four months an abrupt increase in pressure drop build-up and concomitant loss in BTF performance was observed over a 5-day period. Once excess biomass was removed from the BTF unit, normal operation was recovered within 3-4 days.

Steady state operation of the unit was mathematically described with a model involving mass balances for o-DCB, ethanol, and oxygen in three phases: air, recirculating liquid, and biofilm. The model accounts for reaction in both the liquid and biofilm phases. Through the introduction of the notion of effectiveness factors for o-DCB and ethanol, the equations for the biofilm were decoupled from those for the air and liquid allowing for easier numerical solution of the original complex model. The model was found capable of predicting the data on removal rates with a less than 10% - and oftentimes less than 5% - error.

Independent kinetic experiments led to the following conclusions: o-DCB and ethanol were biodegraded following Andrews self-inhibitory kinetics; no kinetic interactions occurred over the concentration ranges tested in the BTF; there was no biomass diversification along the length of the BTF unit.

SIMULTANEOUS REMOVAL OF ortho-DICHLOROBENZENE AND ETHANOL VAPORS IN A BIOTRICKLING FILTER: EXPERIMENTAL RESULTS AND PROCESS MODELING

by
Suchismita Bhattacharya

A Thesis
Submitted to the Faculty of
New Jersey Institute of Technology and
Rutgers, The State University of New Jersey-Newark
in Partial Fulfillment of the Requirements for the Degree of
Doctor of Philosophy in Environmental Science

Department of Chemistry and Environmental Science

January 2002

APPROVAL PAGE

SIMULTANEOUS REMOVAL OF ortho-DICHLOROBENZENE AND ETHANOL VAPORS IN A BIOTRICKLING FILTER: EXPERIMENTAL RESULTS AND PROCESS MODELING

Suchismita Bhattacharya

Dr. Basil C. Baltzis, Thesis Advisor   Date
Professor of Chemical Engineering, NJIT

Dr. Piero Armenante, Committee Member   Date
Distinguished Professor of Chemical Engineering, NJIT

Dr. Gordon Lewandowski, Committee Member   Date
Distinguished Professor of Chemical Engineering, NJIT

Dr. Dittmar Hahn, Committee Member   Date
Assistant Professor of Chemical Engineering, NJIT

Dr. David Kafkewitz, Committee Member   Date
Professor of Biological Sciences, Rutgers-Newark

BIOGRAPHICAL SKETCH

Author:	Suchismita Bhattacharya
Degree:	Doctor of Philosophy
Date:	January 2002

Undergraduate and Graduate Education:

- Doctor of Philosophy in Environmental Science
  New Jersey Institute of Technology, Newark, NJ, 2002

- Bachelor of Chemical Engineering
  University Department of Chemical Technology, Mumbai, India, 1997

Major: Environmental Science

Presentations and Publications:

Baltzis, B.C., Mpanias, C.J, and Bhattacharya S., "Modeling the removal of VOC mixtures in Biotrickling Filters." *Biotechnology and Bioengineering*, Volume 72, Issue 4, Pages 389-401, February 2001.

Bhattacharya S., "Biotrickling filters in air pollution control – Experiments with ethanol and o-dichlorobenzene mixtures." *Ninth Annual Unitech Student Conference* (April, 2000).

Bhattacharya, S and Baltzis, B.C. "Removal of o-dichlorobenzene in a biotrickling filter in the presence of ethanol." *Presented at the 2000 Conference on Biofiltration*, Los Angeles, CA, November 2000.

Bhattacharya, S and Baltzis, B.C. "Long term performance of a biotrickling filter removing o-dichlorobenzene and ethanol mixtures." *Presented at AWMA's 94th Annual Conference and Exhibition*, June 25th-28th, Orlando, FL

Bhattacharya, S and Baltzis, B.C. "Simultaneous Removal of Ethanol and Ortho-Di-Chlorobenzene Vapors From Airstreams in a Biotrickling Filter." *Presented at the AICHE Annual Conference*, November, 2001, Reno, NV.

Bhattacharya, S and Baltzis, B.C. "Modeling the Removal of Dissimilar Volatile Organic Compound (VOC) Mixtures in a Biotrickling Filter." *Presented at the AIChE Annual Conference*, November, 2001, Reno, NV.

This dissertation is dedicated to
my mother, Gauri
my father, Shibabrata
my husband, Anirban
and my sister, Suchayita

ACKNOWLEDGMENT

The author would like to thank her advisor Professor Basil Baltzis for his guidance, insight and constant encouragement throughout the course of this research endeavor.

The author is also grateful to Professors Gordon A. Lewandowski, Piero Armenante, Dittmar Hahn, and David Kafkewitz for serving as members of the committee.

Dr. Larisa Kristopa provided timely and expert assistance with experimental set-up and analytical instruments.

The author would also like to thank the Department of Chemical Engineering and the Department of Chemistry and Environmental Science at NJIT for their financial support during the entire duration of her research.

The author acknowledges the support and assistance of her colleagues Dr. Dilip Mandal, Dr. Otute Akiti, Dr. Jeong-Sheop Shim, Dr. Ernesto Uehara-Nagamine and Ms. Minhee Kim.

TABLE OF CONTENTS

LIST OF TABLES

LIST OF FIGURES

LIST OF FIGURES
(Continued)

Figures   **Page**

Figures   **Page**

LIST OF SYMBOLS

A_S : active (wetted) biolayer surface area per unit volume of BTF (m^{-1})

A_T : total specific surface area of packing material (m^{-1})

b : biomass concentration in a serum bottle (gm^{-3})

b_0 : initial biomass concentration in a serum bottle (gm^{-3})

b'_0 : initial biomass concentration in a serum bottle when solvents are injected (gm^{-3})

b_f : final biomass concentration in a serum bottle (gm^{-3})

b_n : biomass concentration in a serum bottle at n^{th} time instant (gm^{-3})

C_{Gj} : concentration of VOC j in the gas phase in a serum bottle (gm^{-3})

C_{Gje} : equilibrium concentration of VOC j in the gas phase in a serum bottle (gm^{-3})

C_{Gq} : concentration of compound q in air at position h along the BTF (gm^{-3})

$\overline{C}_{Gq}$: dimensionless version of C_{Gq} defined as $\overline{C}_{Gq} = C_{Gq} / C_{Gqi}$

C_{Gqi} : value of C_{Gq} at the inlet of BTF (gm^{-3})

C_{Gqe} : value of C_{Gq} at the exit of BTF (gm^{-3})

C_{Lj} : concentration of VOC j in the liquid phase in a serum bottle (gm^{-3})

C_{Lje} : equilibrium concentration of VOC j in the liquid phase in a serum bottle (gm^{-3})

C_{Lq} : concentration of compound q in the liquid at position h along the BTF (gm^{-3})

$\overline{C}_{Lq}$: dimensionless version of C_{Lq} defined as $\overline{C}_{Lq} = m_q C_{Lq} / C_{Gqi}$

D_{qG} : diffusion coefficient of compound q in the air (m^2h^{-1})

D_{qW} : diffusion coefficient of compound q in water (m^2h^{-1})

d_P : nominal packing diameter (m)

$f(S_O)$: functional dependence-given by relation (6.14)- of biomass specific growth rate on oxygen (dimensionless)

$f(X_V)$: ratio of diffusivity of a compound in the biofilm to that in water

g : gravitational constant (ms^{-2})

h : position in the column (m); h = 0 at the entrance, h = H at the exit for co- current flow; entrance and exit refer to the airstream.

H : total height of BTF bed (m)

K_j : kinetic constant for biodegradation of VOC j (gm^{-3})

K_{ED} : cross-inhibition kinetic constant of o-DCB on biodegradation of ethanol (m^3g^{-1})

K_{Ij} : self-inhibition kinetic constant for biodegradation of VOC j (gm^{-3})

K_O : kinetic constant for oxygen (gm^{-3})

K_{Lq} : overall mass transfer coefficient for compound q (h^{-1})

k_{Gq} : gas-phase mass transfer coefficient for compound q (mh^{-1})

k_{Lq} : liquid-phase mass transfer coefficient for compound q (mh^{-1})

m_q : distribution coefficient between air and water for compound q

Q_G : air flow rate through the BTF (m^3h^{-1})

Q_L : liquid flow rate through the BTF (m^3h^{-1})

R_j : average specific rate of compound j removal in a serum bottle [(g j) (h^{-1})(g^{-1} biomass)]

R_{exp} : experimental removal rate of a VOC in a BTF (gm^{-3}-reactor h^{-1})

R_{pred} : model-predicted removal rate of a VOC in a BTF (gm^{-3}-reactor h^{-1})

S   : cross-sectional area of BTF column (m^2)

S_q : concentration of compound q at a position x in the biofilm (gm^{-3})

$\overline{S}_q$: dimensionless version of S_q defined as $\overline{S}_q = S_q / K_q$

S_q^* : normalized version of S_q defined as $S_q^* = S_q(\theta)/S_q(\theta = 0)$

t : time (h)

u_G : superficial air velocity in the BTF defined as $u_G = Q_G/S$ (mh^{-1})

u_L : superficial liquid velocity in the BTF defined as $u_L = Q_L/S$ (mh^{-1})

V_G : volume of gas phase (headspace) in a serum bottle (m^3)

V_L : volume of liquid phase in a serum bottle (m^3)

V_{LH} : Liquid hold-up volume in BTF-II (m^3)

V_{Sj} : volume of VOC j injected into the serum bottle (m^3)

V_P : volume of the BTF bed (m^3)

X_V : biofilm density (kg dry cells m^{-3})

X_{VL} : biomass density in the recirculating liquid (kg dry cells m^{-3})

x : position in the biofilm (m)

Y_j : yield coefficient of the culture on VOC j (g-biomass g^{-1}-VOC j)

Y_{Oj} : yield coefficient of the culture on oxygen (g-biomass g^{-1}-oxygen) when VOC j is the carbon source

z : dimensionless position in the BTF ($z = h/H$)

Greek Symbols

α_q : dimensionless quantity for compound q defined as $\alpha_q = C_{Gqi} / m_q K_q$

β_E : dimensionless quantity defined as $\beta_E = K_{LE} / K_{LD}$

β_O : dimensionless quantity defined as $\beta_O = K_{LO} / K_{LD}$

γ_D : inverse dimensionless inhibition constant ($\gamma_D = K_D / K_{ID}$)

γ_E : inverse dimensionless inhibition constant ($\gamma_E = K_E / K_{IE}$)

δ : effective biofilm thickness (m)

δ_L : thickness of liquid film (m)

ε_j : effectiveness factor of substrate j (dimensionless)

η_{LD} : dimensionless quantity defined as $\eta_{LD} = \mu_D^* m_D A_S X_{VL} H \delta_L / Y_D C_{GDi} u_L$

η_{LE} : dimensionless quantity defined as $\eta_{LE} = \mu_E^* m_E A_S X_{VL} H \delta_L / Y_E C_{GEi} u_L$

η_D : dimensionless quantity defined as $\eta_D = \mu_D^* m_D A_S X_V H \varepsilon_D \delta \big|_{x=0} / Y_D C_{GDi} u_L$

η_E : dimensionless quantity defined as $\eta_E = \mu_E^* m_E A_S X_V H \varepsilon_E \delta \big|_{x=0} Y_E C_{GEi} u_L$

η_{OD} : dimensionless quantity defined as $\eta_{OD} = \eta_D \omega_D$

η_{OE} : dimensionless quantity defined as $\eta_{OE} = \eta_E \omega_E$

θ : dimensionless position in the biofilm defined as $\theta = x / \delta$

λ_D : dimensionless quantity defined as $\lambda_D = D_{DW} Y_D K_D / D_{OW} Y_{OD} K_O$

λ_E : dimensionless quantity defined as $\lambda_E = D_{EW} Y_E K_E / D_{OW} Y_{OE} K_O$

μ_G : gas (air) viscosity (kgm^{-1}s^{-1})

μ_j^* : kinetic constant for the biodegradation of VOC j (h^{-1})

μ_j : biomass specific growth rate on VOC j (h^{-1})

μ_L : liquid (water) viscosity (kgm^{-1}s^{-1})

ξ : correction factor in expression (7.18)

ξ_{1q} : correction factor in expression (7.19)

ξ_{2q} : correction factor in expression (7.20)

ρ : dimensionless quantity defined as $\rho = K_{LD} H / u_G m_D$

ρ_G : air density (kgm^{-3})

ρ_L : liquid (water) density (kgm^{-3})

ρ_{Sj} : density of VOC j (kgm^{-3})

σ : dimensionless quantity defined as $\sigma = f(X_V)D_{DW}A_S K_D m_D H / u_L \delta C_{GDi}$

σ_L : surface tension of liquid (Nm^{-1})

σ_P : surface tension of packing material (Nm^{-1})

τ : residence time of air in BTF (min)

ϕ_D^2 : dimensionless quantity defined as $\phi_D^2 = X_V \delta^2 \mu_D^* / f(X_V)Y_D D_{DW} K_D$

ϕ_E^2 : dimensionless quantity defined as $\phi_E^2 = X_V \delta^2 \mu_E^* / f(X_V)Y_E D_{EW} K_E$

χ_1 : dimensionless quantity defined as $\chi_1 = C_{GDi}D_{EW}K_E m_E / C_{GEi}D_{DW}K_D m_D$

χ_2 : dimensionless quantity defined as $\chi_2 = C_{GDi}D_{OW}K_O m_O / C_{GOi}D_{DW}K_D m_D$

ψ : dimensionless quantity defined as $\psi_D = K_{LD}H / u_L$

ω_D : dimensionless quantity defined as $\omega_D = C_{GDi}Y_D m_O / C_{GOi}Y_{OD}m_D$

ω_E : dimensionless quantity defined as $\omega_E = C_{GEi}Y_E m_O / C_{GOi}Y_{OE}m_E$

ϑ_E : dimensionless quantity defined as $\vartheta_E = m_D K_{LE} / m_E K_{LD}$

ϑ_O : dimensionless quantity defined as $\vartheta_O = m_D K_{LO} / m_O K_{LD}$

Special Subscripts

$j = E$: VOC j is ethanol

$j = D$: VOC j is o-DCB

$q = E$: compound is ethanol

$q = D$: compound is o-DCB

$q = O$: compound is oxygen

CHAPTER 1

INTRODUCTION

During the last decade a very large number of studies have been undertaken and published on a technology known as biofiltration. This is a technology to clean airstreams contaminated with volatile organic compound (VOC) vapors and is based on VOC degradation by microorganisms. The units used by this technology are known as biofilters.

The wide interest in biofiltration arises from two factors: the nature of contaminants treated and the fundamental basis of the technology itself. Volatile organic compounds (VOCs) may have seriously negative health effects as many of them are suspected carcinogens and classified as hazardous air pollutants (HAPs). Furthermore, VOC emissions have been directly related to either smog formation in the troposphere or ozone depletion in the stratosphere (Mukhopadhyay and Moretti, 1993). Due to the foregoing properties, a number of environmental regulations exist on VOCs and those classified as HAPs are also regulated under the 1990 Clean Air Act Amendments (CAAA). Under CAAA, a 90% reduction in specific HAPs released from major emission sources was to be achieved by the year 2000. This explains the large number of biofiltration studies in the past decade.

The fundamental basis of biofiltration is the biological oxidation of pollutants and their conversion to innocuous final products. Biologically based technologies are environmentally friendly, consume little energy, and thus, are preferable to other

1

technologies achieving the same end. This is the second reason for the increased interest in biofiltration.

To date, there are two generations of biofilters that have been studied as well as applied in the field. The first generation is that of conventional biofilters (usually referred to as, simply, biofilters) and the second generation is that of biotrickling filters (BTFs).

Conventional biofilters are packed with porous particles of organic origin and in them, there is a direct contact of air with the moist biofilms without any regular supply of non-carbon nutrients. On the other hand, biotrickling filters (BTFs) use a well-specified inorganic packing and in them, there is a liquid phase trickling through the bed. The liquid provides, on a continuous basis, additional (non-carbon) nutrients to the biomass while facilitating pH control. Hence, biotrickling filters are preferred over conventional filters for the removal of compounds that are relatively difficult to biodegrade, and/or lead to end products affecting the pH (e.g., chlorinated compounds).

Conventional biofilters have been employed in a wide range of feasibility and modeling studies. Baltzis (1998) reviewed these studies in a book chapter published recently, and a whole book has been published on this issue (Devinny et al., 1999). Studies on conventional biofilters are not reviewed in this dissertation.

The study presented here is one on BTFs. Earlier studies have demonstrated that BTFs lead to removal rates higher than those obtained with conventional biofilters. This has been mainly attributed to larger air/liquid (biofilm) interfacial areas developed in BTFs. Furthermore, since BTFs are better specified systems when compared to conventional biofilters, they are amenable to better engineering and control. It should be mentioned that conventional biofilters may be preferable to BTFs for certain ranges of air flow rates and

for certain types of applications (e.g.. odor control versus treatment of HAPs). Togna and Singh (1994) have discussed practical operating regimes for both conventional biofilters and BTFs.

As reviewed in the next chapter of this dissertation, there are a number of studies on VOC removal in BTFs. However, most of the existing studies have investigated situations in which the airstream passed through a BTF is contaminated due to the presence of a single VOC. When the study reported here was initiated, the few studies on mixed VOC removal in BTFs addressed cases in which pollutants had similar characteristics (solubility, volatility, biodegradability, chemical structure). These studies are reviewed in the next chapter. The study reported here was undertaken with the key objective being to validate or negate the following hypothesis: mixtures of widely different VOCs may be successfully and simultaneously removed in BTFs operating robustly over extended periods of time. The study was based on the treatment of airstreams contaminated with ethanol and ortho-dichlorobenzene (o-DCB) vapors. As discussed in detail in subsequent chapters, the results validated the basic hypothesis. It is interesting that during the course of the work presented here, two studies were published on the removal of dissimilar VOCs. As discussed further in Chapter 2, Okkerse et al. (1999a) found that methylmethacrylate (MMA) significantly hampers dichloromethane (DCM) removal in a BTF. Mohseni and Allen (2000) working with a conventional biofilter that had some features of a BTF (frequent but not continuous passage of a liquid stream through the bed) reported that methanol drastically reduced the removal of α-pinene. Hence, the study reported here is the first to find that two dissimilar VOCs can be successfully and simultaneously removed in a BTF. In fact, it has been found that the presence of ethanol enhances rather than hampers the removal of o-DCB, which is

the much less soluble and much more difficult compound to biodegrade in the mixture considered. The present study also presents a mathematical model that successfully describes and predicts experimental data.

CHAPTER 2

LITERATURE REVIEW

2.1 VOC removal in Biotrickling Filters

Mpanias and Baltzis (1998) investigated the removal of mono-chlorobenzene (m-CB) in a

BTF, and in reporting their findings they also presented a summary of published studies on

the removal of single VOCs in BTFs. Thus, the review presented here only concerns recent

studies not reviewed by the aforementioned authors.

Recent studies have investigated the effects of the packing material and process

parameters such as VOC loading, liquid recirculation rate and air residence time on

performance of BTFs. BTFs in recent studies have been used in treating pollutants that had

not been studied earlier such as methylethylketone (Chou and Huang, 1997), styrene (Chou

and Hsiao, 1998 and Lu et al., 2001a), 1,3-butadiene (Chou and Lu, 1998), methylacetate

(Lu et al., 2001b), N,N-dimethylacetamide (Lu et al., 2001c), ethylacetate (Lu et al.,

2001d), acrylonitrile (Lu et al., 2000b), and nitric oxide (Chou and Lin, 2000). Clearly,

nitric oxide is not a VOC and the study of Chou and Lin (2000) is mentioned here to

indicate that BTFs have been explored in the removal of even inorganic compounds. In

their study with 1,3-butadiene, Chou and Lu (1998) examined the removal of the pollutant

in both a BTF and a BTF in series with a conventional biofilter. Piexoto and Mota (1998)

reported the removal of toluene in a biotrickling filter packed with a material not used in

earlier studies, namely, PVC Raschig rings.

Fortin and Deshusses (1999a) studied methyl tert-butyl ether (MTBE) removal in a BTF and discussed the process of acclimation of a microbial consortium to degrade MTBE. They also presented an analysis on determining the rate-limiting step for the process. During the six week long acclimation period to generate an aerobic microbial consortium capable of degrading MTBE, peat humic substances were added to the recirculating liquid. Almost 97% conversion of MTBE was achieved and no degradation byproducts were found in either the gas or liquid phase. It was found that the process was limited by biological reaction and not mass transfer (Fortin and Deshusses, 1999b). The BTFs were found to adapt quickly to transient conditions and achieve new steady states.

Zuber et al. (1997) presented a design of a small industrial scale BTF. They discussed the scale-up procedure. The cost analysis by the same authors revealed that the full-scale biotrickling filter was more cost-effective than either an airlift bioreactor or a catalytic oxidation unit. Another model for cost-effective operation of biotrickling filters was developed by Deshusses and Cox (1999). They used model simulations to quantify the influence of the nitrate loading on the overall treatment cost. Their results suggested that BTFs were competitive with conventional treatment technologies. A study on the capital and operating costs of a full-scale BTF was presented by Deshusses and Webster (2000) both for chlorinated and non-chlorinated volatile organic compounds.

2.2 Removal of VOC Mixtures in Biotrickling Filters

Sorial et al. (1997) evaluated the performance of a biotrickling filter for BTEX removal and investigated operating parameters such as BTEX loading, empty bed residence time, and backwashing frequency. The same authors also addressed the issue of development of

removal rate constants. Another feasibility study on BTEX vapor removal in a BTF was presented by Lu et al. (2000a). Baltzis et al. (2001) showed that simultaneous removal of mono-chlorobenzene (m-CB) and ortho-dichlorobenzene (o-DCB) is indeed feasible in a BTF. Simulation studies performed by the same authors showed that cross-inhibitory effects played a minor role in the removal of m-CB and o-DCB, two compounds that were similar in structure, biodegradability, and solubility. Pentane and styrene mixture removal was reported by Lu et al. (2001e). The removal rates of styrene were found to be higher than those of pentane and it was concluded that styrene exerted a stronger inhibition on the removal of pentane than pentane did on styrene. Ruokojarvi et al. (2001) studied the oxidation of mixtures of dimethyl sulfide (Me_2S), hydrogen sulfide, and methanethiol (MeSH) using a two-stage biotrickling filter. Almost all of the H_2S and half of the MeSH were oxidized in the first biofilter that operated at a low pH and the rest of MeSH and the Me_2S was oxidized in the second biofilter with neutral pH.

As has already been mentioned in the previous chapter, Okkerse et al. (1999a) studied the removal of methylmethacrylate (MMA) and dichloromethane (DCM) in a BTF. The BTF was originally developed for DCM removal only. Once MMA was introduced into the airstream, simultaneous removal was observed but DCM removal was significantly reduced. The authors concluded that the presence of the easily degradable MMA led to a population shift in the biomass, thus harming DCM removal. Similarly, Mohseni and Allen (2000) working with a hybrid of a BTF and a conventional biofilter, found that the presence of the highly hydrophilic methanol suppressed the growth of the α-pinene degrading microbial community. Thus, the methanol presence reduced the removal rate of the α-pinene. Clearly, the two aforementioned studies have shown simultaneous removal of

dissimilar VOCs but in a non-robust BTF operation. With time, substantial biomass diversification is expected to eventually lead to the suspension of the removal of the less soluble and less biodegradable compound. These results are drastically different from those of the study discussed here.

2.3 Biomass Accumulation Studies

The favorable microbial growth conditions created in the BTF environment lead to biomass accumulation, a problem magnified when easily degradable compounds, such as toluene and ethanol, are fed to a BTF at high loadings. Biomass accumulation hinders the continuous and stable/robust operation of BTFs over prolonged periods of time.

Smith et al. (1996) evaluated two biomass control strategies for high toluene loadings. These involved backwashing with medium fluidization and the use of nitrate instead of ammonia as sole source of nitrogen. The backwashing technique was incorporated as a process variable in a model developed by Alonso et al. (1997). In another study, Smith et al. (1998) reported stable and high removal efficiencies for BTFs highly loaded with toluene under a coordinated biomass control strategy with the objective of maximizing the biofilm specific surface area. It should be noted that 6-mm pelletized Celite particles were used in all these cases as biomass support and backwashing involved fluidizing the bed at an additional pressure drop of 2 psi to a bed expansion of about 40%.

Cox et al. (1999a) examined the effect of adding two protozoan species as well as an uncharacterized protozoan consortium to a toluene degrading biotrickling filter as a means to control biomass accumulation. They found a lower rate of biomass accumulation and improved carbon mineralization in the enriched biotrickling filters after an initial

gestation period. In another study, Cox et al. (1999b) assessed the efficiency of chemical washing of biomass from Pall rings with combinations of compounds such as NaOH, NaClO, and H_2O_2. Washing with NaClO and H_2O_2 resulted in complete inactivity of the unremoved biomass, whereas low residual biological activity was observed with NaOH. This procedure suggested reduction in cleaning frequency but involved additional recovery times for the attached biomass after each wash.

Alonso et al. (1998) developed a method for the calculation of specific biofilm surface area of the reactor as a function of biomass growth. They analyzed three models of reactor porous media to explain the initial increase and subsequent drop in the contaminant removal efficiency while biomass accumulated in the system. They attributed this behavior to the decrease in specific surface area available for contaminant transport into the film with biofilm growth. They also studied the effect of contaminant solubility on biofilter performance concluding that the more soluble the pollutant is, the higher is the removal efficiency due to increased availability for bacterial growth.

A similar study on biomass accumulation and clogging, using dichloromethane as a model pollutant, was carried out by Okkerse et al. (1999b). These authors developed a dynamic model to predict the clogging rate of a filter bed and the time taken by the BTF to adapt to VOC concentration changes at its inlet. The model distinguished between active and inactive biomass and explicitly accounted for changes in pH. The authors suggested the use of the rate of carbon conversion per unit void packing volume in order to compare the performance of different systems on a load basis. Their experimental set-up involved the continuous registration of the weight of the biofilter to study the development of different mass hold-ups and wet biomass on the packing. The exact value of maximum allowable

carbon load was found to depend on the characteristics of the reactor system and the properties of the biomass such as growth rate and density.

2.4 Modeling Studies

Several of the proposed models describing the process in biotrickling filters have been discussed by Mpanias (1998). Diks and Ottengraf (1991a,b) studied dichloromethane (DCM) vapor removal in BTFs. In their model, these authors assumed a zero-order kinetic expression and negligible resistance for the transfer of DCM from the contaminated air to the liquid phase. The data were described by the model relatively successfully. The same data were subsequently analyzed by Hekmat and Vortmeyer (1994) who concluded that a better fit could be obtained if a reaction order between zero and one is assumed. The model of Hekmat and Vortmeyer (1994) assumes no reaction in the liquid phase and negligible mass transfer resistance in it for the VOCs. It considers zero- or first-order reaction kinetics, and diffusion in the biofilm is accounted for via the use of an effectiveness factor. This model successfully described the data, which the authors obtained with airstreams contaminated with either ethanol, or polyalkylated benzene vapors. Regarding ethanol removal, it was concluded that oxygen rather than ethanol availability in the biofilm limited the process. The fact that oxygen may play a determining role in VOC removal in BTFs has also been demonstrated by Kirchner et al. (1996). These authors experimentally demonstrated that oxygen-enriched air could enhance the removal of acetone and iso-propanol vapors in BTFs. For this effect to be described, Kirchner et al. (1996) have used an interactive kinetic expression involving a Monod-type dependence on both oxygen and the VOC concentration in the biofilm.

Alonso et al. (1997) introduced a model that considered a two-phase system, uniform bacterial population, one limiting substrate (toluene) and a quasi-steady state term that accounted for biofilm growth. The model incorporated the variation of specific surface area with bacterial growth and described its effect on the biofilter performance. The potential effect of oxygen was neglected and kinetics were assumed to follow a Monod-type expression with regard to toluene concentration. The liquid phase was neglected, essentially implying that it does not present a resistance for the transfer of toluene to the biofilm and that reaction does not occur in the liquid. A subsequent modification of this model considering three phases and dynamic physical and biological processes was presented by Alonso et al. (1998). These authors also discussed models for reactor porous media as also mentioned in the previous section. In a later study on BTFs, Alonso et al. (1999) considered a three-phase system, non-uniform bacterial population and one limiting substrate – diethyl ether. Unknown parameters were determined experimentally to fit a Monod model of biodegradation of the VOC under steady-state conditions. A study involving nonlinear parameter estimation for the dynamic model was presented by Alonso et al. (2000) with a combination of batch tests and biofilter experiments. Steady state parameters such as maximum rate of substrate utilization, Monod saturation constant and biofilm/water diffusivity ratio for ether were estimated first and then used to estimate the remaining parameters of the dynamic model, namely, the yield coefficient, maximum specific growth rate, and rate of biomass decay and maintenance. The same parameter values were also used in solving a mathematical model describing biofiltration of VOCs and incorporating the effect of nitrate concentration and backwashing (Alonso et al., 2001). The model considered one limiting nutrient (nitrate), one limiting organic substrate, and a

non-homogeneous biomass. Backwashing of the reactor (to remove excess biomass) was introduced in the model as a periodic effect leading to an increase in the biofilm surface area and a decrease in the biofilm thickness. Nitrate limitation was found to be an important factor for the biodegradation rate and parameters corresponding to nitrate limitation were estimated.

Removal of mono-chlorobenzene (m-CB) vapor from airstreams was studied in a biotrickling filter (BTF) operating under counter-current flow of the air and liquid streams (Mpanias and Baltzis, 1998). The process was successfully described with a detailed mathematical model, which accounted for mass transfer and kinetic effects based on m-CB and oxygen availability. Experiments were performed under various values of inlet m-CB concentration, air and/or liquid volumetric flow rates, and pH of the recirculating liquid. There was good agreement between the model-predicted and experimental data on m-CB removal in the BTF.

A modeling study by Baltzis et al. (2001) described the removal of similar compounds, mono-chlorobenzene (m-CB) and ortho-dichlorobenzene (o-DCB) in a BTF. The three-phase model was validated experimentally after the kinetic parameters were determined. A major assumption was that there was no reaction in the liquid phase.

Biodegradation in a biotrickling filter is a complex process and some studies have been performed to identify the operating regime, i.e., reaction or mass transfer limitation/control. Lobo et al. (1999) studied carbon disulphide removal in a BTF and inferred that the rate-controlling step could be identified on the basis of substrate concentration in the liquid phase. They developed a model with two experimentally determined lumped parameters that could be used to size the reactor depending on the rate-

limiting step, the absorption factor, the substrate fractional conversion, and the gas liquid contact pattern. In another study, Barton et al. (1999) presented two methods to predict the relative importance of mass transfer and kinetic limitation in operating BTFs. One method involved altering the total bed temperature while the other varied the amounts of biomass in the recirculating liquid during the process of estimating the effective mass transfer coefficients for varying VOC loading rates. Experiments were performed with a mixed culture capable of consuming two sparingly soluble alkanes, namely, pentane and iso-butane. In experiments with toluene degrading BTFs, Cox et al. (2000) showed that suspended organisms in the recirculating liquid contributed up to 21% of the overall toluene removal rate. They also suggested that the suspended biomass in the recirculating liquid was a result of growth in suspension favored by high nutrient and pollutant loadings rather than a result of biofilm detachment only as suggested by Okkerse et al. (1999). Some more effects of the liquid phase on VOC removal in BTFs were studied by Zhu et al. (1998) who alluded mostly to the liquid remaining and draining from the BTF after periodic backwash to remove biomass.

From the foregoing discussion, it is clear that various modeling attempts made to date have used a wide variety of assumptions due to the high complexity of the biofiltration process. One of the key questions that have not been resolved to date, is whether VOC biodegradation in the liquid present in a BTF is significant relative to the biodegradation occurring in the biofilms or not. In other words, the question of how to properly model the liquid phase recirculating through a BTF still wants an answer.

CHAPTER 3

OBJECTIVES

As has been already mentioned in the Introduction (Chapter 1), this study was undertaken to test the following hypothesis:

Mixtures of widely different VOCs may be successfully and simultaneously treated in BTFs operating robustly over extended periods of time.

To test this hypothesis two widely dissimilar compounds, namely ethanol and ortho-dichlorobenzene (o-DCB) were selected as model compounds. Ethanol has high water solubility, a low Henry's constant, and is readily biodegradable. Its properties are opposite to those of o-DCB. Selection of o-DCB was driven by the fact that this compound had been studied earlier in the laboratory where the present study was performed (Mpanias, 1998).

To test the above hypothesis, a BTF unit was set-up and operated over a period of over three years. Results are presented in Chapter 5. Once the feasibility of simultaneous removal of ethanol and o-DCB in a BTF was established, a number of questions (secondary objectives) were set and addressed.

1. Effect of air residence time on BTF performance.

2. Effect of inlet ethanol and o-DCB concentration on BTF performance.

3. Effect of liquid recirculation rate on BTF performance.

4. Potential interactions between ethanol and o-DCB.

5. Ability of the BTF to perform robustly over extended periods of time.

6. Potential biomass diversification along the BTF column.

7. Contribution of the liquid phase to the overall biodegradation process.

To address objectives 1, 2, and 3, experiments were performed under a wide range of operating conditions and results are reported in Chapter 5.

To address objective 4, two approaches were used. One was based on comparisons of o-DCB removal obtained in the BTF operating with the ethanol/o-DCB mixture with o-DCB removal obtained with a second BTF unit that was never exposed to ethanol. Results of this study are presented in Chapter 5. The second approach was based on kinetic experiments with suspended cultures and their results are presented and discussed in Chapter 7.

To address objective 5, the BTF removing both ethanol and o-DCB was operated over extended periods of time. It was found that after a substantial period of continuous operation, performance deteriorated drastically in a short period of time. A method was developed to quickly restore BTF operation to normal VOC removal rates. Furthermore, reproducibility of results was checked with experiments under given sets of operating conditions repeated at instances that were widely apart. These results are shown in Chapter 5.

To address objective 6, an indirect method was used. Biomass was taken from three positions (top, middle point, and bottom) of the BTF and used as inoculum for suspended culture batch kinetic runs under identical VOC concentrations in separate vials. Experiments were repeated over time. Results are presented in Chapter 7.

Objective 7 was addressed by varying the fraction of the recirculating liquid replenished with fresh nutrient medium over set time periods. This led to variations in the levels of biomass presence in the liquid phase. Results are presented in Chapter 5.

The second major objective set for this study was to model the BTF performance. A new model was developed and is presented in Chapter 6. This model can be viewed as a modification of the models of Mpanias and Baltzis (1998) and Baltzis et al. (2001). The proposed model has a new feature that allows for reaction in the liquid phase, something neglected in the aforementioned earlier studies. In addition, the proposed model uses a simplified approach based on the use of an effectiveness factor that allows for easier description of phenomena in the biofilm phase. The model, its assumptions, and the methodology for numerically solving the equations are presented in Chapter 6.

Chapter 7 presents the model validation using the results presented earlier in Chapter 5. In the same chapter, a detailed description of model parameter estimation is also presented. Estimation of some parameters entailed undertaking kinetic studies that are also discussed in Chapter 7. Furthermore, comparisons of results obtained under the assumption of either significant or negligible contribution of the liquid phase to the overall VOC removal are also presented. Finally, results from sensitivity studies of the model are also shown in Chapter 7.

CHAPTER 4

EXPERIMENTAL DESIGN AND PROCEDURES

4.1 Biotrickling Filter Units

Two biotrickling filters were used in the present study. They were essentially identical except for the fact that one of them, called BTF-I, was employed to treat airstreams carrying o-DCB only and was never exposed to ethanol, whereas the second, called BTF-II, was developed to treat airstreams contaminated with both ethanol and o-DCB vapors. The design of the two units was practically the same as that of the units used by Mpanias (1998) in his study with o-DCB and m-CB vapors. Figure 4.1 shows a schematic representation of BTF-II.

In each set-up, the actual biotrickling filter consisted of a glass column (custom-made, ACE Glass Inc., Vineland, NJ) that was 15 cm in diameter and 80 cm in height. The column was packed with 1/2" Intalox ceramic saddles (Norton Chemical Process Product Corp., Akron, OH) and had three sampling ports at its entrance, exit, and middle point. The packing served as immobilization medium for the biomass. The height of the packed bed was 74 cm in both units. The packed bed in BTF-I was non-segmented, whereas in BTF-II it was segmented into two equal beds (each 37 cm high). The packing in each section of BTF-II and the bottom of BTF-I was supported by a stainless steel screen of 1.5 to 2 mm mesh size (custom-made, ACE Glass Inc., Vineland, NJ). The two sections in BTF-II were separated by a custom-made (ACE Glass Inc.) flanged glass spacer that was 15 cm in diameter and 8 cm in height.

17
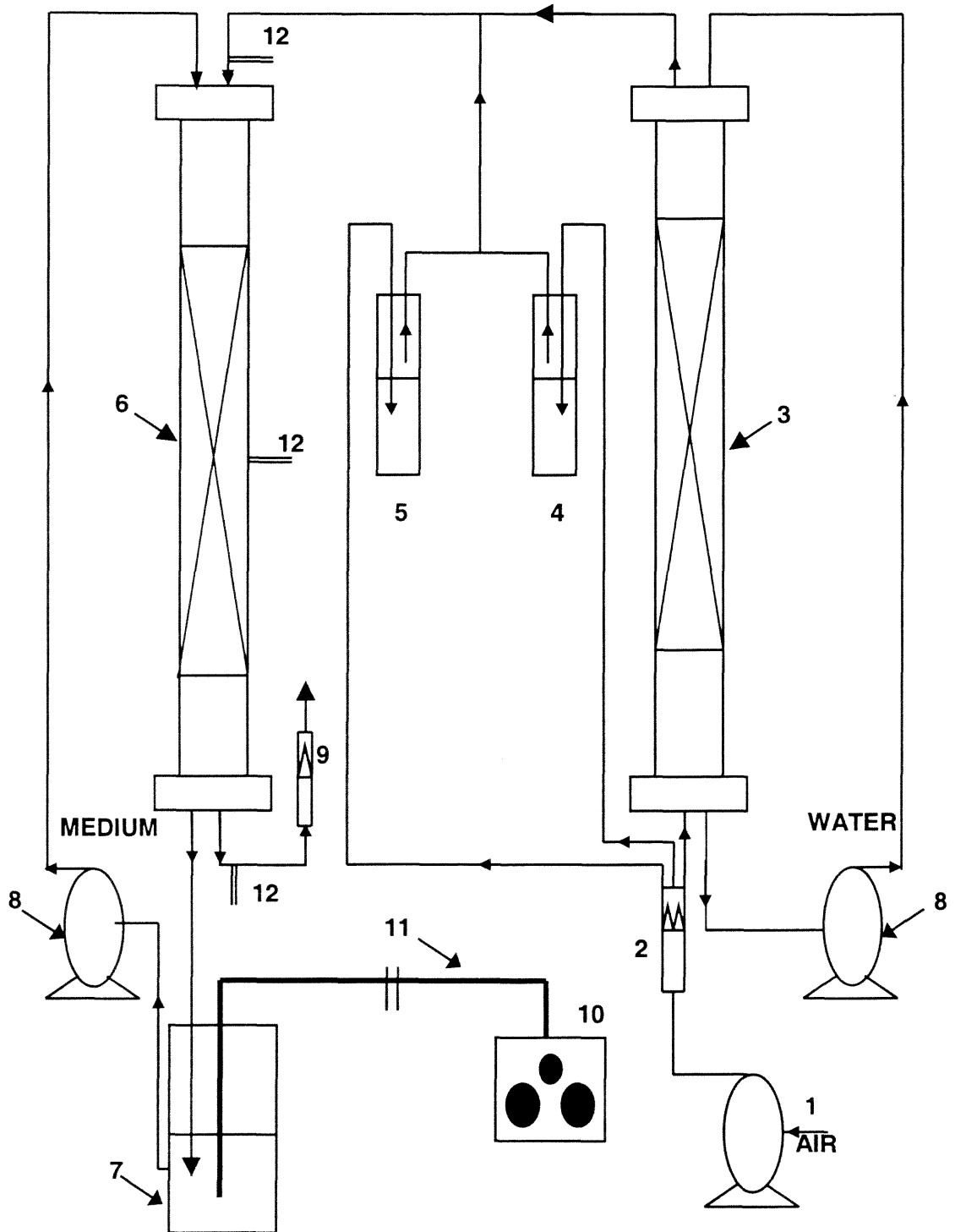
Figure 4.1: Schematic representation of the BTF unit
1. Air pump, 2. Rotameter Assembly, 3. Humidification tower, 4. Ethanol tank, 5. o-DCB tank, 6. Biotrickling Filter, 7. Tank for recirculating medium, 8. Peristaltic pump, 9. Flow meter, 10. pH Electrode, 11. pH Meter, 12. Sampling Port.

Segmentation of the bed in BTF-II allowed for easier disassembling of the unit for excess biomass removal. Biomass removal took place at four month time intervals, as explained later in this chapter. Each BTF column had a flanged custom-made headtop and headbottom (ACE Glass Inc.) made of glass and having various ports for liquid and air passage (supply or removal).

A liquid stream, which contained the nutrient media, was recirculated through the column in a trickling mode. The total volume of the recirculating liquid was 4 L and it was pumped from a tank. As the liquid stream passed through the column, it also removed excess biomass from the surface of the packing. The airstreams supplied to the BTFs were artificially contaminated with ethanol and/or ortho-dichlorobenzene (o-DCB) vapor and flowed co-currently with the liquid. The airstreams supplied to the BTFs were generated by mixing a pre-humidified air stream with slipstreams bubbled through containers carrying the VOCs of interest in liquid form. Prehumidification took place in a 15 cm-diameter glass column packed with 1/2" Intalox ceramic saddles. Each BTF unit had its own prehumidification tower. Each tower was packed to a 55 cm height and air was supplied to it from the bottom. A rotameter assembly (75-350, Gow-Mac Instrument Co., Bound Brook, NJ) was used to vary the flow rates of the air streams and thereby change the VOC concentrations at the BTF inlet. A U-tube filled with water was connected to the airstream exiting the BTF unit to monitor pressure drop across the bed. Experiments were performed at room temperature (about 25 °C)

4.2 Biomass Acclimation and Process Start-up

BTF-I had been used previously in a study on o-DCB removal by Mpanias (1998). The biomass in this unit originated from a stable microbial consortium capable of completely mineralizing o-DCB, while using it as its sole carbon and energy source. An amount of biomass obtained from BTF-I was acclimated to ethanol and o-DCB mixtures in shake flasks. After a number of serial transfers, the biomass was used as inoculum for developing BTF-II as follows. The glass column that eventually became the filter bed of BTF-II was filled with nutrient medium and inoculated with the acclimated consortium described above. Air containing ethanol (2 gm^{-3}) and o-DCB (2 gm^{-3}) was bubbled through the column from its bottom. Once a considerable increase in optical density was observed, indicating sufficient biomass formation, the liquid was temporarily removed from the column. The column was packed with the solid support, the liquid reintroduced, and operation continued in submerged filter mode. In less than a week, a considerable amount of biomass was observed on the packing. The liquid was then drained and fresh nutrient medium started being trickled through the column.

4.3 Recirculating Liquid

The composition of the nutrient medium used in the liquid trickling through the packing was the same as that used by Mpanias (1998). This nutrient medium, a buffer of pH 7.0, consisted of a mixture of two solutions, A and B, at a B:A ratio of 1:99 by volume. Solution A contained the following chemicals per liter of deionized water: 4.0 g Na_2HPO_4 (S374-500 Fisher Scientific Co., Springfield, NJ), 1.5 g KH_2PO_4 (P285-500 Fisher Scientific Co., Springfield, NJ), 1.0 g NH_4NO_3 (S441-500 Fisher Scientific Co.,

Springfield, NJ), and 0.2 g MgSO$_4$.7H$_2$O (M63-500 Fisher Scientific Co., Springfield, NJ). Solution B contained 0.5 g FeNH$_4$-citrate (I72-500 Fisher Scientific Co., Springfield, NJ) and 0.2 g CaCl$_2$ (C77-500 Fisher Scientific Co., Springfield, NJ) per liter of deionized water.

At process start-up, fresh nutrient medium was trickled through the BTF bed. Immediately after start-up, half of the liquid recirculating through the BTFs was replenished with fresh nutrient medium on a daily basis. This approach helped with maintaining a constant pH value in the recirculating liquid and discarding excess biomass from the BTFs. The two units operated at a liquid pH value of about 7 based on the finding of Mpanias (1998), who showed that a value of 6.8 was optimal for o-DCB removal. A pH-controller (Chemcadet model, Cole-Parmer Instrument Co., Niles, IL) was used in some experiments. The controller worked based on automated NaOH addition to the recirculating liquid.

The recirculating liquid was distributed at the top of the BTF beds through six distribution points. As discussed by Mpanias (1998), for the bed diameter of 15 cm and the effective diameter of the packing used, at least two liquid distribution points are needed to ensure good liquid distribution in the BTF units used. The use of six distribution points in this study implies that problems with liquid distribution were avoided.

Some experimental runs were performed to determine the effect of intermittent liquid supply to BTF-II and BTF-I. In these experiments, the power supply to the recirculating pump was alternately stopped for predetermined time intervals using a time controlled outlet strip (Model 1450N, Grasslin Corporation).

As mentioned earlier, half of the liquid recirculating through the BTFs was replenished with fresh nutrient medium on a daily basis. This approach was altered in two sets of experiments with BTF-II. In the first set, once BTF-II attained steady state for a given set of operating conditions, the entire volume (4 L) of the recirculating liquid was discarded and replenished with fresh nutrient medium. The transient response of the process was monitored through VOC concentration measurements till steady state was reached. In the second set, once BTF-II attained steady state for given operating conditions, the experiment was temporarily stopped. The entire amount (4 L) of the recirculating liquid was filtered so that all biomass was removed. The filtered liquid was then used and the experiment repeated under the operating conditions valid before filtering the liquid. The transient response of the process was monitored via VOC concentration measurements till steady state was reached again. The intent of these two sets of transient experiments was to decipher the impact of the biomass presence in the liquid on the biofiltration process.

4.4 Biomass Control

Regular operation of the BTFs entailed daily partial replacement of the liquid (4 L) with fresh nutrient medium while discarding 50% of the used portion. This served as a way of controlling excess biomass build-up in the BTFs. In addition, BTF-I was taken out of service once every two weeks and high volumes of tap water (about 12 L in half hour). were passed through it to remove excess biomass. BTF-II, which carried more biomass, was flushed in the same manner once every ten days. Furthermore, every four months BTF-II required additional treatment as follows. The unit had to be taken out of service for a few hours. The two sections of the glass column were separated and tap water was passed

through each segment (at 8 Lmin^{-1} for 15 min) to remove biomass. Pressure drop was regularly measured to monitor the biomass growth. This was suggested in a study on traditional biofilters by Deront et al. (1998). In fact, the treatment of BTF-II every four months as mentioned above was strongly correlated with pressure drop build-up.

4.5 Kinetic Experiments

Once biomass was acclimated in BTF-II, a stock solution was prepared as follows. A 10 mL sample was taken from the liquid recirculating through BTF-II and placed in a 1L shake flask containing 250 mL of nutrient medium. The nutrient medium had the composition given in section 4.3 of the present chapter. The flask was provided with o-DCB and ethanol at 5 μL each. Degradation was allowed to occur and serial transfers were performed till a stock solution was developed. The stock solution was periodically provided with o-DCB and ethanol at 5 μL each to maintain the biomass. Using the same procedure, a new stock solution was prepared every two months starting with new samples from BTF-II.

Biomass samples from the stock solution were used in suspended culture batch experiments aimed at determining the biodegradation kinetics of o-DCB and ethanol. Experiments were performed with o-DCB only, ethanol only, and o-DCB/ethanol mixtures. Experiments with o-DCB/ethanol mixtures entailed finding whether the two pollutants are involved in kinetic interactions or not.

The kinetic experiments were performed as follows. Samples were taken from the biomass stock solution and diluted with fresh nutrient medium so that the resulting biomass concentration was around 20 gm^{-3} or 65 gm^{-3}. A 10 mL sample of these solutions was placed in a 160 mL serum bottle. The bottle was then sealed using aluminum crimp cap

placed upon a butyl Teflon-faced 20 mm stopper (Wheaton Manufacturers, Millville, NJ). Subsequently, the bottle was provided with the desired amount of o-DCB and /or ethanol and placed in an incubator shaker (200 rpm, 25 °C). Ethanol and o-DCB were supplied to the bottle in liquid form through the stopper using syringes.

Experiments involving o-DCB, either alone or in mixture with ethanol, were performed with initial biomass concentrations of about 20 gm^{-3}. Experiments involving ethanol were performed with initial biomass concentrations of 65 gm^{-3}. The initial biomass concentration values were determined on the basis of several trial runs and with the objective to get measurable and substantial changes in o-DCB and/or ethanol concentrations in 8-10 h time periods. Ethanol was always used in amounts much higher than o-DCB, thus requiring much higher biomass amounts.

Serum bottles were mostly free of liquid (150 mL headspace in 160 mL bottle) to ensure that experiments were not performed under oxygen limitation.

Experiments were monitored via the analysis of headspace samples obtained from the bottles. The analysis was based on determination of the ethanol and/or o-DCB concentration. Air samples from the bottle headspace were obtained at 30-60 min time intervals after the bottle had stayed in the incubator shaker for 2 h. The 2 h period was allowed for establishment of thermodynamic equilibrium distribution of o-DCB and/or ethanol in the gas and liquid phase present in the serum bottle. The 2 h period was determined in several preliminary runs.

Biomass concentrations were measured only in the beginning and end of each kinetic run to determine the yield coefficients.

Some blank experiments were performed along the lines of the kinetic runs but without using biomass. The intent of these experiments was to determine the Henry constants for o-DCB and ethanol and compare the values obtained with those reported in the literature.

Using the approach described above, kinetic experiments were also performed with biomass obtained from BTF-I. These experiments were performed with o-DCB only and their intent was to compare the kinetic parameter values obtained with those reported by Mpanias (1998) who had also experimented with BTF-I.

At 8-9 month intervals, kinetic experiments were performed along the lines of the experiments described earlier in reference to the biomass from BTF-II. In these experiments, instead of using biomass from the stock solution, biomass obtained from the packing of BTF-II was used. This was done as follows. BTF-II was disassembled and biomass samples were scraped off the surface of packing material located at the entrance, middle point, and exit of the filter bed. Biomass scraping was achieved by washing some solid particles from the three locations in the filter bed with autoclaved nutrient medium. After filtration, biomass from each location in the BTF was used in kinetic runs with similar o-DCB and/or ethanol amounts. Comparing the results from these runs one could, indirectly, determine whether biomass diversification (e.g. ethanol degraders versus o-DCB degraders) occurred along the length of the bed in BTF-II.

4.5 Analytical Methods

Air samples obtained from the inlet, outlet and the middle point of the BTF units as well as from the headspace of serum bottles used in kinetic runs were subjected to GC analysis. In

all cases, 500 μL samples were analyzed after they were obtained by using gas-tight syringes (Hamilton, Reno, NV). The GC unit (Hewlett-Packard model 5890 series- II) was equipped with a 6' x 1/8" stainless steel column packed with 80/100 Carbopack C/0.1% SP-1000 (Supelco Inc., Belleforte, PA), and a flame ionization detector. Nitrogen at 21 mLmin^{-1} and 21 psig was used as carrier gas, while hydrogen at 26.3 mLmin^{-1} and 14 psig was used for the detector. The injection port, oven and detector of the GC unit were operated at 210 °C. Both o-DCB and ethanol were simultaneously analyzed in this unit. Retention times were 10.66 min and 0.56 min for o-DCB and ethanol respectively. The area of the chromatogram peaks was determined by a Hewlett Packard 3396A integrator. Calibrations were repeated on a weekly basis. Detection limits were 0.08 gm^{-3} for o-DCB and 0.04 gm^{-3} for ethanol.

Some liquid samples from the exit of BTF-II were sent for GC-MS analysis to the Material Characterization Laboratory at NJIT to check for ethanol/ and or o-DCB presence. The detection limits of the both the analytes were 5 ppm.

Liquid samples from the liquid recirculated through BTF-II and from the serum bottles employed in the kinetic runs were analyzed spectophotometrically (Spectronic 20D, Milton Roy Co.) to determine biomass concentrations. Absorbencies were measured at 540 nm and calibration curves were obtained following the procedures of Mpanias (1998).

CHAPTER 5

RESULTS FROM EXPERIMENTS WITH BIOFILTERS

5.1 Effect of Operating Parameters

Experiments were performed with the biotrickling filters, BTF-I and BTF-II, over a period of 3 years. BTF-I was always fed with o-DCB only, whereas BTF-II was developed to treat o-DCB and ethanol mixtures. Process parameters such as VOC inlet concentrations, liquid recirculation rate (Q_L), and gas phase residence time (τ) were varied among experiments. The VOC concentrations at the inlet, middle point and outlet of each column were recorded. Pressure drop along the columns was monitored, as was the pH of and biomass concentration in the recirculating liquid. VOC analysis of some liquid samples was also carried out. The following quantities were used to evaluate the performance of the BTFs.

$$\text{Removal Rate} = \frac{C_{Gji} - C_{Gje}}{\tau} \quad (\text{gm}^{-3}\text{h}^{-1})$$

$$\text{Loading} = \frac{C_{Gji}}{\tau} \quad (\text{gm}^{-3}\text{h}^{-1})$$

$$\text{Percent Removal} = \frac{C_{Gji} - C_{Gje}}{C_{Gji}} \times 100$$

Results from the performance of BTF-I are shown in Table 5.1. It can be observed that under the different conditions of Q_L and τ tried, o-DCB removal varied from 42% to 71%. The maximum removal rate obtained was 39.2 $\text{gm}^{-3}\text{h}^{-1}$. The groups of experiments designated as 2A and 3A on Table 5.1 were performed under essentially the same air residence time, τ, and o-DCB concentrations. The results show that as the liquid

recirculation rate (Q_L) increases the VOC removal also increases. The experiments of groups 1A and 3A were performed under essentially the same Q_L value. Two of the experiments in the aforementioned groups were performed under very similar o-DCB inlet concentrations. The results show that VOC removal increases with air residence time in the BTF. These tendencies are the same as those found by Mpanias (1998). What is even more interesting is that the results shown in Table 5.1 are quantitatively similar to those obtained

Table 5.1 Removal of o-DCB in BTF-I.

Experiment	Inlet Concentration (gm^{-3})	Percent Removal	Removal Rate (gm^{-3}-reactor h^{-1})
1		$\tau = 6.5$ min; $Q_L = 3.6$ Lh^{-1}	
	1.45	70.4	9.42
A	3.37	68.83	21.41
	4.7	64.51	27.99
	0.91	71.07	5.97
B	2.27	68.44	14.34
2		$\tau = 4.2$ min; $Q_L = 8.7$ Lh^{-1}	
	1.40	64.88	12.98
A	2.74	65.39	25.60
	4.02	68.24	39.19
	1.4	64.88	12.98
B	2.02	65.44	18.88
	3.27	64.32	30.05
3		$\tau = 4.00$ min; $Q_L = 4.2$ Lh^{-1}	
	1.11	51.29	10.20
A	2.56	46.45	21.68
	3.68	41.63	28.50

by Mpanias (1998) who also experimented with o-DCB removal using the same unit. Since the Mpanias study and the study reported here span a period of over 5 years, these results

show an inherently robust performance of BTFs removing o-DCB when the consortium used here is employed.

Initial feasibility studies with ethanol and o-DCB mixtures showed that simultaneous removal of both VOCs was possible in a BTF. Results from systematic experiments with ethanol/o-DCB mixtures in BTF-II are shown in Table 5.2. These experiments were performed over a 3-year period, and results shown are under steady state conditions. The first important conclusion from Table 5.2 is that o-DCB and ethanol can be simultaneously removed in a BTF unit operating over a significant amount of time. Under all conditions tried, ethanol was removed at levels higher than 90% and o-DCB at levels always higher than 70% and often exceeding 90%. Given the fact that analysis of liquid samples indicated no presence of o-DCB or ethanol, removal of the VOCs is attributed to biodegradation only. Removal of ethanol was very high, essentially over 95%, under all conditions tested. This is not surprising as ethanol is a readily biodegradable substrate. Removal rates for ethanol reported in Table 5.2 may be misleading. They are calculated based on the entire BTF volume while in reality ethanol removal was essentially complete within the first section of the BTF bed, as can be seen from the concentration profiles shown in Figure 5.1. If the removal rates for ethanol were calculated based on the volume of the reactor actually involved in ethanol removal, the values would be essentially double those reported in the last column of Table 5.2. Figure 5.1 is important because it shows that o-DCB is removed throughout the column. Since ethanol was removed in the first segment of the filter bed, one could contemplate that o-DCB was removed in the second segment only (sequential removal of VOCs). Clearly, this is not the case and the two VOCs were in fact simultaneously removed.

Table 5.2 Removal of o-DCB and ethanol in BTF-II.

Experiment	Inlet Concentration (gm^{-3})		Percent Removal		Removal Rate $(gm^{-3}\text{-reactor } h^{-1})$	
	o-DCB	Ethanol	o-DCB	Ethanol	o-DCB	Ethanol
1			$\tau = 6.5$ min; $Q_L = 3.6$ Lh^{-1}			
	1.88	2.65	93.10	95.92	16.16	23.46
A	3.46	2.46	92.40	96.41	29.51	21.89
	4.70	2.43	91.97	96.22	39.90	21.58
	1.96	4.36	94.76	97.82	17.14	39.37
B	3.42	4.62	93.11	97.11	29.39	41.41
	4.51	4.15	91.69	97.60	38.17	37.39
	1.05	0.81	78.65	100	7.62	7.48
C	2.11	0.75	73.00	100	14.22	6.92
	3.95	0.90	72.21	100	26.33	8.31
2			$\tau = 4.2$ min; $Q_L = 8.7$ Lh^{-1}			
	0.91	2.51	95.88	95.38	12.46	34.20
A	2.11	2.62	95.24	95.38	28.71	35.70
	3.35	2.35	90.25	97.35	43.19	32.68
B	2.14	5.95	80.12	93.21	37.27	79.23
	2.23	11.53	71.11	92.01	22.65	151.55
3			$\tau = 4.0$ min; $Q_L = 4.5$ Lh^{-1}			
	1.33	2.35	90.53	96.18	17.20	32.29
A	2.2	2.57	85.88	94.36	26.99	34.64
	3.50	2.51	81.89	92.76	40.95	33.26

Figure 5.2 shows the variation of o-DCB removal rates with o-DCB loading under a range of gas phase (air) residence times. These results were obtained from BTF-II, by fixing the ethanol concentration at the inlet and varying the o-DCB concentration. For the same o-DCB loading, the o-DCB removal rate increased with the gas phase residence time as has been also established in previous studies.
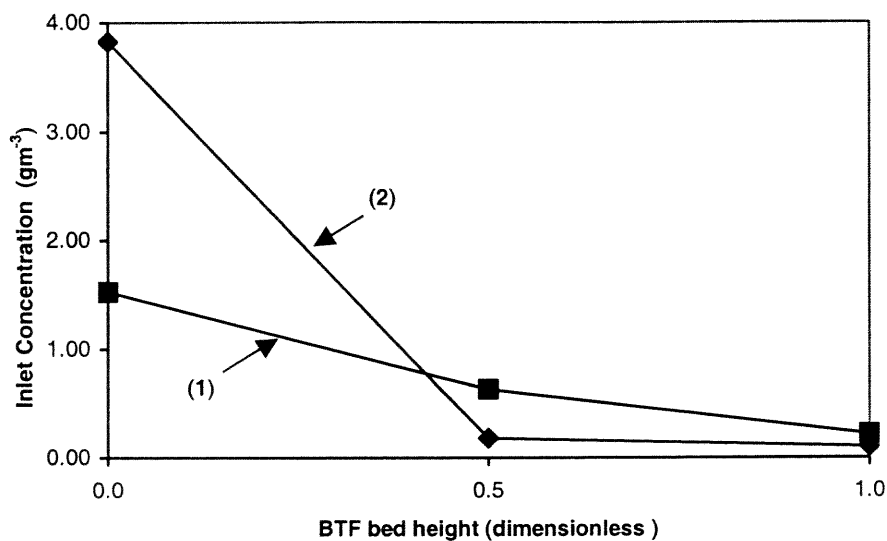
Figure 5.1 Concentration profiles along the BTF-II bed when $\tau = 6.5$ min and $Q_L = 7.6$ Lh^{-1}. Curves 1 and 2 are for o-DCB and ethanol, respectively.
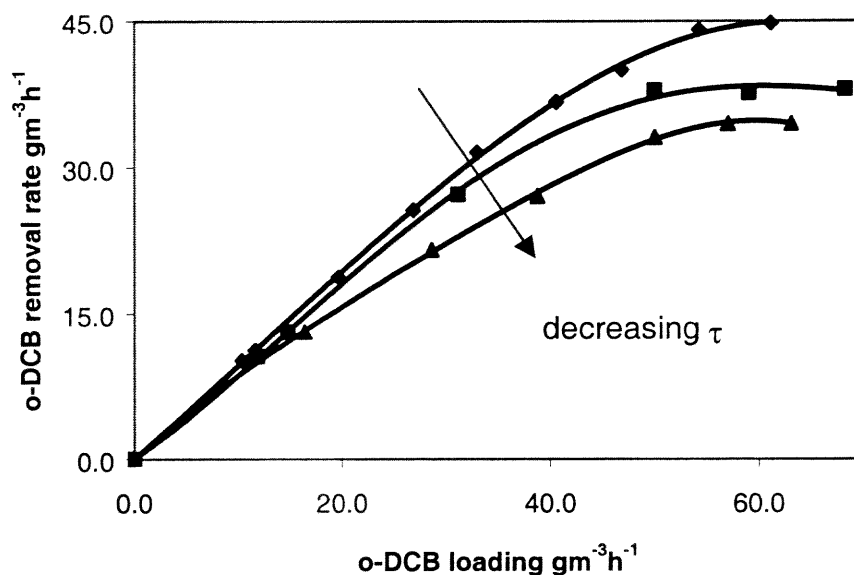
Figure 5.2 Effect of gas phase residence time under constant liquid recirculation rate of 7.8 Lh^{-1} and inlet ethanol concentration of 3.5 gm^{-3}. ◆ denotes $\tau = 5.25$ min, ■ denotes $\tau = 4.2$ min, and ▲ denotes $\tau = 3.25$ min.

Comparing o-DCB removal in BTF-I (Table 5.1) and BTF-II (Table 5.2), it can be seen that the performance of BTF-II is much better. This suggests that the presence of ethanol has a positive effect on o-DCB removal. In order to further investigate this observation, BTF-II was operated for some time on o-DCB alone. The results from this study are listed in Table 5.3. It was found that there was a reduction in o-DCB removal under these conditions.

Table 5.3 Removal of o-DCB in BTF-II in the absence of ethanol.

Experiment	Inlet Concentration (gm^{-3})	Percent Removal	Removal Rate $(gm^{-3}\text{-reactor } h^{-1})$
1		$\tau = 6.5$ min; $Q_L = 3.6$ Lh^{-1}	
A	1.07	80.00	7.90
	2.27	79.12	16.58
2		$\tau = 4.2$ min; $Q_L = 8.7$ Lh^{-1}	
	1.12	81.44	22.34
A	1.92	78.39	12.54
	3.45	75.9	37.41
3		$\tau = 4.2$ min; $Q_L = 4.5$ Lh^{-1}	
	1.4	79.33	15.87
A	2.15	78.12	23.99
	3.62	73.2	37.85

Table 5.4 helps comparing the performance of BTF-I and II under similar conditions of Q_L and τ. It can be seen that the reduction in removal rate of o-DCB in BTF-II when ethanol is absent is by about 15% under similar experimental conditions. Compared to BTF-I, however, the o-DCB removal rates in BTF II in the absence of ethanol were higher. Visual inspection of the BTFs revealed higher biomass presence in BTF-II as compared to BTF-I. This leads one to conclude that the higher amounts of biomass in the BTF system, due to ethanol, has a positive effect on o-DCB removal. These findings are in contrast with two other published studies (Okkerse et al., 1999a and Mohseni et al., 2000)

that have concluded that the presence of a readily biodegradable and highly water soluble VOC has a negative impact on the removal of a more recalcitrant and sparingly water soluble VOC.

Table 5.4 Comparison of o-DCB removal in BTFs

Inlet Concentration of o-DCB (gm^{-3})	Percent Removal	Removal Rate $(gm^{-3}$-reactor $h^{-1})$
$\tau = 4.2$ min ; $Q_L = 8.7$ Lh^{-1}		
In BTF-II when inlet Ethanol concentration is 2.5gm^{-3}		
2.1	95.2	28.7
3.4	90.3	43.2
In BTF-I which treats only oDCB		
2.0	64.9	13.0
3.3	65.4	25.6
In BTF-II in absence of Ethanol		
1.9	81.4	22.3
3.5	75.9	37.4

The variation of o-DCB removal with the ethanol concentration at the BTF inlet can also be deduced from Figure 5.3. The data show that for the same o-DCB loading, the o-DCB removal is higher when ethanol is present. On the other hand, the figure also shows that as the ethanol concentration increases the removal rate drops and exhibits a tendency to approach the performance obtained in the absence of ethanol. In reality, as can be seen from Figure 5.4, the o-DCB removal rate initially increases with the inlet ethanol concentration. It reaches, however, a maximum and then a drop is observed. This effect is less prominent at high values for the air residence time. One can then conclude that for a given set of operating parameters there is a range of concentrations where the ethanol

presence has a beneficial effect on o-DCB removal. It was found that variation in o-DCB inlet concentration did not have any significant effect on ethanol removal rates.
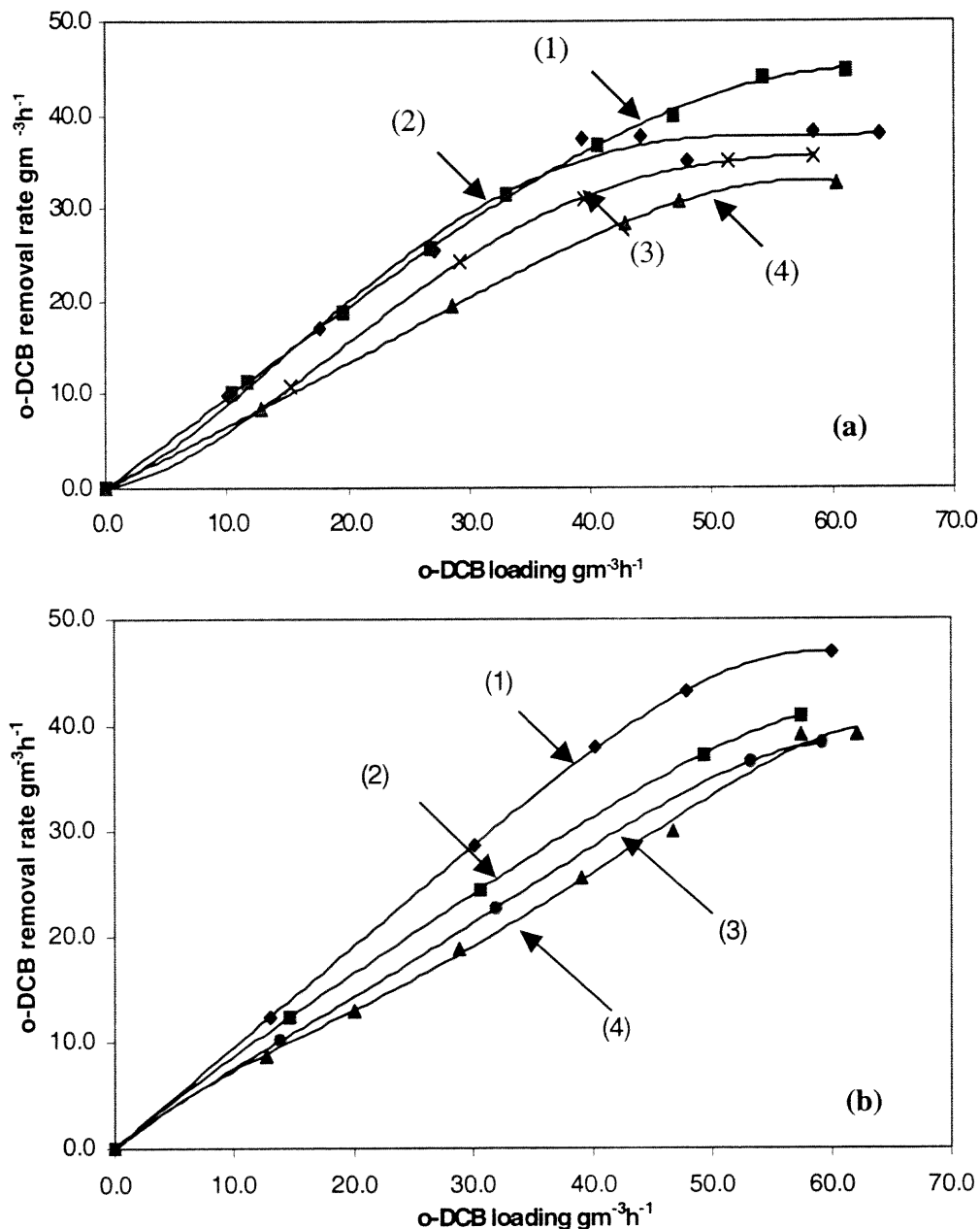
Figure 5.3 Removal rates for o-DCB as a function of o-DCB loading when Q_L = 7.8 Lh^{-1}. The τ-values are 5.25 and 4.2 min in (a) and (b), respectively. Curves 4 refer to data from BTF-I (no-ethanol). The inlet ethanol concentrations are 1.5, 3.5, and 0 gm^{-3} for curves 1, 2, and 3, respectively in (a) and 2.6, 6.1 and 11.6 gm^{-3} for curves 1, 2, and 3, respectively in (b)
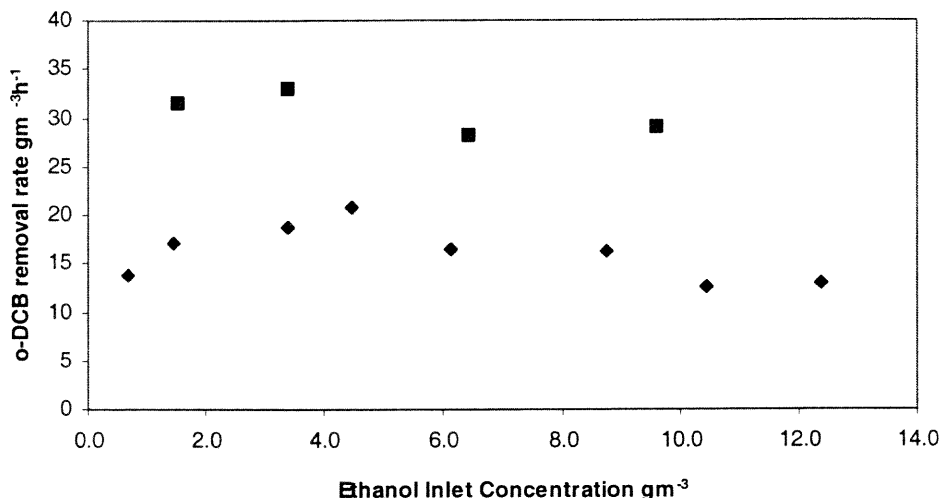
Figure 5.4 o-DCB removal rates as a function of inlet ethanol concentration when $Q_L =$ 7.5 Lh^{-1} and the inlet o-DCB concentration is 2.5 gm^{-3}. Symbols ■ and ◆ represent data for τ-values of 3.25 and 5.25 min, respectively.

5.2 Contribution of Liquid Phase

Compared to BTF-I, there was a high biomass presence both on the packing and in the recirculating liquid in BTF-II. To further examine the contribution of the liquid phase to the overall reaction process, a new set of experiments was carried out in BTF-II while it was operating at steady state under a set of conditions. Instead of replenishing only 50% of the recirculating liquid with fresh medium, the entire liquid phase was replaced with fresh medium. Thus the only factor varied was the amount of biomass in the liquid phase.

Figure 5.5 shows the result of such an experiment. Over the 3 h period of the experiment, the inlet concentrations of o-DCB and ethanol were kept constant. It can be observed that there was an increase in the VOC concentrations at the center of the BTF column. The o-DCB concentrations (Figure 5.5a) increased by about 50% whereas ethanol concentrations (Figure 5.5b) showed a minor increase. Observe that concentrations in Figure 5.5b are on a logarithmic scale. However, this decrease in performance in the first

segment was compensated for in the second half of the column, denoted by the constant exit concentrations. As biomass build-up in the liquid increased with time, there was an improvement in removal as compared to initial time. This can be attributed to the increased nutrient supply with the fresh medium.

Figure 5.6 shows a similar experiment. In this case, instead of replenishing the recirculating liquid with fresh medium, filtered used medium was used so that the nutrient supply was not changed. Again a similar behavior was obtained as in the previous case regarding ethanol and o-DCB at the middle point of the column. At the exit, the o-DCB concentration was found to increase and eventually recover its initial value. Exit ethanol concentration was found to remain constant. All these observations indicate that VOC removal occurs in the liquid phase as well as the biomass immobilized on the packing.

These results are similar to the findings of a study on toluene vapor removal in a BTF (Cox et al., 2000) and another on sparingly soluble alkanes in a BTF (Barton et al, 1999). This can have a profound effect on the long term performance of BTFs as liquid phase contributions can be used to adjust the VOC removal capacity of the unit. Furthermore, the study on alkanes concluded that these results could also help to determine the mechanism controlling the process. The VOC concentration in the effluent depends on the biomass loading in the liquid stream and thus the process appears to be under kinetic control.

A series of experiments (not shown) were carried out to verify the effect of intermittent liquid recirculation. Medium recirculation was stopped for 6 hr intervals. There was a slight drop in o-DCB removal during the "dry periods" but no significant change in ethanol removal. It was concluded that no benefit was obtained from the elimination of

liquid mass transfer effects during the "dry periods". In fact, it was concluded that the absence of the biodegradation contribution from the liquid phase led to a reduction in o-DCB removal.
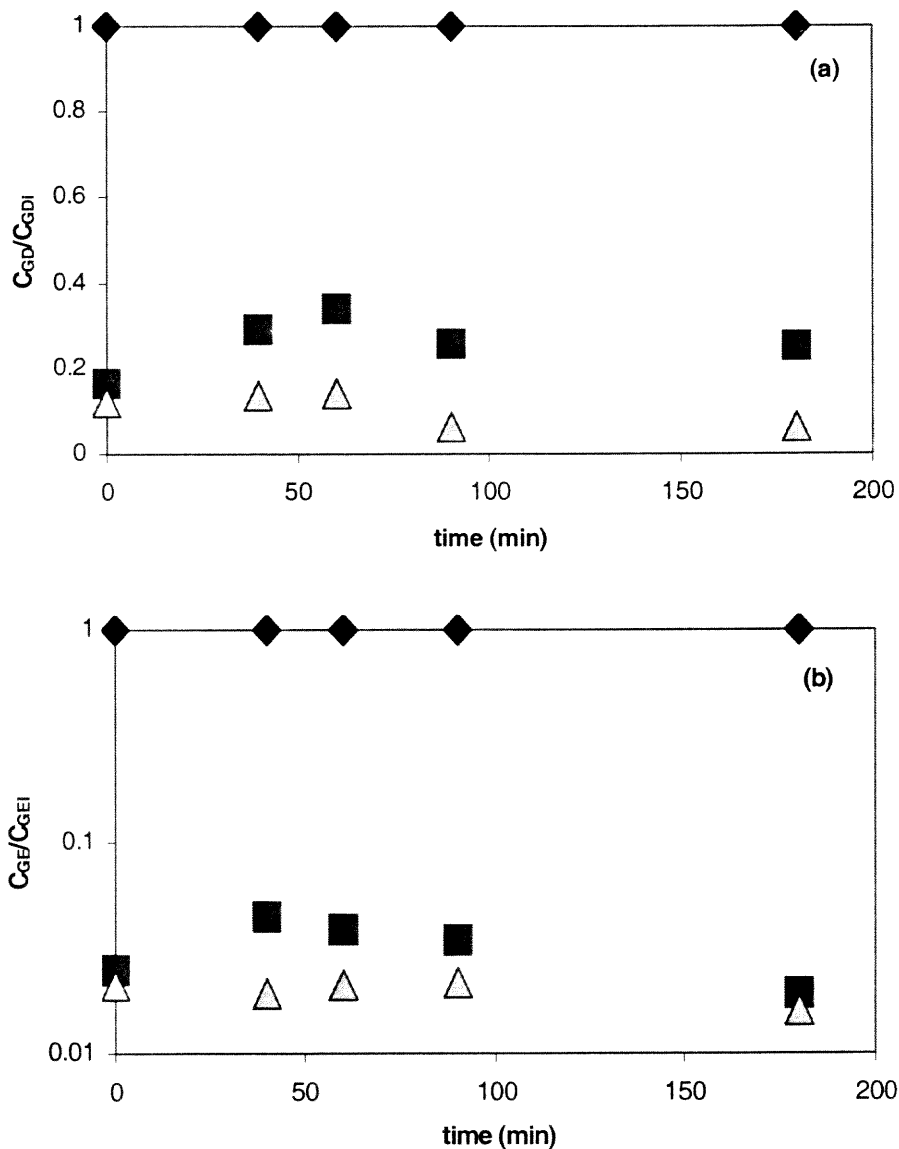
Figure 5.5 Normalized concentration profiles of o-DCB (a) and ethanol (b) at the inlet (♦), middle point (■), and outlet (△) of the BTF bed after complete replenishment of the liquid with fresh medium. Operating conditions: $\tau = 4.33$ min, $Q_L = 8.7$ Lh^{-1} and inlet concentrations of 0.94 gm^{-3} and 3.5 gm^{-3} for o-DCB and ethanol, respectively.
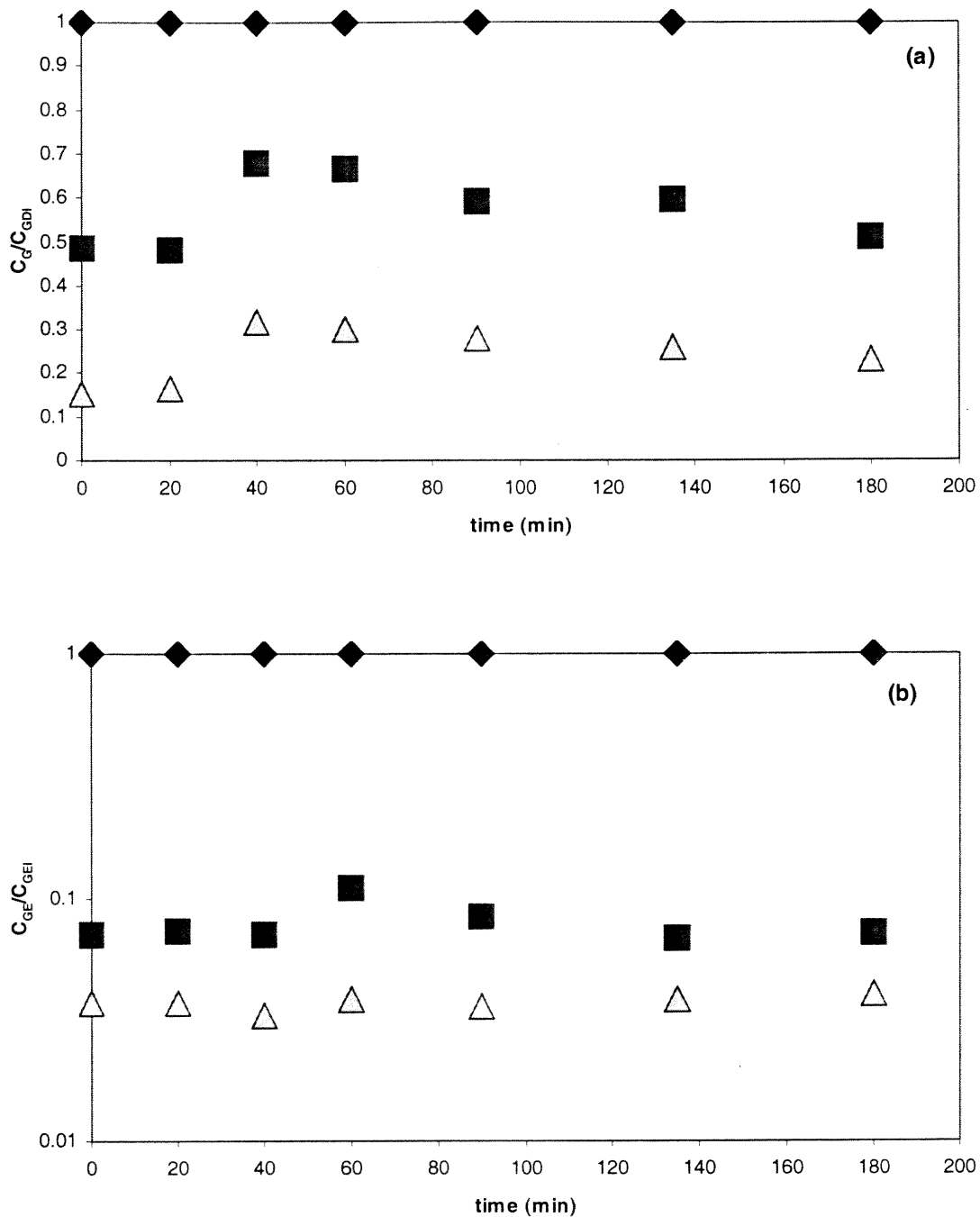
Figure 5.6 Normalized concentration profiles of o-DCB (a) and ethanol (b) at the inlet (♦), middle point (■), and outlet (△) of the BTF bed after complete replenishment of the liquid with filtered used medium. Operating conditions: $\tau = 4.41$ min, $Q_L = 9.8$ Lh^{-1} and inlet concentrations of 1.25 gm^{-3} and 3.43 gm^{-3} for o-DCB and ethanol, respectively.

5.3 Effect of Biomass Build-up

Although an increased amount of biomass in the system assists in VOC removal, too much of biomass has a negative effect. Biomass build-up over long time periods can lead to clogging of the column and cause a detrimental effect on the performance of the BTF. In BTF-II, this was observed once every four months. When the BTF was operated under high ethanol loadings, this occurred more frequently. This drop in performance did not occur during the 3 years of BTF-I operation (no ethanol). Whenever the performance of BTF-II declined, it happened fast and necessitated removal of excess biomass. This was done by disassembling the unit and flushing its two segments with tap water as described in Chapter 4. Results from two such performance decline and recovery occurrences are recorded in Table 5.5 and 5.6. In the first case, in a period of 5 days, o-DCB removal dropped from 93% to 27%. Ethanol removal also dropped to less than 90%. In the second case, o-DCB removal dropped from 90% to 42% in four days. During the same period, the gas phase pressure drop almost doubled. However, in both cases, once the column was cleaned and reassembled, recovery was fast. Within three days, the performance of the BTF returned to its optimum value. It can be concluded that pressure drop monitoring is important to predict clogging in BTFs.

5.4 Long Term Performance

Table 5.7 records the performance of BTF-II over a period of 2 years. It can be seen that in spite of periodic clogging of the column, removal data could be replicated for same operating conditions at steady state. This indicates that the column was robust and gave predictable performance over long periods of time.

Table 5.5 Deterioration and recovery of BTF-II performance (excess biomass problems) when $\tau = 5.23$ min and $Q_L = 9.8$ Lh^{-1}.

DAY	Inlet Concentration (gm^{-3})		Percent Removal		Removal Rate (gm^{-3}-reactor h^{-1})		Pressure drop	
	o-DCB	Ethanol	o-DCB	Ethanol	o-DCB	Ethanol	inches H$_2$O	PSI
-4	1.55	2.67	92.34	94.56	16.41	28.68	1.5	0.0542
-3	1.98	2.75	83.82	93.37	19.04	29.45	1.5	0.0542
-2	1.41	2.61	54.06	92.01	8.74	27.55	-	-
-1	1.48	2.72	44.06	90.07	7.48	28.08	-	-
0	1.44	2.71	27.98	88.09	4.62	27.38	2.5	0.0904
1	1.46	2.80	64.13	95.19	10.74	30.57	1.25	0.0452
2	2.12	2.56	87.39	96.56	21.25	28.35	-	-
3	2.23	2.67	97.51	97.12	24.95	29.74	1.5	0.0542

Table 5.6 Deterioration and recovery of BTF-II performance (excess biomass problems) when $\tau = 4.41$ min; $Q_L = 8.4$ Lh^{-1}.

DAY	Inlet Concentration (gm^{-3})		Percent Removal		Removal Rate (gm^{-3}-reactor h^{-1})		Pressure drop	
	o-DCB	Ethanol	o-DCB	Ethanol	o-DCB	Ethanol	inches H$_2$O	PSI
-4	1.25	3.72	90.0	94.5	15.32	47.88	1.5	0.0542
-3	1.17	3.58	80.16	95.19	12.78	46.37	1.75	0.0632
-2	1.3	3.85	71.00	93.7	12.57	49.13	2	0.072
-1	1.35	3.47	56.43	90.3	10.36	42.67	2.5	0.0904
0	1.27	3.61	42.11	89.5	7.26	44.00	2.5	0.0904
1	1.15	3.8	66.05	95.86	10.34	49.61	1.25	0.0452
2	1.32	3.52	73.44	96.32	13.18	46.17	1.5	0.0542
3	1.45	3.78	85.31	94.21	16.83	48.50	1.5	0.0542

Table 5.7 Duplication of results with BTF-II for a 2.5 years period

Date	Inlet Concentration (gm^{-3})		Percent Removal	
	o-DCB	Ethanol	o-DCB	Ethanol
$\tau = 6.5$ min; $Q_L = 3.6$ Lh^{-1}				
Feb 99	1.88	2.65	93.10	95.92
	3.46	2.46	92.40	96.41
	4.70	2.43	91.97	96.22
Nov 99	1.96	2.36	94.76	97.82
	3.42	2.62	94.82	97.11
	4.51	2.15	95.69	97.60
Sept 00	1.92	2.81	93.6	98.3
	3.35	2.75	95.3	97.6
	4.6	2.90	93.6	97.3
April 01	2.0	2.51	95.6	97.6
	3.5	2.62	94.0	98.9
	4.8	2.35	92.9	96.6

CHAPTER 6

DEVELOPMENT OF THE MATHEMATICAL MODEL

In this chapter, a mathematical model describing removal of two VOCs in a BTF under steady state conditions is presented. The basic concepts of the model are shown schematically in Figure 6.1. Liquid and air flow cocurrently through the packed column (A). The packing material may be either completely or partially covered with biofilm (B).

Contaminated air   Liquid   Packing material

A   h   B

C

GAS   LIQUID   BIOFILM

C_{Gq} C_{Lq} **I**   **II**

$S_{q2,3}$

S_{q1} **Solid Support**

δ_L 0 δ

X $\longrightarrow$
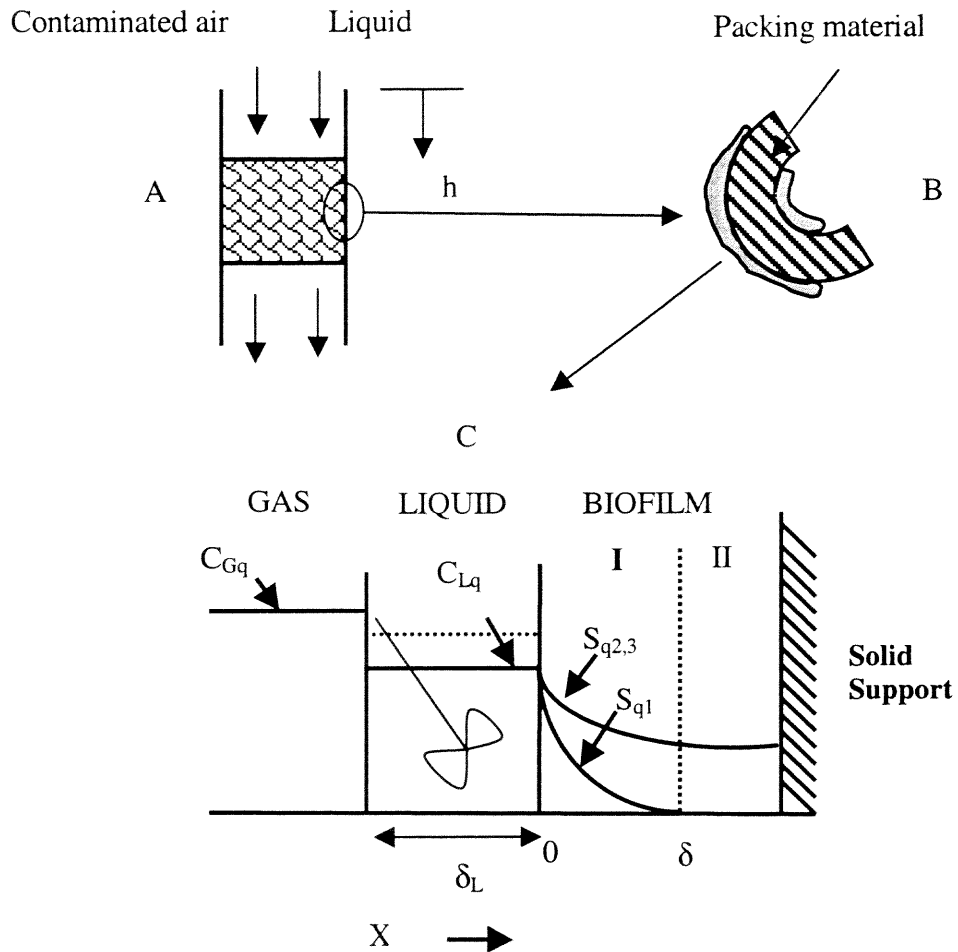
Figure 6.1 Schematic representation of the basic model concepts at a cross-section of the BTF column

At any cross-section of the BTF, the VOCs and oxygen are transferred from the air to the liquid medium wetting the biofilm. Biodegradation occurs in the liquid medium due to biomass presence. The liquid phase is modeled as a CSTR. VOCs and oxygen not consumed in the liquid phase diffuse through and react in the biofilm attached on the packing material (C).

The proposed model is a modification/extension of the work of Mpanias and Baltzis (1998) and Baltzis et al. (2001). The earlier models neglected reaction in the liquid phase and were validated with data from m-CB, o-DCB, and m-CB/o-DCB mixtures in BTFs. The model proposed here reduces to the earlier models mentioned above, when the reaction terms in the liquid phase are set equal to zero.

6.1 Model Formulation

The model describes removal of two VOCs in a BTF. In deriving the model, the following assumptions have been made.

1. The rate of biodegradation depends on the concentration of the VOCs and oxygen, and the rate expressions can be determined from suspended culture experiments.

2. VOCs and oxygen transfer into the biofilm through the side surfaces of biofilm patches that partially cover the surface of the packing can be neglected. Therefore, diffusion/reaction in the biofilm needs to be described only in the direction perpendicular to the main surface of the patch.

3. Reaction in the biolayer occurs only in a fraction called effective biofilm. The effective biofilm thickness (δ) is determined by the depletion of either oxygen or the VOCs. The value of δ may vary along the BTF bed.

4. The thickness of the effective biofilm is very small compared to the surface curvature of the packing material. Hence, planar geometry can be used.

5. Anaerobic degradation of the VOCs does not take place if oxygen gets depleted in the biofilm.

6. Liquid and air streams flow cocurrently through the column.

7. There are no radial concentration gradients in the gas and liquid films and there is negligible mass transfer resistance from the bulk liquid to the biofilm.

8. The air stream passes through the trickling filter in plug flow.

9. Reaction may take place in the liquid phase at each cross-section of the biotrickling filter. The liquid film is modeled as a CSTR.

10. The density of the biofilm is constant throughout the BTF, as is the biomass concentration in the recirculating liquid.

11. At equilibrium, the concentrations of the VOCs and oxygen at the air/liquid interface follow Henry's law.

12. The concentrations of the VOCs and oxygen in the biofilm at the liquid/biofilm interface are equal to those in the liquid phase.

13. Diffusivities of the VOCs and oxygen in the biofilm are corrected from the diffusivities in water using a biomass density dependent factor (Mpanias, 1998).

14. The void fraction of the filter bed is constant implying that the amount of biomass produced in the biofilm is sloughed off into the liquid and then discarded from the system during medium replenishment. Thus, a biomass balance is not needed.

15. The liquid trickling through the bed is recirculated in the unit. No reaction occurs in the recirculation line.

16. Supplemental nutrients, such as nitrogen and phosphorus sources are not exerting rate limitation on the process.

17. The composition of biomass does not change either along the column, or in the direction of the depth of the biofilm.

Under the assumptions above, removal of two VOCs from airstreams in a biotrickling filter can be described by nine mass balances, three on each VOC and three on oxygen, as follows.

I. Mass balances in the biofilm, at a position h along the column,

$$f(X_V)D_{DW}\frac{d^2S_D}{dx^2} = \frac{X_V}{Y_D}\mu_D(S_E,S_D)f(S_O) \tag{6.1}$$

$$f(X_V)D_{EW}\frac{d^2S_E}{dx^2} = \frac{X_V}{Y_E}\mu_E(S_E,S_D)f(S_O) \tag{6.2}$$

$$f(X_V)D_{OW}\frac{d^2S_O}{dx^2} = \left\{\frac{X_V}{Y_{OE}}\mu_E(S_E,S_D) + \frac{X_V}{Y_{OD}}\mu_D(S_E,S_D)\right\}f(S_O) \tag{6.3}$$

With corresponding boundary conditions

$$S_D = C_{LD}; \ S_E = C_{LE}; \ \text{and} \ S_O = C_{LO} \ \text{at} \ x = 0 \tag{6.4}$$

$$\frac{dS_E}{dx} = \frac{dS_D}{dx} = \frac{dS_O}{dx} = 0 \ \text{at} \ x = \delta \tag{6.5}$$

II. Mass Balances in the liquid phase along the column,

$$u_L\frac{dC_{LD}}{dh} = K_{LD}\left(\frac{C_{GD}}{m_D} - C_{LD}\right) + f(X_V)D_{DW}A_S\left[\frac{dS_D}{dx}\right]_{x=0}$$
$$- \delta_L\frac{X_{VL}A_S}{Y_D}\mu_D(C_{LE},C_{LD})f(C_{LO}) \tag{6.6}$$

$$u_L \frac{dC_{LE}}{dh} = K_{LE}\left(\frac{C_{GE}}{m_E} - C_{LE}\right) + f(X_V)D_{EW}A_S\left[\frac{dS_E}{dx}\right]_{x=0}$$
$$- \delta_L \frac{X_{VL}A_S}{Y_E}\mu_E(C_{LE},C_{LD})f(C_{LO})$$

(6.7)

$$u_L \frac{dC_{LO}}{dh} = K_{LO}\left(\frac{C_{GO}}{m_O} - C_{LO}\right) + f(X_V)D_{OW}A_S\left[\frac{dS_O}{dx}\right]_{x=0}$$
$$- \delta_L X_{VL}\left[\frac{A_S}{Y_{OD}}\mu_D(C_{LD},C_{LE})f(C_{LO}) + \frac{A_S}{Y_{OE}}\mu_E(C_{LD},C_{LE})f(C_{LO})\right]$$

(6.8)

With corresponding boundary conditions

$$C_{LD}(h=0) = C_{LD}(h=H)$$
$$C_{LE}(h=0) = C_{LE}(h=H)$$
$$C_{LO}(h=0) = C_{LO}(h=H)$$

(6.9)

III. Mass balances in the gas phase along the column,

$$u_G \frac{dC_{GD}}{dh} = K_{LD}\left(C_{LD} - \frac{C_{GD}}{m_D}\right)$$

(6.10)

$$u_G \frac{dC_{GE}}{dh} = K_{LE}\left(C_{LE} - \frac{C_{GE}}{m_E}\right)$$

(6.11)

$$u_G \frac{dC_{GO}}{dh} = K_{LO}\left(C_{LO} - \frac{C_{GO}}{m_O}\right)$$

(6.12)

With corresponding boundary conditions

$$C_{GD} = C_{GDi}; \ \ C_{GE} = C_{GEi}; \ \text{and} \ C_{GO} = C_{GOi} \ \text{at} \ \ h=0$$

(6.13)

Functions $f(S_O)$ and $f(C_{LO})$ appearing in equations (6.1) through (6.3) and (6.6)

through (6.8), respectively, express the dependence of the biomass specific growth rate on

the oxygen concentration in the environment considered and are given by,

$$f(S_O) = \frac{S_O}{K_O + S_O} \text{ and } f(C_{LO}) = \frac{C_{LO}}{K_O + C_{LO}} \tag{6.14}$$

Functions $\mu_j(S_j, S_q)$ appearing in equations (6.1) through (6.3) express the specific growth rate of biomass on substrate (pollutant) j, j = D, E. When two substrates are involved, the specific growth rate of biomass on substrate j may depend not only on the availability of substrate j but the availability of substrate q (j ≠ q) as well; this happens when the two substrates are involved in kinetic interactions.

Equations (6.1)-(6.13) have been written for the case where the liquid and air are in co-current flow. For counter-current flow operation, equations (6.10)-(6.12) have to be modified by multiplying their right hand side by minus one (-1) and equations (6.13) are valid at h = H rather than h = 0.

The equations above have been written with the model mixture in mind, i.e., subscripts E and D imply ethanol and o-DCB, respectively. However, it is clear that the same equations can be used for any mixture of two VOCs provided that one has a stable microbial consortium that simultaneously utilizes both pollutants. As is being discussed later in Chapter 7, kinetic experiments with suspended cultures have revealed that the biomass consortium used in the present study degrades both ethanol and o-DCB following an Andrews' expression for the specific growth rate, when biomass is presented with each compound individually. Furthermore, experiments with mixtures have led to the conclusion that kinetic interactions can be neglected. Hence, for the system considered in this study,

$$\mu_j(S_j, S_q) = \frac{\mu_j^* S_j}{K_j + S_j + \dfrac{S_j^2}{K_{Ij}}}, j = D, E \tag{6.15}$$

Similarly, $\mu_j(C_{Lj}, C_{Lq})$, $j \neq q$, $j = D$, E are given by equation (6.15) provided that C_{Lj} is substituted for S_j.

Boundary conditions (6.9) express that the liquid is recirculated through the column and the assumption that no reaction occurs in the pipe carrying the liquid from the bottom to the top of the column. Boundary conditions (6.5) reflect the assumption, also used in earlier studies (Mpanias and Baltzis, 1998; Baltzis et al., 2001; Shareefdeen and Baltzis, 1994), that an effective biofilm thickness (δ) exists in the biolayer. The value of δ may vary along the biofilter column and is numerically determined as the position where S_E, S_D, or S_O becomes essentially equal to zero. Quantitatively, the term "essentially" implies here that S_O or S_E and S_D, becomes equal to 0.0001 gm^{-3}.

Equations (6.6)-(6.8), involve VOC biodegradation terms under the assumptions that there is neither axial dispersion nor radial gradients in the liquid film. The thickness of the liquid film (δ_L) can be determined from the liquid holdup of the column and the wetted area, which are both functions of the liquid flow rate. The biomass concentration (X_{VL}) in the liquid phase has been assumed to be constant throughout the length of the reactor due to recirculation and was determined experimentally. When either X_{VL} or δ_L is very low, reaction in the liquid phase is negligible and the model reduces to that of Baltzis et al. (2001).

By introducing the following dimensionless quantities,

$$\overline{S}_D = \frac{S_D}{K_D}, \quad \overline{S}_E = \frac{S_E}{K_E}, \quad \overline{S}_O = \frac{S_O}{K_O}, \quad \lambda_E = \frac{D_{EW} Y_E K_E}{D_{OW} Y_{OE} K_O},$$

$$\lambda_D = \frac{D_{DW} Y_D K_D}{D_{OW} Y_{OD} K_O}, \quad \phi_E{}^2 = \frac{X_V \delta^2 \mu_E^*}{f(X_V) Y_E D_{EW} K_E}, \quad \phi_D{}^2 = \frac{X_V \delta^2 \mu_D^*}{f(X_V) Y_D D_{DW} K_D},$$

$$\theta = \frac{x}{\delta}, \ \gamma_D = \frac{K_D}{K_{ID}}, \ \gamma_E = \frac{K_E}{K_{IE}}, \ z = \frac{h}{H},$$

$$\overline{C}_{LD} = \frac{m_D C_{LD}}{C_{GDi}}, \ \overline{C}_{LE} = \frac{m_E C_{LE}}{C_{GEi}}, \ \overline{C}_{LO} = \frac{m_O C_{LO}}{C_{GOi}}, \ \overline{C}_{GD} = \frac{C_{GD}}{C_{GDi}}, \ \overline{C}_{GE} = \frac{C_{GE}}{C_{GEi}},$$

$$\overline{C}_{GO} = \frac{C_{GO}}{C_{GOi}}, \ \alpha_E = \frac{C_{GEi}}{m_E K_E}, \ \alpha_D = \frac{C_{GDi}}{m_D K_D}, \ \alpha_O = \frac{C_{GOi}}{m_O K_O},$$

$$\sigma = \frac{f(X_v) D_{DW} A_S K_D m_D H}{u_L \delta C_{GDi}}, \ \chi_1 = \frac{C_{GDi} D_{EW} K_E m_E}{C_{GEi} D_{DW} K_D m_D};$$

$$\chi_2 = \frac{C_{GDi} D_{OW} K_O m_O}{C_{GOi} D_{DW} K_D m_D}; \ \psi = \frac{K_{LD} H}{u_L}, \ \beta_E = \frac{K_{LE}}{K_{LD}},$$

$$\beta_O = \frac{K_{LO}}{K_{LD}}, \ \rho = \frac{K_{LD} H}{u_G m_D}, \ \vartheta_E = \frac{m_D K_{LE}}{m_E K_{LD}}, \ \vartheta_O = \frac{m_D K_{LO}}{m_O K_{LD}},$$

$$\eta_{LD} = \frac{\mu_D^* m_D A_S X_{VL} H \delta_L}{Y_D C_{GDi} u_L}, \ \eta_{LE} = \frac{\mu_E^* m_E A_S X_{VL} H \delta_L}{Y_E C_{GEi} u_L}$$

$$\omega_D = \frac{C_{GDi} Y_D m_O}{C_{GOi} Y_{OD} m_D}, \ \omega_E = \frac{C_{GEi} Y_E m_O}{C_{GOi} Y_{OE} m_E}$$

equations (6.1) to (6.13), when expressions (6.14) and (6.15) are also used, can be written as

$$\frac{d^2 \overline{S}_D}{d\theta^2} = \phi_D^{\ 2} \frac{\overline{S}_D \overline{S}_O}{(1 + \overline{S}_D + \gamma_D \overline{S}_D^2)(1 + \overline{S}_O)} \tag{6.16}$$

$$\frac{d^2 \overline{S}_E}{d\theta^2} = \phi_E^{\ 2} \frac{\overline{S}_E \overline{S}_O}{(1 + \overline{S}_E + \gamma_E \overline{S}_E^2)(1 + \overline{S}_O)} \tag{6.17}$$

$$\frac{d^2 \overline{S}_O}{d\theta^2} = \lambda_D \phi_D^{\ 2} \frac{\overline{S}_D \overline{S}_O}{(1 + \overline{S}_D + \gamma_D \overline{S}_D^2)(1 + \overline{S}_O)} + \lambda_E \phi_E^{\ 2} \frac{\overline{S}_E \overline{S}_O}{(1 + \overline{S}_E + \gamma_E \overline{S}_E^2)(1 + \overline{S}_O)} \tag{6.18}$$

$$\overline{S}_E = \alpha_E \overline{C}_{LE}; \ \overline{S}_D = \alpha_D \overline{C}_{LD}; \ \text{and} \ \overline{S}_O = \alpha_O \overline{C}_{LO} \ \text{at} \ \theta = 0 \tag{6.19}$$

$$\frac{d\overline{S}_E}{d\theta} = \frac{d\overline{S}_D}{d\theta} = \frac{d\overline{S}_O}{d\theta} = 0 \quad at \quad \theta = 1 \tag{6.20}$$

$$\frac{d\overline{C}_{LD}}{dz} = \psi\left(\overline{C}_{GD} - \overline{C}_{LD}\right) + \sigma\left[\frac{d\overline{S}_D}{d\theta}\right]_{\theta=0}$$
$$- \eta_{LD}\frac{\alpha_D\alpha_O\overline{C}_{LD}\overline{C}_{LO}}{(1 + \alpha_D\overline{C}_{LD} + \gamma_D\alpha_D^2\overline{C}_{LD}^2)(1 + \alpha_O\overline{C}_{LO})} \tag{6.21}$$

$$\frac{d\overline{C}_{LE}}{dz} = \psi\beta_E\left(\overline{C}_{GE} - \overline{C}_{LE}\right) + \sigma\chi_1\left[\frac{d\overline{S}_E}{d\theta}\right]_{\theta=0}$$
$$- \eta_{LE}\frac{\alpha_E\alpha_O\overline{C}_{LE}\overline{C}_{LO}}{(1 + \alpha_E\overline{C}_{LE} + \gamma_E\alpha_E^2\overline{C}_{LE}^2)(1 + \alpha_O\overline{C}_{LO})} \tag{6.22}$$

$$\frac{d\overline{C}_{LO}}{dz} = \psi\beta_O\left(\overline{C}_{GO} - \overline{C}_{LO}\right) + \sigma\chi_2\left[\frac{d\overline{S}_O}{d\theta}\right]_{\theta=0}$$
$$- \eta_{LD}\omega_D\frac{\alpha_D\alpha_O\overline{C}_{LD}\overline{C}_{LO}}{(1 + \alpha_D\overline{C}_{LD} + \gamma_D\alpha_D^2\overline{C}_{LD}^2)(1 + \alpha_O\overline{C}_{LO})}$$
$$- \eta_{LE}\omega_E\frac{\alpha_E\alpha_O\overline{C}_{LE}\overline{C}_{LO}}{(1 + \alpha_E\overline{C}_{LE} + \gamma_E\alpha_E^2\overline{C}_{LE}^2)(1 + \alpha_O\overline{C}_{LO})} \tag{6.23}$$

$$\overline{C}_{LD}(z=0) = \overline{C}_{LD}(z=1)$$
$$\overline{C}_{LE}(z=0) = \overline{C}_{LE}(z=1) \tag{6.24}$$
$$\overline{C}_{LO}(z=0) = \overline{C}_{LO}(z=1)$$

$$\frac{d\overline{C}_{GD}}{dz} = \rho(\overline{C}_{LD} - \overline{C}_{GD}) \tag{6.25}$$

$$\frac{d\overline{C}_{GE}}{dz} = \rho\vartheta_E(\overline{C}_{LE} - \overline{C}_{GE}) \tag{6.26}$$

$$\frac{d\overline{C}_{GO}}{dz} = \rho\vartheta_O(\overline{C}_{LO} - \overline{C}_{GO}) \tag{6.27}$$

$$\overline{C}_{GD} = \overline{C}_{GE} = \overline{C}_{GO} = 1 \text{ at } z = 0 \tag{6.28}$$

Solution of equations (6.16)-(6.28) would involve using an exhaustive trial and error method. An initial guess would be required for the VOC and oxygen concentrations in the liquid phase at $z = 0$. Equations (6.16)-(6.18) would have to be solved with an assumed value of δ and the value of δ would have to be adjusted until boundary conditions (6.20) were met. Once the right value of δ was determined, concentration slopes at $\theta = 0$ would have to be calculated and VOC and oxygen concentrations in the liquid and airstream at a position Δz away from z would be determined. The procedure would be repeated till $z = 1$ and if the liquid phase concentrations at $z = 1$ did not match those at $z = 0$ in accordance with condition (6.24), the procedure would have to be repeated with a new initial guess for the liquid phase concentrations at $z = 0$. This approach has in fact been used in the past by Mpanias and Baltzis (1998) and Baltzis et al. (2001), who, however, did not account for reaction in the liquid phase. As an alternative, leading to considerable simplification, a new approach is proposed in the next section.

6.2 Model Simplification

In order to simplify the model, the concept of effectiveness factor was introduced. While describing the transient biofiltration of a single substrate in a conventional biofilter, Shareefdeen and Baltzis (1994) had used a similar approach. They had been able to express the effectiveness factor as a linear function of the gas phase VOC concentration. Along the same lines, the effectiveness factor is defined here as

$$\varepsilon_j = \frac{\text{amount of reactant consumed after being transferred into the biofilm via diffusion}}{\text{amount of reactant consumed under no diffusion limitation}}$$

Using the definition above, effectiveness factors with respect to each compound can be defined as follows,

$$\varepsilon_D = \frac{-f(X_V)D_{DW}\left(\dfrac{dS_D}{dx}\right)_{x=0}}{\delta\dfrac{X_V}{Y_D}[\mu_D(S_E,S_D)f(S_O)]_{x=0}} \tag{6.29}$$

$$\varepsilon_E = \frac{-f(X_V)D_{EW}\left(\dfrac{dS_E}{dx}\right)_{x=0}}{\delta\dfrac{X_V}{Y_E}[\mu_E(S_E,S_D)f(S_O)]_{x=0}} \tag{6.30}$$

$$\varepsilon_O = \frac{-f(X_V)D_{OW}\left(\dfrac{dS_O}{dx}\right)_{x=0}}{\delta\left[\dfrac{X_V}{Y_{OE}}\mu_E(S_E,S_D)f(S_O)+\dfrac{X_V}{Y_{OD}}\mu_D(S_D,S_E)f(S_O)\right]_{x=0}} \tag{6.31}$$

Lobo et al. (1999) used a similar method for analysis of a trickle-bed bioreactor for carbon disulfide removal. A gas-liquid mass transfer effectiveness factor and a diffusion-bioreaction effectiveness factor term were lumped to obtain a global effectiveness factor term for all local processes occurring in the bioreactor differential volume. A biocatalytical effectiveness factor was also used by Hekmat and Vortemeyer (1994) to model reaction in the biofilm. Another analysis of effectiveness factor in the biofilm of a toluene-degrading conventional biofilter was presented by Hwang and Tang (1997) in order to determine the rate limiting factor of the toluene biofiltration process.

Using the boundary condition (6.4) at $x = 0$, S_E, S_D, and S_O can be replaced by C_{LE}, C_{LD} and C_{LO} respectively. Substituting equations (6.29), (6.30) and (6.31) in equations (6.6), (6.7) and (6.8) we get,

$$u_L \frac{dC_{LD}}{dh} = K_{LD}\left(\frac{C_{GD}}{m_D} - C_{LD}\right) - \varepsilon_D \delta \frac{X_v A_s}{Y_D} \mu_D(C_{LE}, C_{LD}) f(C_{LO})$$
$$- \delta_L \frac{X_{VL} A_s}{Y_D} \mu_D(C_{LE}, C_{LD}) f(C_{LO}) \qquad (6.32)$$

$$u_L \frac{dC_{LE}}{dh} = K_{LE}\left(\frac{C_{GE}}{m_E} - C_{LE}\right) - \varepsilon_E \delta \frac{X_v A_s}{Y_E} \mu_E(C_{LE}, C_{LD}) f(C_{LO})$$
$$- \delta_L \frac{X_{VL} A_s}{Y_E} \mu_E(C_{LE}, C_{LD}) f(C_{LO}) \qquad (6.33)$$

$$u_L \frac{dC_{LO}}{dh} = K_{LO}\left(\frac{C_{GO}}{m_O} - C_{LO}\right)$$
$$- \varepsilon_O \delta X_v \left[\frac{A_s}{Y_{OD}} \mu_D(C_{LD}, C_{LE}) f(C_{LO}) + \frac{A_s}{Y_{OE}} \mu_E(C_{LD}, C_{LE}) f(C_{LO})\right] \qquad (6.34)$$
$$- \delta_L X_{VL} \left[\frac{A_s}{Y_{OD}} \mu_D(C_{LD}, C_{LE}) f(C_{LO}) + \frac{A_s}{Y_{OE}} \mu_E(C_{LD}, C_{LE}) f(C_{LO})\right]$$

Multiplying equation (6.1) by $-Y_D/Y_{OD}$ and equation (6.2) by $-Y_E/Y_{OE}$ and then adding the resulting two equations and equation (6.3) one gets,

$$D_{OW} \frac{d^2 S_O}{dx^2} - \frac{Y_D}{Y_{OD}} D_{DW} \frac{d^2 S_D}{dx^2} - \frac{Y_E}{Y_{OE}} D_{EW} \frac{d^2 S_E}{dx^2} = 0 \qquad (6.35)$$

When equation (6.35) is integrated once and boundary condition (6.5) is taken into account, the following equation is found to hold for any value of x,

$$D_{OW} \frac{dS_O}{dx} = \frac{Y_D}{Y_{OD}} D_{DW} \frac{dS_D}{dx} + \frac{Y_E}{Y_{OE}} D_{EW} \frac{dS_E}{dx} \qquad (6.36)$$

Because of relation (6.36) the following relation results, when the definitions of effectiveness factors [equations (6.29) through (6.31)] are considered,

$$\varepsilon_O \delta X_v \left[\frac{1}{Y_{OE}} \mu_E (C_{LE}, C_{LD}) + \frac{1}{Y_{OD}} \mu_D (C_{LD}, C_{LE}) \right] f(C_{LO})$$

$$= \varepsilon_E \delta X_v \frac{1}{Y_{OE}} \mu_E (C_{LE}, C_{LD}) f(C_{LO}) + \varepsilon_D \delta X_v \frac{1}{Y_{OD}} \mu_D (C_{LD}, C_{LE}) f(C_{LO})$$

(6.37)

Due to relation (6.37), equation (6.34) can be written in the following form,

$$u_L \frac{dC_{LO}}{dh} = K_{LO} \left(\frac{C_{GO}}{m_O} - C_{LO} \right)$$

$$- \varepsilon_D \delta X_v \frac{A_S}{Y_{OD}} \mu_D (C_{LD}, C_{LE}) f(C_{LO}) - \varepsilon_E \delta X_v \frac{A_S}{Y_{OE}} \mu_E (C_{LD}, C_{LE}) f(C_{LO})$$

$$- \delta_L X_{VL} \left[\frac{A_S}{Y_{OD}} \mu_D (C_{LD}, C_{LE}) f(C_{LO}) + \frac{A_S}{Y_{OE}} \mu_E (C_{LD}, C_{LE}) f(C_{LO}) \right]$$

(6.38)

It should be mentioned that in the presence of only one VOC j (j = D, E), equation (6.37)

implies that $\varepsilon_O = \varepsilon_j$.

Equations (6.32), (6.33), and (6.38) can be written in dimensionless form as

$$\frac{d\overline{C}_{LD}}{dz} = \psi \left(\overline{C}_{GD} - \overline{C}_{LD} \right)$$

$$- (\eta_D + \eta_{LD}) \frac{\alpha_D \alpha_O \overline{C}_{LD} \overline{C}_{LO}}{(1 + \alpha_D \overline{C}_{LD} + \gamma_D \alpha_D^2 \overline{C}_{LD}^2)(1 + \alpha_O \overline{C}_{LO})}$$

(6.39)

$$\frac{d\overline{C}_{LE}}{dz} = \psi \left(\overline{C}_{GE} - \overline{C}_{LE} \right)$$

$$- (\eta_E + \eta_{LE}) \frac{\alpha_E \alpha_O \overline{C}_{LE} \overline{C}_{LO}}{(1 + \alpha_E \overline{C}_{LE} + \gamma_E \alpha_E^2 \overline{C}_{LE}^2)(1 + \alpha_O \overline{C}_{LO})}$$

(6.40)

$$\frac{d\overline{C}_{LO}}{dz} = \psi \beta_O \left(\overline{C}_{GO} - \overline{C}_{LO} \right)$$

$$- (\eta_D + \eta_{LD}) \omega_D \frac{\alpha_D \alpha_O \overline{C}_{LD} \overline{C}_{LO}}{(1 + \alpha_D \overline{C}_{LD} + \gamma_D \alpha_D^2 \overline{C}_{LD}^2)(1 + \alpha_O \overline{C}_{LO})}$$

$$- (\eta_E + \eta_{LE}) \omega_E \frac{\alpha_E \alpha_O \overline{C}_{LE} \overline{C}_{LO}}{(1 + \alpha_E \overline{C}_{LE} + \gamma_E \alpha_E^2 \overline{C}_{LE}^2)(1 + \alpha_O \overline{C}_{LO})}$$

(6.41)

where,

$$\eta_D = \frac{\mu_D^* m_D A_S X_V H}{Y_D C_{GDi} u_L} \varepsilon_D \delta, \quad \eta_E = \frac{\mu_E^* m_E A_S X_V H}{Y_E C_{GEi} u_L} \varepsilon_E \delta$$

and all other quantities as defined earlier. The boundary conditions for equations (6.39) through (6.41) are given by relations (6.24).

With the approach presented in this section, BTF performance can be described and predicted by solving equations (6.25) through (6.27) and (6.39) through (6.41) along with the corresponding boundary conditions, provided that effectiveness factors are known as functions of the VOCs and oxygen concentrations in the liquid phase. Effectiveness factors can be calculated by independently solving equations (6.16) through (6.18) along with the corresponding boundary conditions for various values of liquid phase concentrations (C_{LE}, C_{LD}, and C_{LO}). In other words, the approach presented here requires solving two separate problems, each in one direction only, rather than solving one problem in two directions simultaneously. This decoupling of the original model equations changes the original PDE problem into two ODE problems.

6.3 Numerical Methods

The two decoupled ODE problems were solved numerically as follows. The 2nd-order ODE problem described by equations (6.16) through (6.18) along with boundary conditions (6.19) and (6.20) was solved by using the method of orthogonal collocation (Finlayson, 1980; Villadsen and Stewart, 1967). The method used 10 points in the θ-direction (biofilm thickness). The functions for determining the collocation matrices were obtained by modifying those proposed by Lin et al. (1999) for the problem of diffusion and reaction in a

catalyst pellet. These functions as well as the main program that solves the resulting set of equations were written in MATLAB®. Since the value of δ is not known, the numerical methodology employs successive iterations (trial and error). A value of δ is assumed and based on it the values of ϕ_D and ϕ_E are determined. The equations are then solved and the values of $\bar{S}_D$, $\bar{S}_E$ and $\bar{S}_O$ at $\theta = 1$ are checked. If the value of oxygen or the VOCs in dimensional terms is 0.0001 gm^{-3} (i.e. practically zero) at $\theta = 1$, the assumed value of δ is accepted as the correct one, otherwise a new value of δ is assumed and the approach is repeated. The code for solving this problem is given in Appendix A of this dissertation. Solution of the equations (6.16) through (6.18) along with their corresponding boundary conditions led to the determination of quantities $\varepsilon_D\delta$ and $\varepsilon_E\delta$ as functions of C_{LD}, C_{LO} and C_{LE}. These quantities are needed for solving the second problem (z- direction).

The VOC and oxygen concentrations in the air and liquid along the BTF length were obtained solving equations (6.25) through (6.27) and (6.39) through (6.41) subject to the boundary conditions (6.28) and (6.24), respectively. These equations were solved simultaneously via a 4th-order Runge-Kutta algorithm. The code for solving the ODE problem in the z-direction is given in Appendix B of this dissertation and works as follows. The liquid phase concentration values of the two VOCs and oxygen at z = 0 are assumed and the code runs at Δz increments of size 1/500 till z = 1 is reached. At each z-position, the required values of $\varepsilon_D\delta$ and $\varepsilon_E\delta$ are read using a look-up function (inbuilt in MATLAB®) based on interpolation between nearest neighbors in three-dimensional matrices. The entries of these matrices were obtained by solving equations (6.16) through (6.20), as discussed earlier. If the computed liquid phase VOC and oxygen concentrations at z = 1 match the assumed values at z = 0, then conditions (6.24) are satisfied and the

program stops. If the VOC and oxygen concentrations in the liquid phase at $z = 0$ and $z = 1$ do not satisfy conditions (6.24), new values are assumed for the liquid phase concentrations at $z = 0$ and the procedure is repeated.

The code given in Appendix B works both for the case when reaction is assumed to occur in the liquid phase ($\eta_{Lj} \neq 0$, j = D, E) and the case where reaction is assumed not to occur in the liquid phase ($\eta_{LD} = \eta_{LE} = 0$).

Most studies on biofilter modeling have used computer codes developed specifically for each study. MATLAB®-based codes used in the present study is a recent development in the biofiltration area (Amanullah et al., 2000).

CHAPTER 7

VALIDATION OF THE MATHEMATICAL MODEL

The mathematical model developed and presented in Chapter 6 was tested for its ability to describe and predict the experimental results shown in Chapter 5. Results of model validation studies are presented in this chapter.

To test the model, a number of parameters had to be either experimentally determined or taken from the literature. Hence, the following first part of the present chapter presents the work done on parameter estimation.

7.1 Model Parameter Estimation

7.1.1 Henry's constants

The value of Henry's constant for o-DCB was taken from Mpanias (1998) as $m_D = 0.119$. Henry's constant for ethanol, m_E, was experimentally determined by injecting various volumes of liquid ethanol, V_{SE}, in closed serum bottles carrying a known volume of nutrient medium (without biomass) and monitoring the ethanol concentration in the headspace of the bottles. When the headspace ethanol concentration stayed unchanged, C_{LEe}, the liquid phase ethanol concentration was computed via the formula,

$$C_{LEe} = \frac{V_{SE}\rho_{SE} - V_G C_{GEe}}{V_L} \tag{7.1}$$

Values of C_{GEe} were plotted versus the corresponding values of C_{LEe} as shown in Figure 7.1, and the data regressed to a straight line forced through the (0,0) - point, i.e., through the origin. As can be seen from figure 7.1, there was excellent agreement between the data

and the fitted line. The slope of the line was 0.00028 and this was taken as the value of m_E.

The m_E - value found here agrees very nicely with the 0.0003 value reported by Yaws et al. (1997) and Sander (1999).
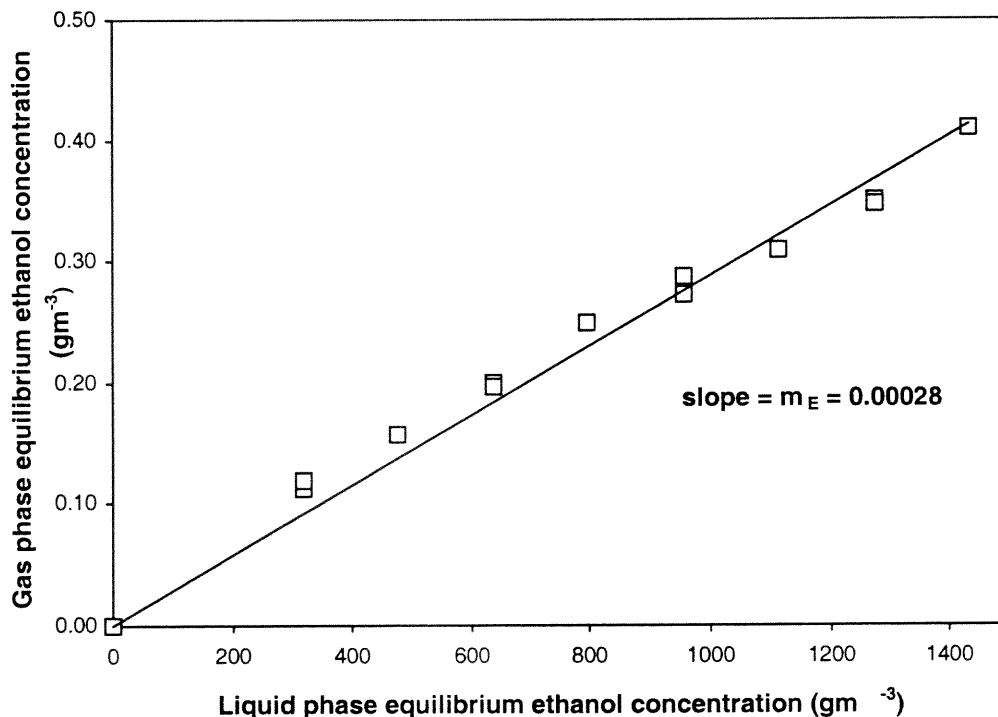
Figure 7.1 Equilibrium ethanol concentrations in the air and the liquid medium. Experimental values (symbols) were regressed to a straight line.

It is interesting to observe that there is a three-order of magnitude difference between the m_E and m_D values indicating that ethanol is a much more water soluble substrate when compared to o-DCB.

7.1.2 Kinetic Parameters

Determination of kinetic parameters required undertaking an independent study on biodegradation with suspended cultures. The experimental methods for this study have been described in Chapter 4. As discussed in Chapter 4, experiments were performed with two cultures that originated from the biomass in BTF-I and BTF-II. In the remaining, the cultures will be referred to as culture BTF-I and culture BTF-II, in correspondence to their origin.

7.1.2.1 Yield Coefficients.   Yield coefficients of cultures BTF-I and BTF-II on o-DCB, as well as of culture BTF-II on ethanol were determined as follows. For each kinetic run enough time was allowed for the entire amount of the solvent (o-DCB or ethanol) to be consumed. This amount was $\rho_{Sj} V_{Sj}$, $j = D, E$, where ρ_{Sj} is the density of the solvent and V_{Sj} is the volume of the liquid solvent injected into the serum bottle. Biomass concentration was measured in the beginning and end of each run, b_0 and b_f, respectively. The yield coefficient was determined via the formula,

$$Y_j = \frac{(b_f - b_0)V_L}{\rho_{Sj} V_{Sj}} \tag{7.2}$$

where V_L is the volume of the liquid suspension in the serum bottle.

Results from experiments with culture BTF-I and o-DCB showed that Y_D was 0.398 gg^{-1}, which is also the value reported by Mpanias (1998).

The yield coefficients of culture BTF-II on o-DCB and ethanol were found to be 0.258 and 0.444 gg^{-1}, respectively. As shown in Figure 7.2 there was insignificant variation

of the values of Y_D and Y_E among experimental runs. This implies that loss of biomass due to either death or maintenance requirements can be safely neglected.
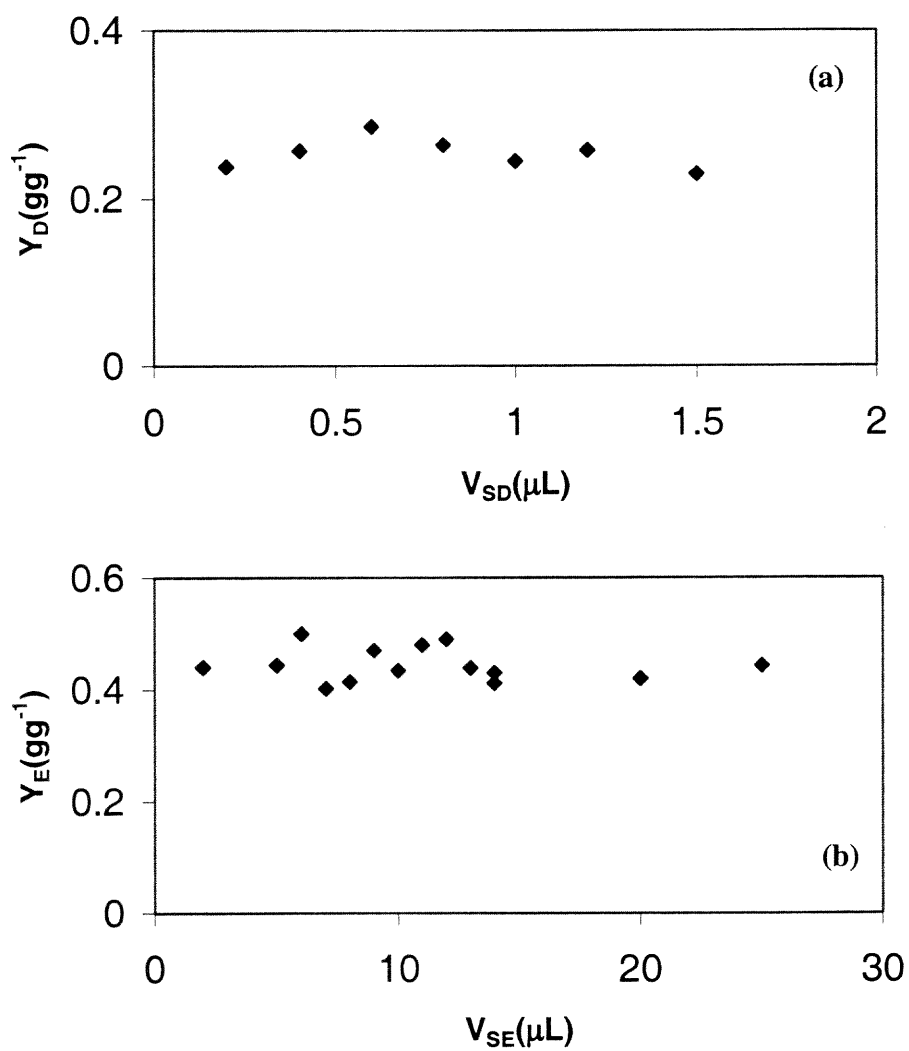
Figure 7.2 Yield coefficients of culture BTF-II on o-DCB (a) and ethanol (b) as functions of the amount of solvent used in experimental runs.

7.1.2.2 Biomass Specific Growth Rate on Single Substrates. Three series of experiments were performed in serum bottles in order to determine the specific growth rate expressions for cases in which biomass is presented with either o-DCB or ethanol as sole carbon and energy source. In the first series, culture BTF-I was grown on o-DCB, in the second series culture BTF-II was grown on o-DCB, and in the third series culture BTF-II was grown on ethanol. In all cases the culture was assumed to be in the exponential growth phase [thus, the specific growth rate was constant] and the rate-limiting substrate (o-DCB or ethanol) distributed between the liquid suspension and the headspace of the bottle according to equilibrium, i.e.,

$$C_{Gj} = m_j C_{Lj}, j = D, E \tag{7.3}$$

The specific growth rate corresponding to the substrate (o-DCB or ethanol) concentration at the beginning of each experimental run was determined via the well-known equation,

$$\ln \frac{b}{b_0} = \mu_j(C_{Lj})t \tag{7.4}$$

as the slope of the ln b/b_0 versus t line. This line was obtained by regressing ln b/b_0 versus t values to a straight line using the least squares method for error minimization.

Since biomass concentration values were measured only in the beginning and end of each run, b(t) values were computed using the measured headspace concentration values through the formula (Mpanias, 1998),

$$b(t) = b_0 + \frac{1}{V_L}\left[Y_j V_{Sj} \rho_{Sj} - \frac{Y_j(V_L + m_j V_G)C_{Gj}}{m_j}\right] \tag{7.5}$$

Equation (7.5) is valid only when the substrate is in equilibrium distribution between the liquid and the headspace of the serum bottle. To ensure that this was true,

equation (7.5) was used with C_{Gj} values obtained starting two hours after the bottle had been injected with the carbon source. The C_{Gj} value at t = 2 h was used to determine, via equation (7.3), the C_{Lj} value to which the specific growth rate was attributed.

Figure 7.3 shows two examples of ln b/b_o versus t plots. It is clear that the data, as in all cases, fell nicely on a straight line.

Values of $\mu_j(C_{Lj})$ obtained were plotted versus the corresponding C_{Lj} (j = D, E) values as shown in Figures 7.4 through 7.6. As can be seen from all three graphs, the data showed that $\mu_j(C_{Lj})$ initially increases with C_{Lj} and, after reaching a maximum, decreases at high C_{Lj} values. This trend is indicative of Andrews kinetics, implying that $\mu_j(C_{Lj})$ can be expressed as,

$$\mu_j(C_{Lj}) = \frac{\mu_j^* C_{Lj}}{K_j + C_{Lj} + \frac{C_{Lj}^2}{K_{Ij}}} \tag{7.6}$$

Since Mpanias (1998) had worked with BTF-I and o-DCB and had determined kinetic values, his values (reported in Table 7.1) were used in generating the Andrews curve shown in Figure 7.4. As can be seen from the figure, the data obtained here agree very nicely with the model prediction. This implies that culture BTF-I was a stable one and had undergone no apparent change in the 5-year period that spans the present study and that of Mpanias (1998).
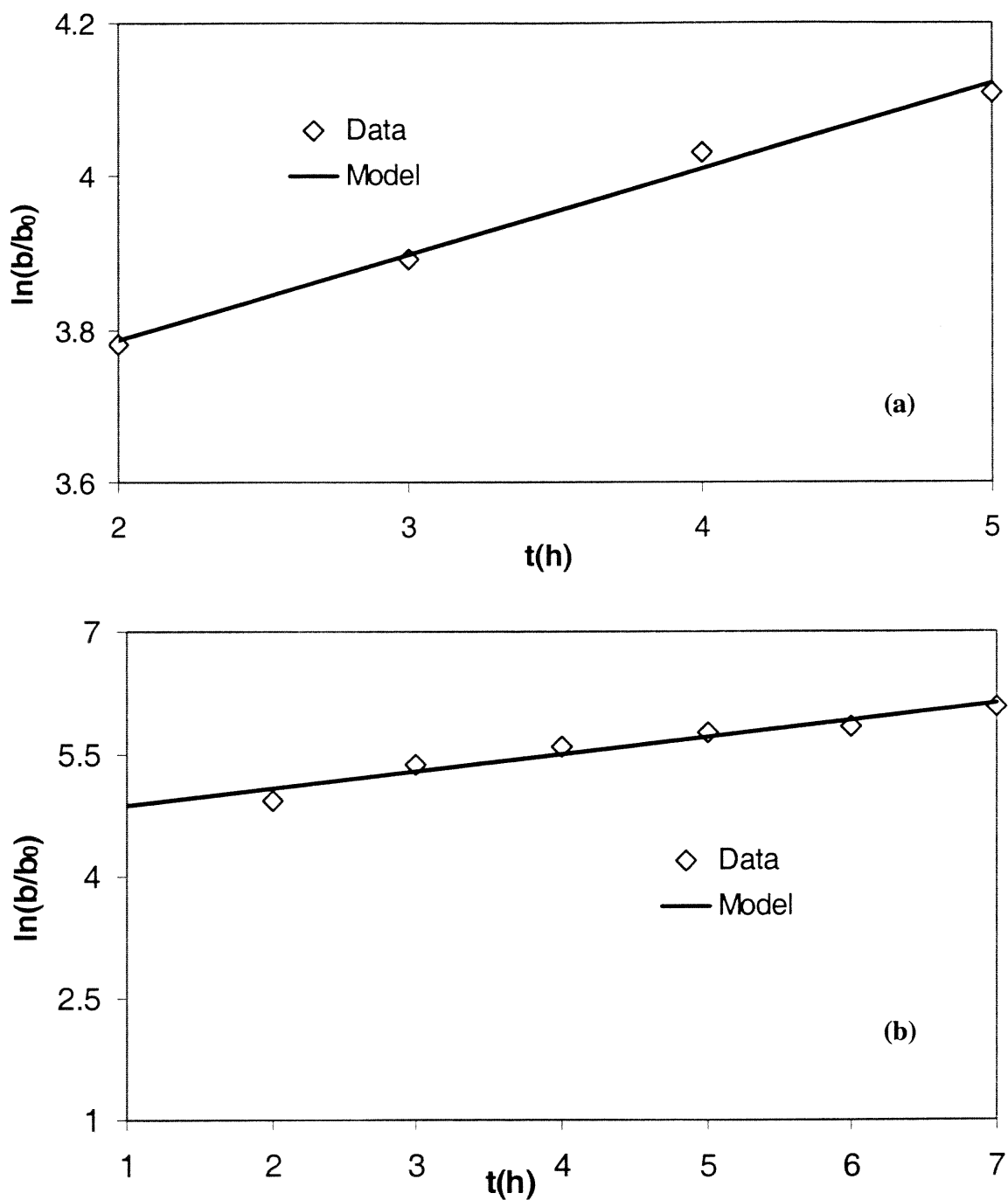
Figure 7.3 Semilogarithmic plots of biomass concentration versus time for specific growth rate determination. Culture, substrate, and initial biomass concentration are (a) BTF-I, o-DCB and 27.5 gm^{-3}, and (b) BTF-II, ethanol and 66.5 gm^{-3}.
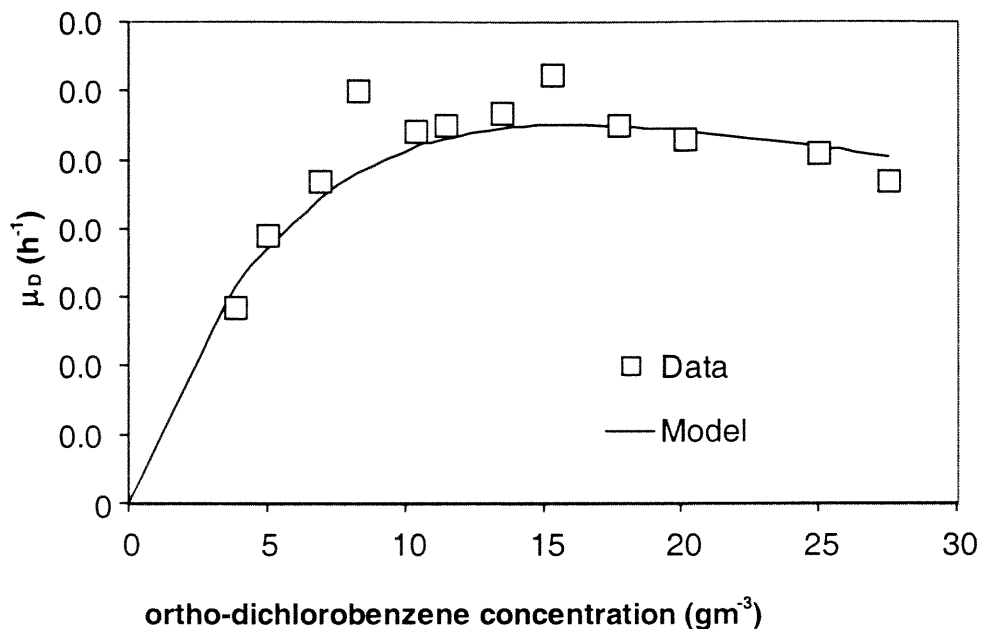
Figure 7.4 Specific growth rate of culture BTF-I as a function of ortho-dichlorobenzene concentration in the liquid medium. Data (symbols) are compared to the predictions (curve) of the model of Mpanias (1998).
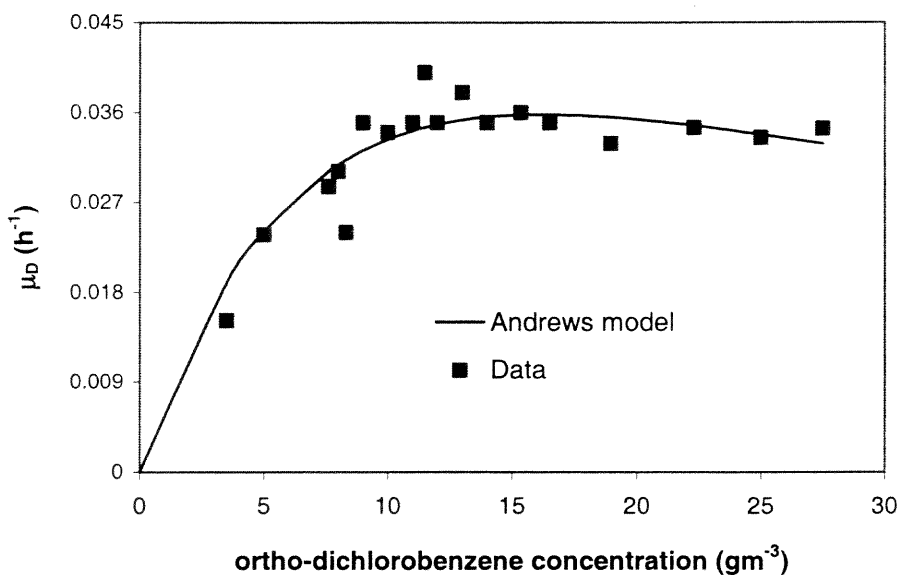
Figure 7.5 Specific growth rate of culture BTF-II as a function of o-DCB concentration in the liquid medium. Data (symbols) have been fitted to the Andrews model (curve).
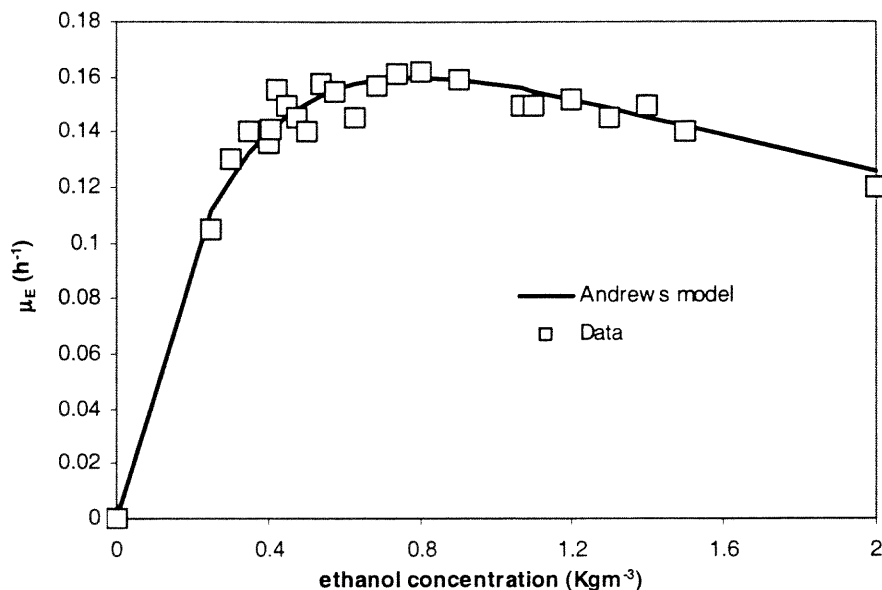
Figure 7.6 Specific growth rate of culture BTF-II as a function of ethanol concentration in the liquid medium. Data (symbols) have been fitted to the Andrews model (curve).

The data obtained with culture BTF-II were regressed to the Andrews model using the Levenberg-Marquardt subroutine in MATLAB®. The values obtained from the regressions are given in Table 7.1 for o-DCB and Table 7.2 for ethanol. Using these values the Andrews curves were generated and plotted in Figures 7.5 and 7.6. These figures show a very good agreement between data and the fitted curves.

Having the kinetic parameters, o-DCB and ethanol concentrations in the headspace of serum bottles were generated by solving the following two equations (Mpanias, 1998),

$$\frac{db}{dt} = \mu_j(C_{Lj})b \tag{7.7}$$

$$\frac{dC_{Gj}}{dt} = -\frac{m_j V_L}{V_L + m_j V_G} \frac{1}{Y_j} \mu_j(C_{Lj})b \tag{7.8}$$

and also using equation (7.3).

Table 7.1 Growth characteristics and parameters of cultures BTF-I and BTF-II on o-DCB

	Ortho-Dichlorobenzene (Andrews Kinetics)	
	Culture BTF-I (Mpanias, 1998)	Culture BTF-II
Kinetic Parameters		
μ_D^* (h^{-1})	0.146	0.095
K_D (gm^{-3})	13.389	13.389
K_{ID} (gm^{-3})	19.657	19.657
Yield Coefficient (gg^{-1})	0.398	0.258

Table 7.2 Growth characteristics and parameters of culture BTF-II on Ethanol

	Ethanol (Andrews Kinetics)
Kinetic Parameters	
μ_E^* (h^{-1})	0.39
K_E (gm^{-3})	570
K_{IE} (gm^{-3})	1100
Yield Coefficient (gg^{-1})	0.444

Equations (7.7) and (7.8) were numerically solved using a fourth-order Runge-Kutta algorithm.

Figure 7.7 shows experimentally determined C_{Gj} values, j = D, E along with model-predicted values. Predictions were obtained by numerically solving equations (7.7) and (7.8) along with equation (7.3) and using the parameter values reported in Tables 7.1 and 7.2. As can be seen from the graphs, there was excellent agreement between data and predictions.
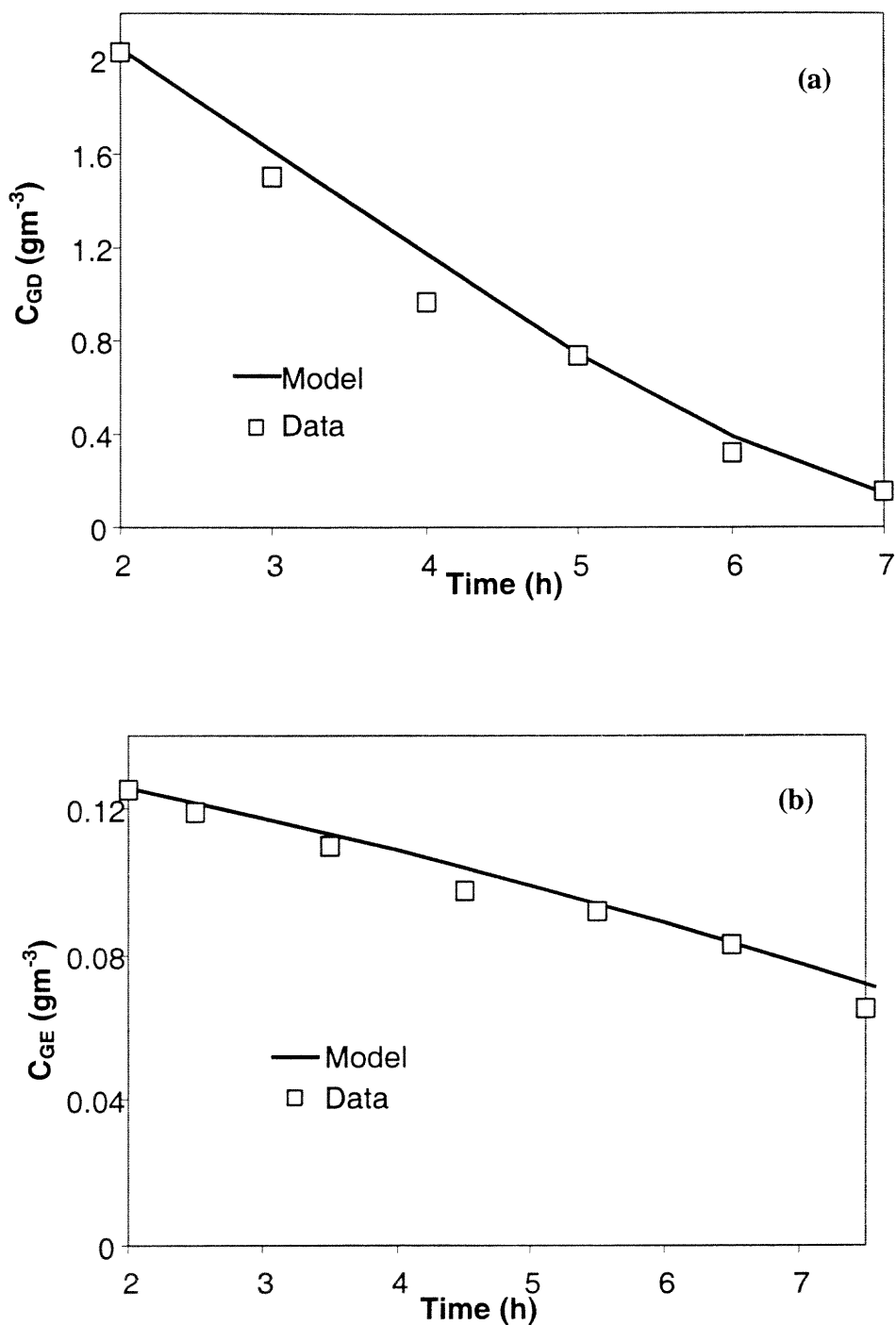
Figure 7.7 Experimental values and model-predicted concentration profiles for (a): o-DCB and (b) ethanol in the headspace of serum bottles. Experiments with stock culture BTF-II with initial biomass and liquid phase solvent concentration values of (a): 24.4 and 17.0 gm^{-3} and (b): 64 and 420 gm^{-3}.

7.1.2.3 Comparison of Growth Kinetics of Stock Culture BTF-II and Culture Obtained from the Biofilter Unit. As mentioned in section 7.1.2.2, the kinetic parameters of culture BTF-I did not change over a 5-year period and thus, the values reported in Table 7.1 for culture BTF-I could be safely used in describing biofilter performance in unit BTF-I, as discussed later in this chapter.

Regarding culture BTF-II the kinetic parameters reported in Tables 7.1 and 7.2 were obtained by using a stock culture prepared as described in Chapter 4. To ensure that these values could be used for describing biofiltration in unit BTF-II, the following things were done.

First, kinetic experiments were periodically performed using biomass taken directly from the liquid stream recirculating through BTF-II. This biomass was used in kinetic runs without going through serial transfers, as opposed to the stock-culture BTF-II preparation. Data were compared to model predictions based on equations (7.3), (7.7) and (7.8) and using the kinetic parameter values reported in Tables 7.1 and 7.2. In all cases, an excellent agreement between data and model predictions was found. Two examples, one for o-DCB and one for ethanol, are shown in Figure 7.8.

Second, the question was asked regarding the differences between the biomass found in the liquid recirculating through BTF-II and the biomass immobilized on the particles at various locations along BTF-II. Variations of biomass along the BTF-II unit could possibly arise due to exposure to two substrates, o-DCB and ethanol. To answer the foregoing questions, kinetic runs were performed with biomass directly obtained from the surface of solid particles found in three different locations along unit BTF-II. The experimental methodology is discussed in Chapter 4.
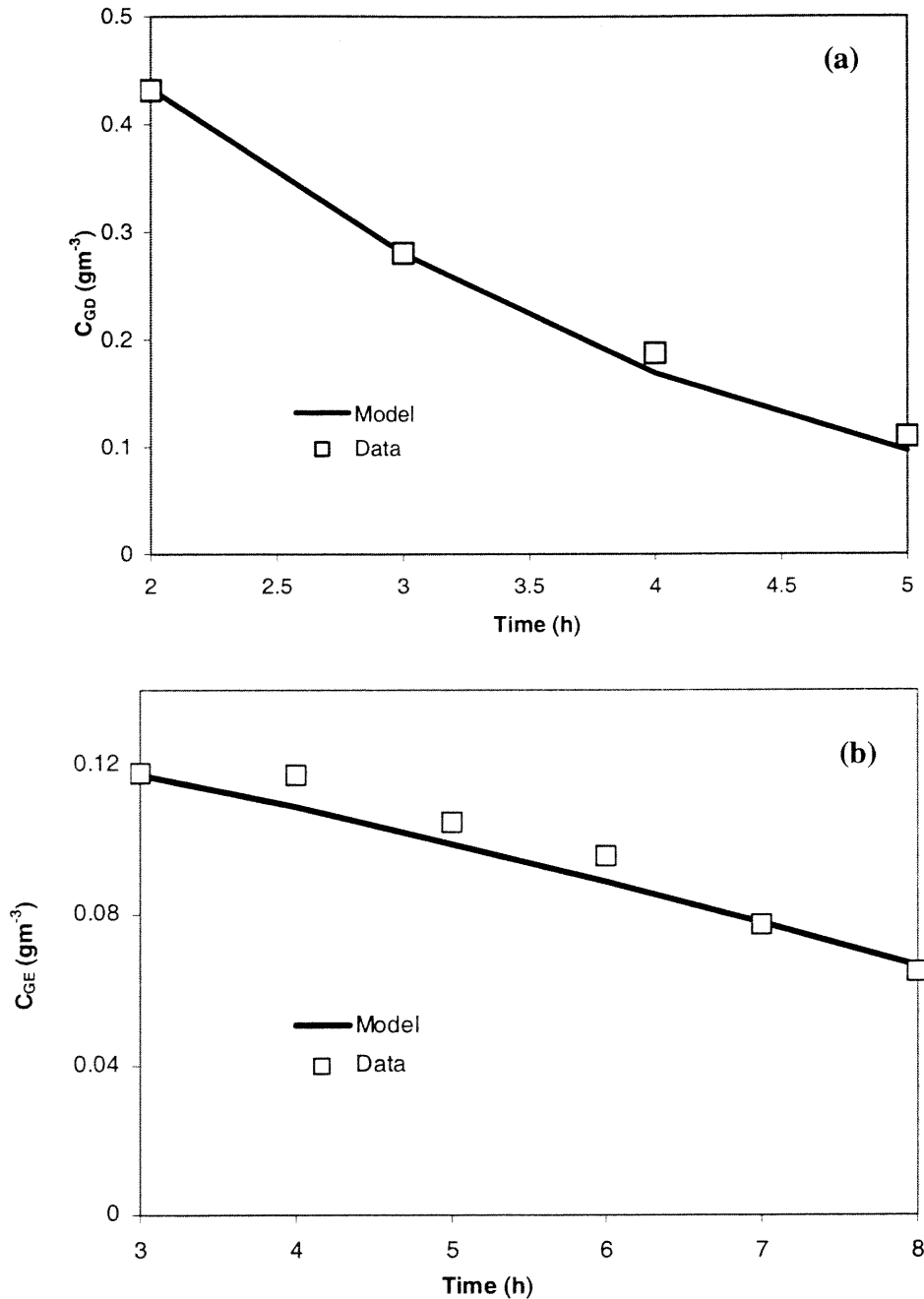
Figure 7.8 Experimental values and model-predicted concentration profiles for (a): o-DCB and (b) ethanol in the headspace of serum bottles. Experiments with culture BTF-II taken from the liquid stream recirculating through the biofilter. Initial biomass and liquid phase solvent concentration values of (a): 21 and 5.4 gm^{-3} and (b): 65 and 400 gm^{-3}.

Figure 7.9 shows results from three experiments on o-DCB removal and three experiments on ethanol removal. The data show that the origin (location) of the biomass

does not alter the concentration profiles, especially in the case of ethanol. Furthermore, comparisons of the data and concentration profiles obtained by integrating equations (7.7) and (7.8) using the kinetic parameters reported in Tables 7.1 and 7.2 indicate that there is very good agreement (especially for ethanol) between the two.
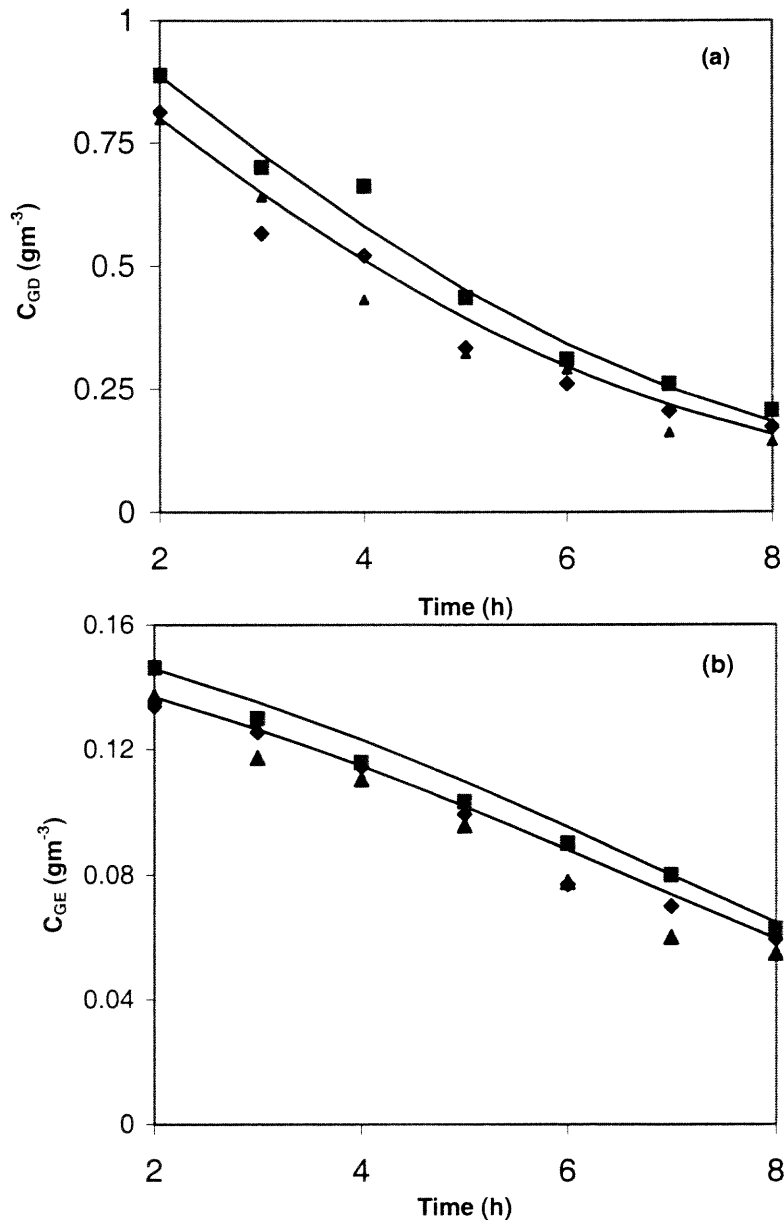
Figure 7.9 Experimental values (symbols) and model-predicted (curves) concentration profiles for (a): o-DCB and (b) ethanol in the headspace of serum bottles using biomass from the top (▲), middle-point (■), bottom (◆) of BTF-II. Initial biomass and liquid phase solvent concentration values are (a) 20 and 6.5–7.5 gm^{-3} and (b) 61.35 and 700-750 gm^{-3}.

The foregoing results led to the conclusion that there is no apparent variation of biomass composition along BTF-II and that for engineering purposes the kinetic parameters obtained from experiments with suspended cultures can be safely used in describing biodegradation rates in the BTF-II unit.

7.1.2.4 Biodegradation Kinetics of o-DCB/Ethanol Mixtures Using Stock-culture BTF-II. Simultaneous degradation of similar (e.g., mono-chlorobenzene and o-DCB, Baltzis et al., 2001) or dissimilar (e.g., phenol and glucose, Wang et al., 1996) substrates by either a stable microbial consortium or a pure culture usually leads to kinetic interactions between the two substrates. Since most of the experiments performed in the present study involved the simultaneous removal of o-DCB and ethanol in BTF-II, the issue of potential kinetic interactions between the two substrates was addressed.

Experiments were performed to investigate the effects of ethanol presence on o-DCB and vice versa. The experimental protocol was different from that discussed in Chapter 4 regarding kinetic studies with single substrates. This is because of the following. Experiments with o-DCB were performed with initial biomass concentrations in the range of 20-25 gm^{-3} to enable monitoring of o-DCB concentrations in the headspace of serum bottles. With such low biomass concentrations and the range of ethanol concentrations used, ethanol concentrations in the headspace varied little to lead to accurate results. Use of smaller ethanol amounts led to inaccurate detection in the headspace due to the high water solubility of ethanol. For these reasons, it was decided to use the usual low biomass values for o-DCB monitoring in the headspace and direct measurement of biomass concentration through the sacrifice of a serum bottle at various instants of time. More specifically, 12 experiments were performed with various combinations of o-DCB and ethanol amounts

used. For each combination, 5 serum bottles were used, all five having the same initial biomass concentration and receiving the same amounts of o-DCB and ethanol. Each one of the bottles involved in a particular combination was sacrificed at a different instant of time so that biomass concentrations could be measured. Gas phase ethanol concentration values were computed based on C_{GD} values, biomass concentration measurements, the amounts of o-DCB and ethanol injected into each serum bottle, and the assumption that yield coefficients are same as those determined from experiments with single compounds using the following relation,

$$b_n = b_o^{'} + \frac{1}{V_L} \sum_{j=1}^{2} \left[Y_j V_{Sj} \rho_{Sj} - \frac{Y_j (V_L + m_j V_G) C_{Gj,n}}{m_j} \right], \; n = 0,\ldots,4 \qquad (7.9)$$

where $b_o^{'}$ is the biomass concentration in the liquid of the serum bottle at the time of injection of the solvents. The C_{Gj} values were converted to C_{Lj} values via equation (7.3).

Values of C_{Lj} in conjunction with biomass concentration values allowed for determination of an average value for the specific (i.e., per unit amount of biomass) removal rate of each VOC, R_j, (j = D, E), using the approach of Wang et al. (1996) and the equation

$$R_j = \frac{(C_{Lj,0} - C_{Lj,n}) \sum_{k=0}^{n} t_k}{(t_n - t_0) \sum_{k=0}^{n} t_k b_k}, \; \text{with } n = 4 \text{ and } j = D, E \qquad (7.10)$$

Results are reported in Table 7.3 and 7.4. Essentially three series of experiments were performed. In each series, the amount of o-DCB used was kept constant and the amount of ethanol used was varied. As can be seen from Table 7.3, the R_D values for a given amount of o-DCB did not vary with the ethanol amount used. It was, thus, concluded

that -at least for the concentration ranges tested and used in BTF experiments - ethanol does not affect the biodegradation kinetics of o-DCB. Table 7.4 analyses the R_E values in a similar manner to examine the effect of o-DCB on ethanol. The same data sets were rearranged in three series so that in each series the amount of ethanol was kept constant and the amount of o-DCB was varied. Since no experiments were performed with ethanol only, under the protocol described here, rates R_E with no o-DCB present were computed from equations (7.7) and (7.8) solved for ethanol parameter values from Table 7.2. From Table 7.4 one can see that especially for high ethanol amounts used, the presence of o-DCB reduces the R_E-values. A cross-inhibition expression of the form,

Table 7.3 Average specific rate of o-DCB removal (R_D) by culture BTF-II in the presence of ethanol

Experiment	V_{SD} (μL)	V_{SE} (μL)	R_D (g o-DCB h^{-1} g^{-1} – biomass)
1	0.5	0	0.00956
2	0.5	2	0.00875
3	0.5	5	0.00892
4	0.5	10	0.00976
5	1.0	0	0.01149
6	1.0	2	0.01077
7	1.0	5	0.01130
8	1.0	10	0.01052
9	1.5	0	0.01532
10	1.5	2	0.01554
11	1.5	5	0.01469
12	1.5	10	0.01444

Table 7.4 Average specific rate of ethanol removal (R_E) by culture BTF-II in the presence of o-DCB

Experiment	V_{SD} (µL)	V_{SE} (µL)	R_E (g o-DCB h^{-1} g^{-1} – biomass)
	0	2	0.107
2	0.5	2	0.081
6	1	2	0.107
10	1.5	2	0.053
	0	5	0.203
3	0.5	5	0.165
7	1	5	0.114
11	1.5	5	0.093
	0	10	0.287
4	0.5	10	0.239
8	1	10	0.165
12	1.5	10	0.126

$$\mu_E(C_{LE}) = \frac{\mu_E^* C_{LE}}{K_E + C_{LE} + \frac{C_{LE}^2}{K_{IE}} + K_{ED}C_{LE}C_{LD}} \qquad (7.11)$$

was used. Equation (7.8) was written twice, once for o-DCB with $\mu_D(C_{LD})$ as per expression (7.6) and once for ethanol with $\mu_E(C_{LE})$ as per expression (7.11). These two equations were simultaneously solved along with

$$\frac{db}{dt} = [\mu_D(C_{LD}) + \mu_E(C_{LE})]b \qquad (7.12)$$

under various assumed values for K_{ED}. The results led to predictions for C_{GD}, C_{GE}, and b

profiles versus time. The predicted profiles were compared to experimental C_{GD} and b

values as well as computed C_{GE} values from (7.9). A value of $K_{ED} = 0.5$ was found to

minimize the error between data and model predictions. Results are shown in Figure 7.10

where a nice agreement is found in both cases.
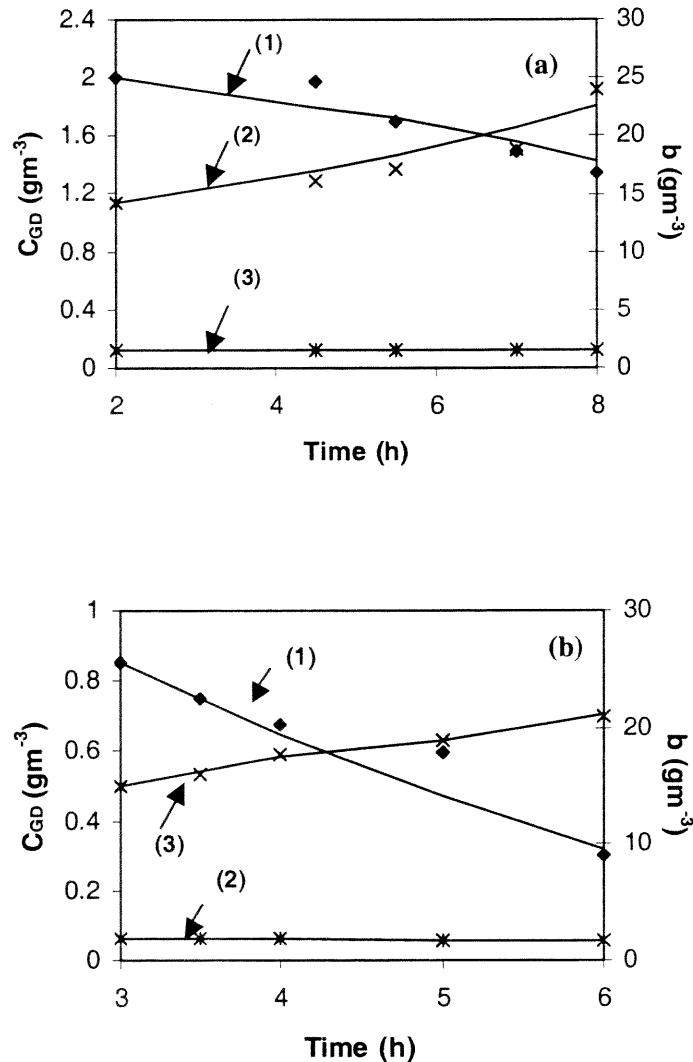
Figure 7.10 Experimental values (symbols) and model-predicted (curves) concentration profiles for (1) o-DCB, (2) ethanol (along the primary y-axis), and (3) biomass along the (secondary y-axis). Data from experiments 12 and 6 are shown in (a) and (b), respectively.

For the o-DCB and ethanol concentration ranges used in the BTF, predictions of $\mu_E(C_{LE})$ values from (7.11) with either $K_{ED} = 0$ or $K_{ED} = 0.5$ are almost identical. For this reason, kinetic parameter values obtained from experiments with single substrates (section 7.1.2.2) were also used for the case of simultaneous removal of ethanol and o-DCB with expression (7.6) unaltered for both compounds.

7.1.3 Yield Coefficients on Oxygen

Using the values of yield coefficients of the biomass on the carbon source (see Tables 7.1 and 7.2), the values of the yield coefficient of the biomass on oxygen were calculated from the reaction stoichiometric equations following the methods used by Shareefdeen et al. (1993) and Mpanias (1998). The method assumes a biomass composition described by the "molecular" formula $CH_{1.8}O_{0.5}N_{0.2}$ (Shuler and Kargi, 1992) and that the nitrogen source for the biomass is the ammonium ion in NH_4NO_3.

The stoichiometric equations are as follows:

1. Biomass BTF-I growing on o-DCB,

$$C_6H_4Cl_2 + 0.428\,H_2O + 0.476\,NH_4NO_3 + 4\,O_2 \rightarrow$$
$$2.38\,CH_{1.8}O_{0.5}N_{0.2} + 0.476\,HNO_3 + 2\,HCl + 3.62\,CO_2 \qquad (7.13)$$

2. Biomass BTF-II growing on o-DCB,

$$C_6H_4Cl_2 + 0.308\,NH_4NO_3 + 4.883\,O_2 \rightarrow$$
$$1.54\,CH_{1.8}O_{0.5}N_{0.2} + 0.308\,HNO_3 + 2\,HCl + 4.46\,CO_2 + 0.076\,H_2O \qquad (7.14)$$
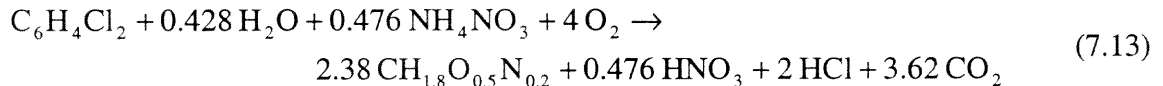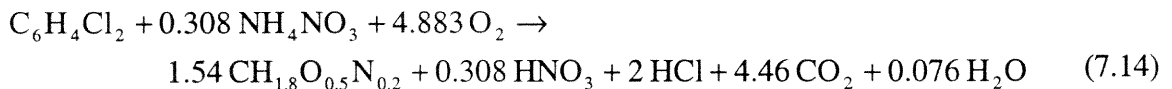
3. Biomass BTF-II growing on ethanol,

$$C_2H_6O + 2.13\,O_2 + 0.166\,NH_4NO_3 \rightarrow$$
$$0.83\,CH_{1.8}O_{0.5}N_{0.2} + 2.5\,H_2O + 1.17\,CO_2 + 0.166\,HNO_3 \qquad (7.15)$$
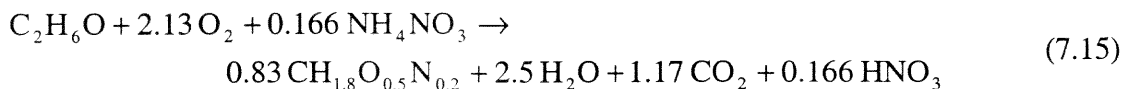
Based on equation (7.13), the value of Y_{OD} for culture BTF-I is found to be 0.457 (g-biomass/g-oxygen). This value is slightly different from 0.363 value used by Mpanias (1998) who experimented with culture BTF-I and o-DCB and found identical kinetics on o-DCB. Mpanias (1998) assumed that the entire nitrogen contained in NH_4NO_3 could be incorporated into the biomass. However, NO_2-nitrogen can be incorporated into the biomass only under anaerobic/anoxic conditions and the process considered here is aerobic. This is the main reason for the discrepancy in Y_{OD} values for culture BTF-I, and the value computed here is considered a better estimate. For culture BTF-II, using equations (7.14) and (7.15), one can calculate $Y_{OD} = 0.242$ gg^{-1} and $Y_{OE} = 0.3$ gg^{-1}. The Y_{OD} and Y_{OE} values computed in this section are also listed in Table 7.6.

7.1.4 Effectiveness Factor and Effective Biofilm Thickness

As has been discussed in Chapter 6, in order to get VOC (and oxygen) profiles along the BTF unit and, from them, predict the BTF performance one can solve equations (6.25) through (6.27) and (6.39) through (6.41) along with the corresponding boundary conditions. To do so, one needs to know the value of δ at each location of the BTF length as well as the values of effectiveness factors ε_D and ε_E. In fact, one needs to know the values of products $\varepsilon_D\delta$ and $\varepsilon_E\delta$ in order to determine the values of η_D and η_E, respectively.

The value of δ, as has been also discussed in Chapter 6, can be determined by solving (independently) equations (6.16) through (6.18) along with the corresponding boundary conditions. Solution of the same equations allows for computation of the values of effectiveness factors through the following equations,

$$\varepsilon_D = \left(\frac{d\overline{S}_D}{d\theta}\right)\left(\phi_D{}^2 \frac{\overline{S}_D \overline{S}_O}{(1+\overline{S}_D + \gamma_D \overline{S}_D{}^2)(1+\overline{S}_O)}\right)^{-1}\Bigg|_{\theta=0} \qquad (7.16)$$

$$\varepsilon_E = \left(\frac{d\overline{S}_E}{d\theta}\right)\left(\phi_E{}^2 \frac{\overline{S}_E \overline{S}_O}{(1+\overline{S}_E + \gamma_E \overline{S}_E{}^2)(1+\overline{S}_O)}\right)^{-1}\Bigg|_{\theta=0} \qquad (7.17)$$
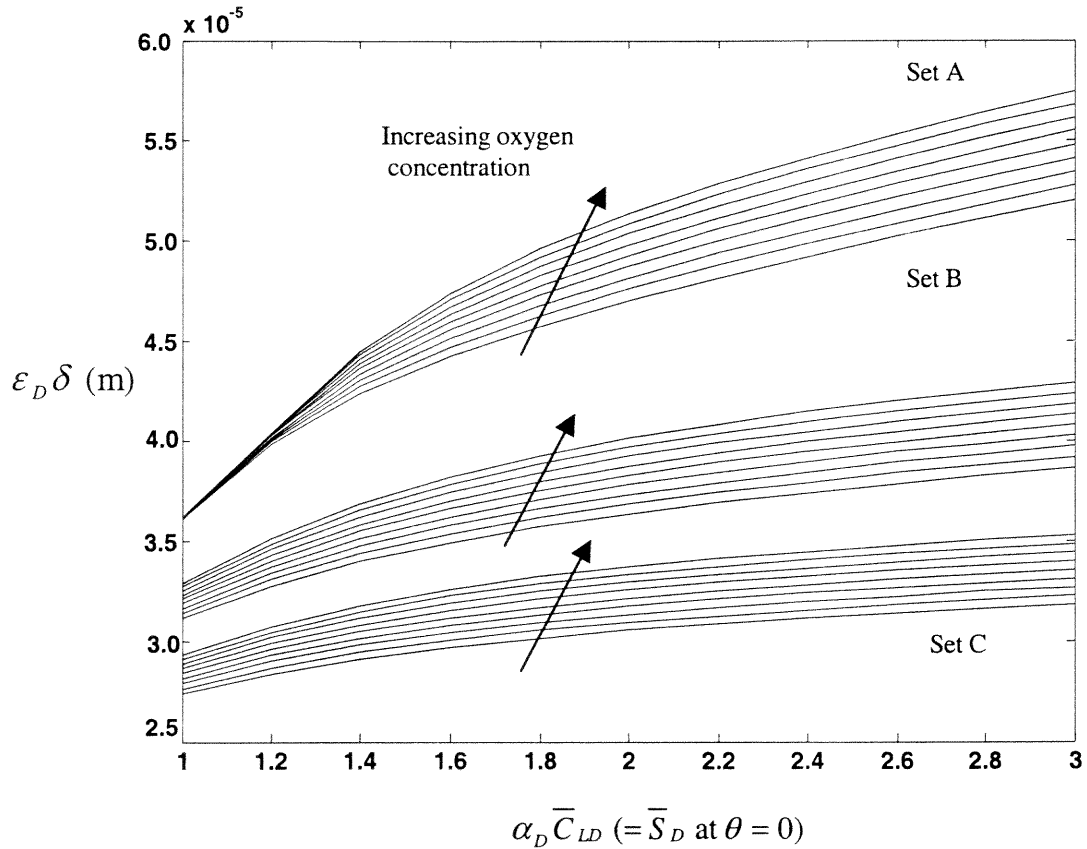
Figure 7.11 Variation of $\varepsilon_D \delta$ with the dimensionless o-DCB concentration at the liquid/biofilm interface for different ethanol and oxygen concentrations. Curves of Set A are for the case where no ethanol is present ($\alpha_E \overline{C}_{LE} = 0$). Curves of Set B and C are for cases where the $\alpha_E \overline{C}_{LE}$ values are 0.05 and 1.5, respectively. The top curve in each set corresponds to oxygen saturation conditions for the liquid ($C_{LO} = 8$ ppm). The oxygen concentration is equally reduced in subsequent curves to reach 60% saturation for the bottom curve in each set.

Values of $\varepsilon_D\delta$ and $\varepsilon_E\delta$ as functions of C_{LD}, C_{LO} and C_{LE} have been obtained as discussed in section 6.3 of Chapter 6.

Figures 7.11 through 7.13 show the variation of $\varepsilon_D\delta$ and $\varepsilon_E\delta$ with the concentrations of o-DCB, ethanol, and oxygen. The concentration ranges used in Figures 7.11 through 7.13 are those encountered in the BTF experiments.

In the absence of ethanol and for low o-DCB concentrations, it was found that $\varepsilon_D\delta$ did not depend on the oxygen concentration. This is reflected in Figure 7.11 as all curves of Set A collapse into a single curve for low o-DCB concentration values. In these cases, it was found that the value of δ is determined by depletion of o-DCB in the biofilm when equations (6.16) through (6.18) are solved along with their boundary conditions. In all other cases shown in Figures 7.11 through 7.13 the value of δ was determined by depletion of oxygen in the biofilm.
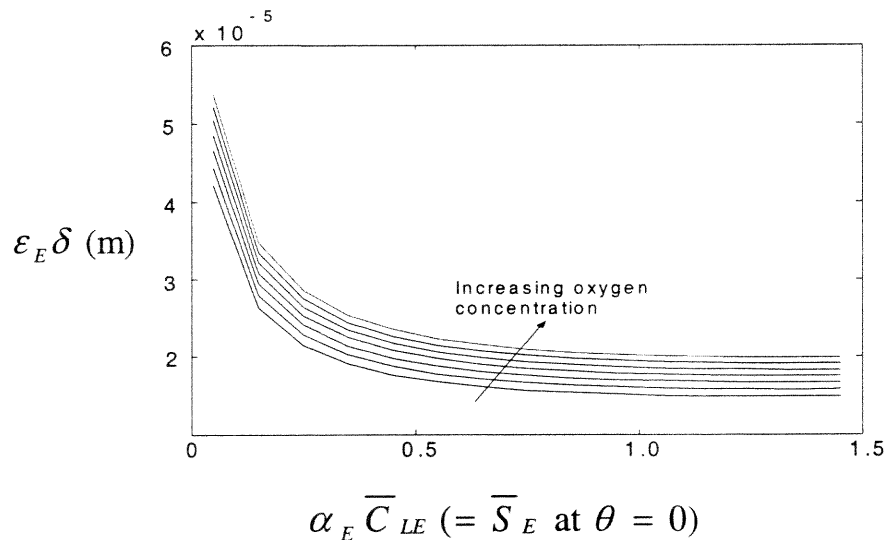
Figure 7.12 Variation of $\varepsilon_E\delta$ with the dimensionless ethanol concentration at the liquid /biofilm interface when there is no o-DCB presence. The top curve corresponds to oxygen saturation conditions for the liquid (C_{LO} = 8 ppm).The oxygen concentration is equally reduced in subsequent curves to reach 70 % saturation for the bottom curve.

Oxygen plays an important role in o-DCB removal in the biofilm even in the absence of ethanol when o-DCB is present at higher levels (right hand side part of curves in Set A, Figure 7.11).
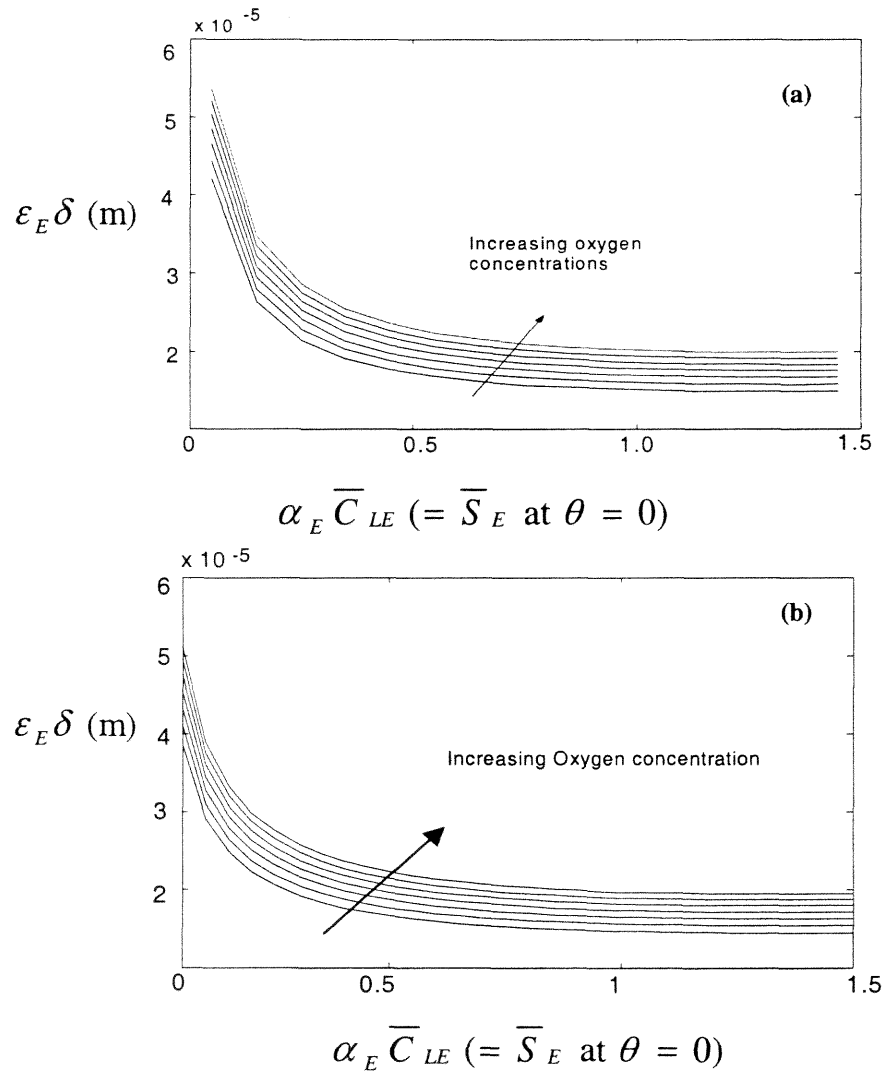
Figure 7.13 Variation of $\varepsilon_E \delta$ with the dimensionless ethanol concentration at the liquid /biofilm interface when o-DCB is present at $\alpha_D \overline{C}_{LD}$ values of 1.0 and 2.0 for (a) and (b), respectively. Oxygen presence as in Figure 7.12.

For the majority of cases shown in Figure 7.11 and for a given set of o-DCB and ethanol concentration values, the $\varepsilon_D \delta$ - value increases with the oxygen concentration. For a given set of o-DCB and oxygen concentration values, Figure 7.11 shows that the $\varepsilon_D \delta$ - value decreases when the ethanol concentration value increases.

Figures 7.12 and 7.13 suggest that the o-DCB concentration has a very small effect on the $\varepsilon_E \delta$ - values. The same figures also suggest that for a given set of ethanol and o-DCB concentration values, the $\varepsilon_E \delta$ - value increases with the oxygen concentration (common feature with Figure 7.11 regarding $\varepsilon_D \delta$)

It is interesting to observe that $\varepsilon_D \delta$ increases with the o-DCB concentration value (Figure 7.11), whereas the value of $\varepsilon_E \delta$ deceases with the ethanol concentration value. (Figures 7.12 and 7.13).

7.1.5 Specific Wetted Surface Area and Mass-Transfer Coefficients

The values of the specific wetted surface area of the biofilm, and the gas and liquid phase mass transfer coefficients (k_{Gq}, k_{Lq}; q = O for oxygen, q = E for ethanol, and q = D for o-DCB) were obtained from the following modified Onda correlation (Mpanias, 1998),

$$\frac{A_S}{\xi A_T} = 1 - \exp\left\{-1.45\left(\frac{\sigma_P}{\sigma_L}\right)^{0.75}\left(\frac{Q_L \rho_L}{SA_T \mu_L}\right)^{0.1}\left(\frac{A_T}{\rho_L^2 g}\right)^{-0.05}\left[\left(\frac{Q_L \rho_L}{S}\right)^2 \frac{1}{\rho_L \sigma_L A_T}\right]^{0.2}\right\} \quad (7.18)$$

$$\frac{\xi_{1q} k_{Gq}}{A_T D_{qG}} = 5.23\left(\frac{Q_G \rho_G}{SA_S \mu_G}\right)^{0.7}\left(\frac{\mu_G}{\rho_G D_{qG}}\right)^{\frac{1}{3}}\left(A_T d_P\right)^{-2} \quad (7.19)$$

$$\xi_{2q} k_{Lq}\left(\frac{\rho_L}{\mu_L g}\right)^{\frac{1}{3}} = 0.0051\left(\frac{Q_L \rho_L}{SA_S \mu_L}\right)^{\frac{2}{3}}\left(\frac{\mu_L}{\rho_L D_{qW}}\right)^{-0.5}\left(A_T d_P\right)^{-0.4} \quad (7.20)$$

The numerical coefficients in the right hand side of expressions (7.19) and (7.20) reflect the physical characteristics of the packing material used. The packing was identical to that used by Mpanias (1998).

Except for Q_G and Q_L that varied among experiments, the values of all parameters appearing in relations (7.18) through (7.20) as well as their source are given in Table 7.6.

Based on the k_{Gq} and k_{Lq} values determined via relations (7.19) and (7.20) the required values of the overall mass transfer coefficients K_{Lq} (q = O, D, E) were determined via the following equation,

$$\frac{1}{K_{Lq}} = \frac{1}{m_q k_{Gq} A_S} + \frac{1}{k_{Lq} A_S}$$

(7.21)

For ξ_{1q} and ξ_{2q}, q = D, O the values determined by Mpanias (1998) were used. Due to lack of any better estimate, for ethanol it was assumed that $\xi_{1E} = \xi_{1D}$ and $\xi_{2E} = \xi_{2D}$. This turns out to be a good estimate for the following reasons. Hekmat and Vortemeyer (1994) who studied ethanol removal in a BTF packed with polypropylene particles determined, through fitting of their data, a 3,600 h^{-1} value of the overall gas side mass transfer coefficient (K_{GE}). Using expressions (7.19) and (7.20) with the assumed ξ_{1E} and ξ_{2E} values (both equal to 2.55) and for the operating conditions and properties of the packing used by Hekmat and Vortemeyer (1994) one can predict K_{GE} values between 3,200 and 3,800 h^{-1}, i.e., values very close to the reported value of 3,600 h^{-1}.

The value of parameter ξ appearing in relation (7.19) was determined by fitting some data sets to the solution of the model equations, as discussed later in this chapter.

7.1.6 Liquid Film Thickness

The thickness of the liquid film, δ_L, was calculated via the following equation,

$$\delta_L = \frac{V_{LH}}{A_S V_P} \tag{7.22}$$

where V_{LH} is the volume of the liquid hold-up in the BTF, V_P is the volume of the BTF

bed, and A_S is the specific wetted surface area calculated via correlation (7.18).

Values of V_{LH} were measured via draining the BTF after it had operated for some

time under a given value for the liquid recirculation rate, Q_L, and measuring the volume of

drained liquid. For the range of Q_L- values used in the study, it was found that V_{LH} is a

linear function of Q_L as shown in Figure 7.14 where a straight line has been passed through

the data using the least squares error minimization method.

Table 7.5 lists the characteristic values of δ_L at the Q_L - values used in the BTF

experiments. The same table lists the corresponding A_S and V_{LH} values, that also depend on

Q_L.
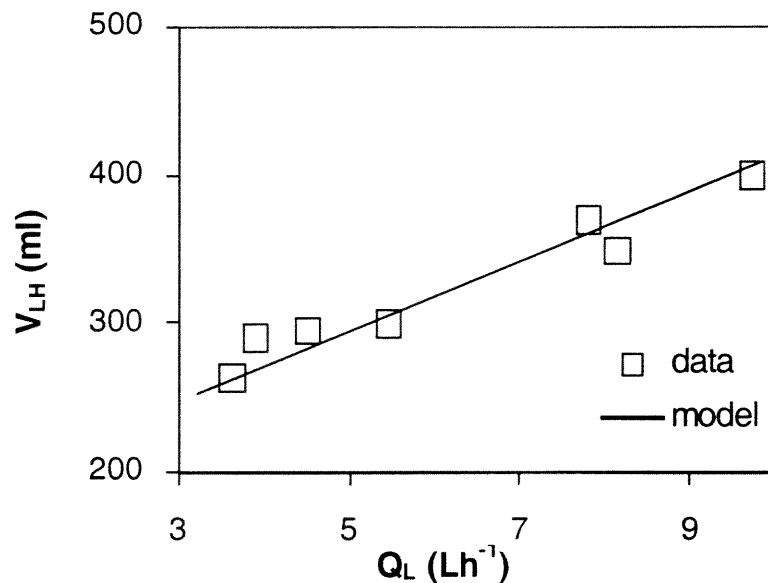
Figure 7.14 Volume of liquid hold-up in the BTF as a function of liquid recirculation rate. Data points (symbols) have been regressed to a straight line.

Table 7.5 Thickness of the liquid film, δ_L, as a function of Q_L.

Q_L (Lh^{-1})	A_S (m^{-1})	Liquid Hold-up (L)	δ_L (m)
3.6	139.20	0.271	0.000155
4.5	151.63	0.292	0.000153
7.8	186.96	0.371	0.000158
9.8	203.79	0.419	0.000163

7.1.7 Other Parameters

Other parameters such as diffusivities of ethanol, o-DCB, and oxygen in water and air (D_{qW}, D_{qG}; q = E, D, O), the biomass density in the biofilm, X_V, the biomass concentration in the liquid recirculating through the BTF, X_{VL}, the correction factor for diffusivities in the biofilm, f(X_V), etc. were mostly taken from the literature and some measured during the course of this study. The values of these parameters and their source are listed in Table 7.6. In fact, Table 7.6 presents a complete listing of all model parameters except for the kinetic parameters that are listed in Tables 7.1 and 7.2. The only parameter not listed in the tables is ξ, since this was a fitted parameter and its determination is discussed later in this chapter.

Table 7.6 Model parameter values for biofiltration of ethanol and o-DCB

Parameter	Numerical Value	Unit	Reference
Physical Parameters for Ethanol			
m_E	0.00028	-	Present study
D_{EW}	1.01 x 10^{-9}	m^{2}s^{-1}	Perry and Green (1999)
D_{EG}	1.0 x 10^{-5}	m^{2}s^{-1}	Perry and Green (1999)

Table 7.6 Model parameter values for biofiltration of ethanol and o-DCB (Continued)

Parameter	Numerical Value	Unit	Reference
	Physical Parameters for o-DCB		
m_D	0.119	-	Mpanias (1998)
D_{DW}	0.78×10^{-9}	m^2s^{-1}	Perry and Green (1999)
D_{DG}	0.69×10^{-5}	m^2s^{-1}	Mpanias (1998)
	Physical Parameters for oxygen		
C_{GOi}	275	gm^{-3}	Mpanias (1998)
m_O	34.4	-	Mpanias (1998)
D_{OW}	2.39×10^{-9}	m^2s^{-1}	Perry and Green (1999)
D_{OG}	2.03×10^{-5}	m^2s^{-1}	Perry and Green (1984)
	Kinetic Parameters for oxygen		
K_O	0.260	-	Mpanias (1998)
Y_{OE}	0.3	gg^{-1}	Present study
Y_{OD} (BTF- I)	0.457	gg^{-1}	Present study
Y_{OD} (BTF-II)	0.242	gg^{-1}	Present study
	Physical Parameters for Biomass		
X_V	75	Kgm^{-3}	Mpanias (1998)
$f(X_V)$	0.253	-	Mpanias (1998)
X_{VL} (mixtures)	1.0	Kgm^{-3}	Present study
X_{VL} (o-DCB)	0.0	Kgm^{-3}	Present study / Mpanias (1998)

Table 7.6 Model parameter values for biofiltration of ethanol and o-DCB (Continued)

Parameter	Numerical Value	Unit	Reference
Physical Parameters for Air			
μ_G	0.18×10^{-3}	$Kgm^{-1}s^{-1}$	Perry and Green (1999)
ρ_G	1.193	Kgm^{-3}	Perry and Green (1999)
Physical Parameters for Water			
μ_L	0.982×10^{-3}	$Kgm^{-1}s^{-1}$	Perry and Green (1999)
ρ_L	997.85	Kgm^{-3}	Perry and Green (1999)
σ_L	72×10^{-3}	Nm^{-1}	Mpanias (1998)
Parameters for Packing material			
A_T	623.36	m^{-1}	Mpanias (1998)
d_P	0.0127	m	Mpanias (1998)
σ_P	61×10^{-3}	Nm^{-1}	Mpanias (1998)
Column Dimensions			
V_P	1.3×10^{-2}	m^3	Present Study
S	1.82×10^{-2}	m^2	Present Study
Other parameters			
ξ_{1D}, ξ_{2D}	2.55	-	Mpanias (1998)
ξ_{1E}, ξ_{2E}	2.55	-	Present Study
ξ_{1O}	0	-	Mpanias (1998)
ξ_{2O}	7.12	-	Mpanias (1998)

7.2 Preliminary Model Testing

As discussed in Chapter 6, the introduction of the notion of effectiveness factors allows for decoupling of the mass balance equations in the biofilm from the mass balances in the gas (air) and liquid phases. This decoupling constitutes an approximation to the original model equations. In order to test if the approximation is a reasonable one, the following test was performed.

Mpanias (1998) had experimented with unit BTF-I to remove o-DCB vapors from airstreams flowing counter – currently with the liquid stream through the BTF unit. He had also described his data by solving the original model equations without any approximation. His data, along with the percent error between experimentally determined and model predicted o-DCB removal rates, are shown in Table 7.7.

The same data were described by the approximate model proposed here as follows. The $\varepsilon_D \delta$ - values were determined by solving equations (6.16) and (6.18) with $\overline{S}_E = 0$ and using the appropriate boundary conditions from (6.19) and (6.20). Concentration profiles in the gas and liquid phase for o-DCB and oxygen were obtained by solving equations (6.25a), (6.27a), (6.28a), (6.39), (6.41), and (6.24) with $C_{LE} = 0$. Equation (6.25a) is a modified version of equation (6.25); to get (6.25a) one needs to multiply the right hand side of (6.25) by –1. Similarly, equation (6.27a) is obtained from (6.27) by multiplying the right hand side of equation (6.27) by –1. Finally, equation (6.28a) is a modified version of (6.28); the modifications are to disregard $\overline{C}_{GE}$ and let the equality hold at z = 1 rather that z = 0. The foregoing modifications were needed because Mpanias (1998) experimented with BTF-I under counter-current flow conditions.

In solving the model equations, the parameter values are those shown in Table 7.1 (for culture BTF-I) and Table 7.6. The only exception was the Y_{OD} value. Instead of the 0.457 gg^{-1} value shown in Table 7.6, a value of 0.363 gg^{-1} was used to ensure that all

Table 7.7 Experimental data (Mpanias, 1998) and model predictions (comparison of two models) for biofiltration of ortho-dichlorobenzene under counter-current flow of air and liquid.

[a]C_{GDi}	[b]X_{exp} (%)	[c]R_{exp} (gm^{-3}-reactor h^{-1})	[d]R_{pred} (gm^{-3}-reactor h^{-1})	[e]E (%) new model	[f]E (%) old model
[g]τ = 6.2 min; [h]Q_L = 1.2 Lh^{-1}
1.20	71.80	8.28	7.92	-5.03	+2.42
2.30	64.00	14.15	14.64	+2.79	+10.88
τ = 4.5 min; Q_L =1.9 Lh^{-1}
0.65	76.40	6.62	5.77	-12.79	-6.95
3.50	60.00	27.98	27.05	-3.39	+7.58
τ = 3.25 min; Q_L = 3.3 Lh^{-1}
0.75	63.80	9.0	8.51	+2.71	+5.89
2.10	57.50	22.42	22.59	+4.43	+11.19

[a] o-DCB concentration in the air entering the BTF; [b] percent o-DCB removal based on experimental values and defined as $100 \times (C_{GDi} - C_{GDe,1})/C_{GDi}$, where $C_{Gde,1}$ is the experimentally measured o-DCB concentration in the air exiting the BTF, [c] experimentally determined o-DCB removal rate defined as $(C_{GDi} - C_{GDe,1})/\tau$, [d] o-DCB removal rate determined by the approximate model and defined as $(C_{GDi} - C_{GDe,2})/\tau$ where $C_{Gde,2}$ is the predicted o-DCB concentration in the air exiting the BTF, [e] percent error in predicted o-DCB removal rate defined as $100 \times (R_{pred} - R_{exp})/R_{exp}$, [f] percent error in o-DCB removal rate predicted by solving the original model (Mpanias 1998), [g] air residence time, and [h] liquid flow rate.

parameters were same as those used by Mpanias (1998) and thus, allow for a fair comparison of the two models. Furthermore, since Mpanias (1998) had that assumed no reaction occurs in the liquid phase, the same assumption was made here ($\eta_{LD} = 0$). Some of the data sets were used for determining the value of ξ through a fitting approach also followed by Mpanias (1998). The value of ξ found here was 1.75 whereas Mpanias (1998) had found a 2.36 value. Using $\xi = 1.75$, predictions were made for the o-DCB removal rate for all data sets and are shown in Table 7.7 along with percent error between model-predicted and experimentally obtained values for the o-DCB removal rates.

As can be seen from Table 7.7, the approximation used in the present study predicts the data equally well if not better than the original model. Hence it was concluded that the approximation introduced in the present study is one that can be used with confidence.

7.3 Modeling the Data from Unit BTF-I

The experimental data on o-DCB removal in unit BTF-I under co-current flow of air and the liquid stream obtained during the course of the present study and presented in Chapter 5 have been described with the approximate model proposed here as follows.

Values for $\varepsilon_D \delta$ were obtained by solving equations (6.16) and (6.18) with $\overline{S}_E = 0$ and using the appropriate boundary conditions from (6.19) and (6.20). Measurements for the biomass concentration in the recirculating liquid revealed a very low value of 0.075 kgm^{-3} and it was, thus, assumed that no reaction occurs in the liquid phase ($\eta_{LD} = 0$). Equations (6.25) and (6.27), along with boundary conditions (6.28), were simultaneously solved with equations (6.39) and (6.41), along with boundary conditions (6.24). In all foregoing equations, ethanol concentration values were set equal to zero wherever they

appear. The model parameters used are shown in Tables 7.1 (culture BTF-I) and 7.5. The

value of ξ was determined by fitting data from three data sets to the solution of the model

equations. A value of $\xi = 1.5$ was obtained.

Table 7.8 shows experimental and model-predicted values for the removal rate of o-

DCB vapor. As can be seen from the table the model predicts the data within a less than 6

% error in all cases and in many cases the error is less than 3 %.

Table 7.8 Experimental data and model predictions for biofiltration of ortho-dichlorobenzene (o-DCB) in BTF-I [a].

C_{GDi}	X (%)	R_{exp} (gm^{-3}-reactor h^{-1})	R_{pred} (gm^{-3}-reactor h^{-1})	E (%)
		$\tau = 6.5$ min; $Q_L = 3.6$ Lh^{-1}		
1.45	70.01	9.37	9.93	5.95
4.70	64.27	27.88	28.04	0.56
		$\tau = 4.2$ min; $Q_L = 8.7$ Lh^{-1}		
2.74	65.39	25.60	26.53	3.63
4.02	68.24	39.19	36.75	-6.23
		$\tau = 4.00$ min; $Q_L = 4.2$ Lh^{-1}		
1.11	61.29	10.20	9.93	-2.64
2.56	56.45	21.68	21.32	-1.67
3.68	51.63	28.50	28.6005	0.35

[a]All symbols as defined in Table 7.7; air and liquid in co-current flow.

Figure 7.15 shows model predicted concentration values for o-DCB and oxygen within the effective biofilm thickness at three locations along the length of unit BTF-I. In this case, concentrations have been normalized with the corresponding values at $\theta = 0$. According to Figure 7.15, at locations close to the BTF entrance oxygen is depleted before o-DCB in the biofilm and thus, determines the value of δ. At locations away from the BTF entrance (Figures 7.15b and 7.15c), and as the o-DCB concentration in the air decreases, o-DCB rather than oxygen is depleted first within the biofilm and thus determines the value of δ. For low inlet o-DCB concentrations, C_{GDi}, it has been found that o-DCB gets depleted before oxygen throughout the BTF unit.

Figure 7.16 shows two examples of the variation of the effective biofilm thickness, δ, along the length of unit BTF-I. It has been found that for low o-DCB concentrations in the air entering the BTF, there is little variation of the value of δ (curve 1). In such cases, the depletion of o-DCB in the biofilm determines the value of δ throughout the biotrickling filter. At higher o-DCB concentrations in the air entering the BTF, there is significant variation of the value of δ along the BTF length (curve 2). In such cases, δ is determined by oxygen depletion at low values of z and by o-DCB depletion at large values of z. In fact, the peak of curve 2 (and any similar curve) occurs at the value of z at which there is a switch of the compound depleted first in the biofilm.
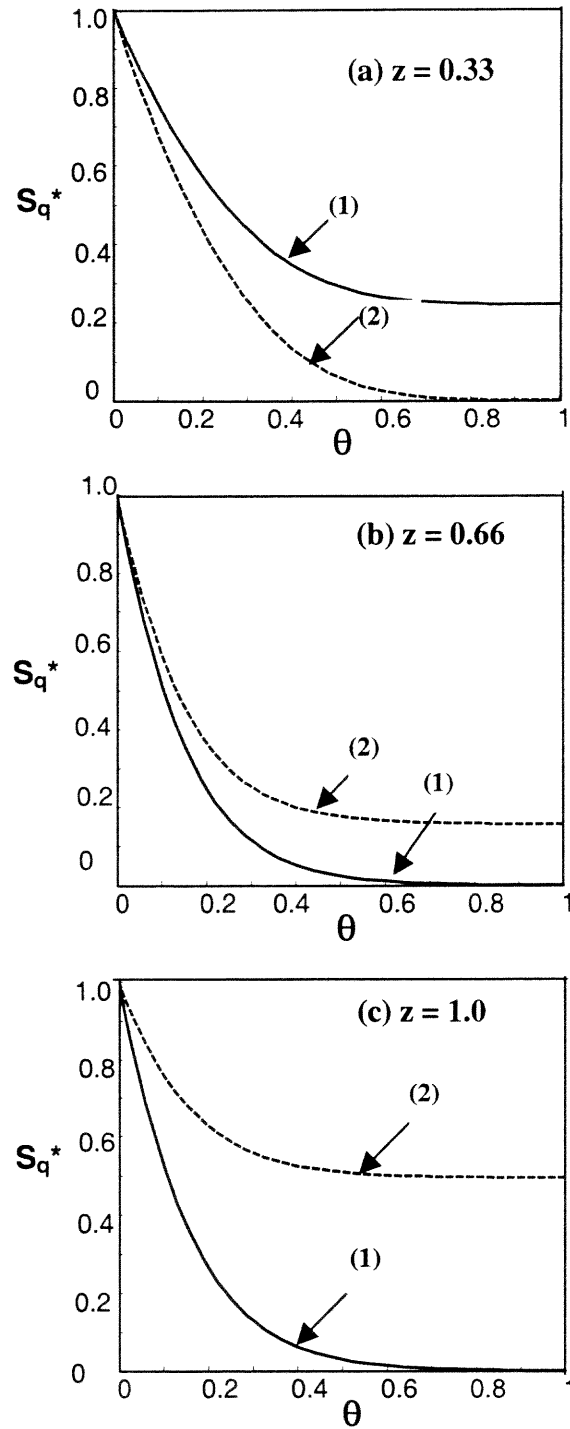
Figure 7.15 Model predicted normalized concentration profiles in the active biofilm for o-DCB (curves 1) and oxygen (curves 2) at three locations along BTF-I when $C_{GDi} = 4.7$ gm^{-3}, $Q_L = 3.6$ Lh^{-1} and $\tau = 6.5$ min.
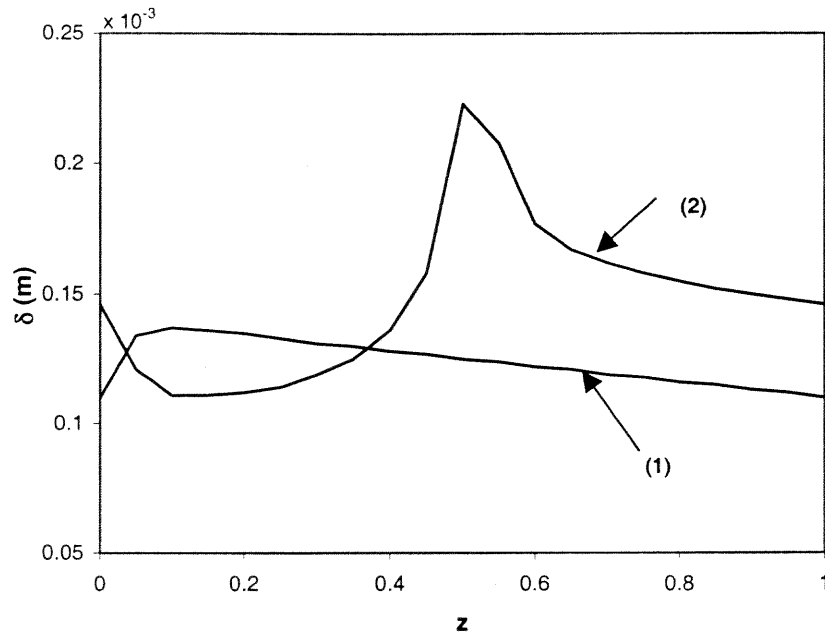
Figure 7.16 Model predicted effective biofilm thickness along the length of unit BTF-I when $Q_L = 3.6$ Lh^{-1} and $\tau = = 6.5$ min. The value of C_{GDI} is 1.06 and 4.7 gm^{-3} for curves 1 and 2, respectively.

7.4 Modeling the Data from Unit BTF-II

As has been shown in Chapter 5, unit BTF-II has been used extensively in experiments with air streams carrying both o-DCB and ethanol vapors. The data obtained have been modeled using equations (6.16) through (6.20) to determine $\varepsilon_D\delta$ and $\varepsilon_E\delta$ and then separately equations (6.24) through (6.28) and (6.39) through (6.41) following the methodology described in section 6.3. Two cases were considered, one in which reaction in the liquid phase was assumed to occur and one in which reaction in the liquid phase was neglected. Except for ξ, the values of the parameters used are those listed in Tables 7.1 (culture BTF–II), 7.2, and 7.6

BTF-II has been also used in experiments with air streams carrying o-DCB only, as discussed in Chapter 5. An attempt was made to model these data sets with the equations mentioned in Section 7.3 of this chapter. Parameter values used were those listed in Tables 7.1 (culture BTF-II) and 7.6. Results from the foregoing modeling studies are presented in the following subsections.

7.4.1 Removal of o-DCB/ethanol Mixtures With Reaction in the Liquid Phase

The value of parameter ξ was determined as follows. Five data sets were selected and using their operating parameter values, the model equations were solved under an assumed ξ-value. From the predicted o-DCB and ethanol concentration values at the exit of BTF-II, the model-predicted o-DCB and ethanol removal rates were computed. Subsequently, the absolute value of the errors in predictions of o-DCB and ethanol removal rates were computed (errors defined as in Table 7.7). The mean of these absolute errors for the five data sets was computed for both o-DCB and oxygen. The procedure was then repeated for another assumed ξ-value and the goal was to find the value of ξ that minimizes the mean absolute error for both o-DCB and ethanol. No such common value of ξ was found. As shown in Figure 7.17, the value of ξ that minimized the error for o-DCB was slightly above 3. A much lower value of ξ (not shown in Figure 7.17) would minimize the error for ethanol at considerable increase, however, in the error for o-DCB. For this reason, a value of $\xi = 3.0$ was used in modeling all data sets (i.e., both those used in the fitting approach as well as those not used in the fitting). It should be mentioned that the method described above was also used in determining the value of ξ reported in sections 7.2 and 7.3 for unit BTF-I.
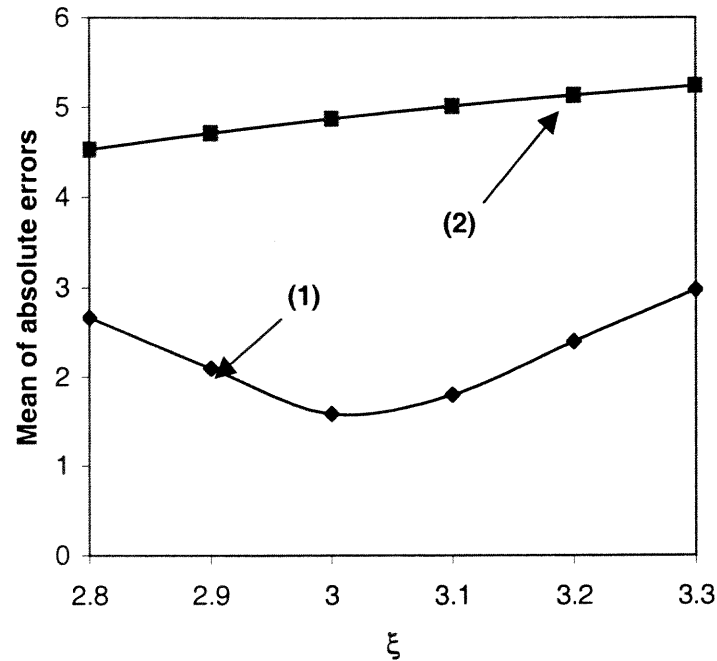
Figure 7.17 Determination of the optimal value of ξ for BTF-II when reaction is assumed to occur in the liquid phase. Mean values of $\left| 100 \times (R_{pred} - R_{exp})/R_{exp} \right|$ for both o-DCB (curve 1) and ethanol (curve 2) from 5 data sets were used in determining the best value of ξ.

Table 7.9 shows experimental data (also shown in Chapter 5) along with model predictions. As can be seen from the table, there is an almost excellent agreement between experimental and model predicted values. With very few exceptions, the percent error in predicting the experimental removal rate of both o-DCB and ethanol is less than ±5%; furthermore the error never exceeds 8.5%. It can be also seen from the table that the model does a much better job in predicting o-DCB removal when compared to predictions of ethanol removal; this can be attributed in the value of ξ used which, as discussed above, is better for o-DCB. Furthermore, the model consistently over-predicts the experimentally determined ethanol removal rate, whereas for o-DCB, in some cases the experimental removal rate is under-predicted and in some cases over-predicted by the model.

Table7.9 Experimental data and model predictions for biofiltration of o-dichlorobenzene and ethanol in BTF-II when reaction is assumed to occur in the liquid phase[1].

	Inlet Concentration (gm^{-3})	Percent Removal (%)		Removal Rate $(gm^{-3}\text{-reactor } h^{-1})$		Error %
		X_{exp}	X_{pred}	R_{exp}	R_{pred}	
$\tau = 6.5$ min ; $Q_L = 3.6$ Lh^{-1}						
o-DCB	1.88	93.10	93.15	16.16	16.68	3.23
Ethanol	2.65	95.92	98.91	23.46	24.96	6.40
o-DCB	4.70	91.97	89.06	39.90	39.87	-0.09
Ethanol	2.43	96.22	98.86	21.58	22.88	6.02
$\tau = 5.5$ min ; $Q_L = 7.8$ Lh^{-1}						
o-DCB	3.44	95.2	96.69	35.87	36.96	2.18
Ethanol	1.39	95.43	99.81	14.56	15.42	5.68
$\tau = 4.2$ min ; $Q_L = 8.35$ Lh^{-1}						
o-DCB	0.87	92.00	94.31	11.48	11.72	2.08
Ethanol	2.23	96.76	99.7	30.84	31.76	2.99
$\tau = 4.2$ min ; $Q_L = 8.7$ Lh^{-1}						
o-DCB	3.35	90.25	91.84	43.19	43.95	1.76
Ethanol	2.35	97.35	99.43	32.68	33.38	2.14
o-DCB	2.11	95.24	92.54	28.71	27.90	-2.83
Ethanol	2.62	95.38	99.43	35.70	37.21	4.24
$\tau = 4.00$ min ; $Q_L = 4.5$ Lh^{-1}						
o-DCB	2.20	85.88	84.63	26.99	26.60	-1.45
Ethanol	2.57	94.36	98.45	34.64	36.14	4.34
o-DCB	3.50	81.89	81.32	40.95	40.66	-0.71
Ethanol	2.51	92.76	98.39	33.26	35.28	6.07
$\tau = 4.2$ min ; $Q_L = 7.8$ Lh^{-1}						
o-DCB	2.87	92.38	93.09	37.88	38.17	0.77
Ethanol	1.05	91.91	99.44	13.79	14.92	8.19
o-DCB	3.17	91.98	93.31	41.65	42.26	1.45
Ethanol	0.53	99.31	99.46	7.52	7.53	0.15

[1]All symbols as defined in Table 7.7; air and liquid in co-current flow.

Figure 7.18 shows model-predicted concentration profiles in the air along the length of unit BTF-II. Predictions are compared with data and a good agreement can be observed. The agreement is not very satisfactory for ethanol concentration values at the exit of the BTF. It should be mentioned, however, that ethanol concentrations at the BTF exit were always very low and close to the detection limit of the GC unit. Hence, there may be an error involved in the measured ethanol concentration values in the air exiting the BTF unit. In general, the model predicted and measured o-DCB concentrations agreed within 5% at the middle point of the BTF and within 10% at its exit. Regarding ethanol, the agreement was within 15-20% at the middle point and within 50% at the exit of the BTF.

Figure 7.19 shows an example of model-predicted dimensionless concentration profiles in both gas and liquid phases for all three compounds (o-DCB, ethanol, and oxygen). It can be seen from the plots that there is a large difference between gas and liquid phase concentrations at the inlet of the BTF leading to high gradients for mass transfer. The predicted actual (dimensional) o-DCB concentration value in the liquid exiting the BTF never exceeds 1 gm^{-3} for all C_{GDi} values used in the experiments. For ethanol, the concentration in the liquid is predicted to be low throughout the BTF unit. In terms of actual (dimensional) ethanol concentrations, the predicted values in the liquid exiting the BTF were between 1 and 5 gm^{-3} for all C_{GEi} values used in the experiments. The very low o-DCB and ethanol concentration values explain why neither of the two compounds was detected when liquid samples taken from the exit of the BTF were analyzed as mentioned earlier in this dissertation. Regarding oxygen, there is insignificant variation in the gas phase concentration along the BTF but significant variation in the liquid phase reaching values as low as 60% of the saturation value.
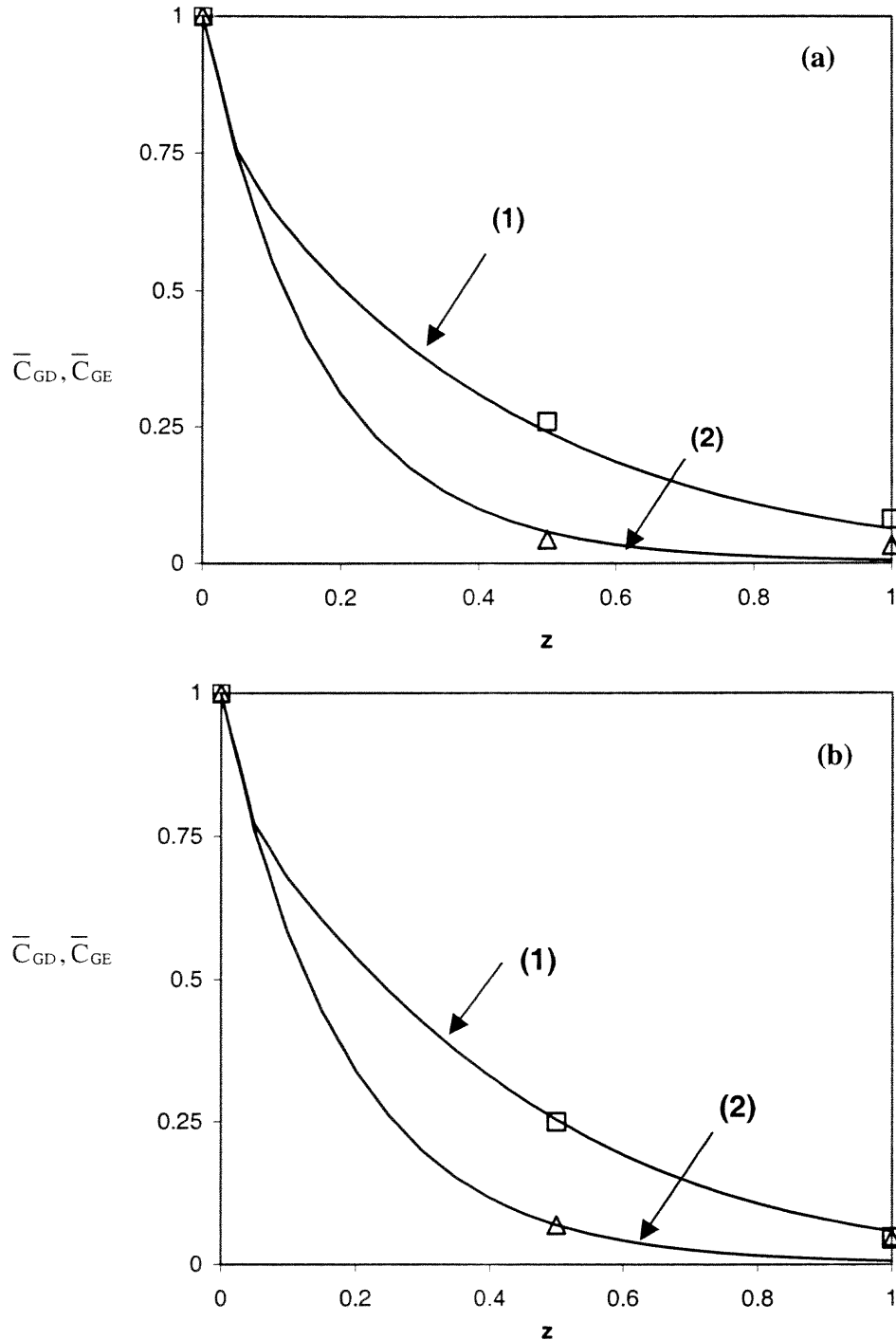
Figure 7.18 Model-predicted dimensionless concentration profiles of o-DCB(curves 1) and ethanol (curves 2) in BTF-II in the air along BTF-II when reaction is assumed to occur in the liquid phase. Symbols represent experimental data. The values for C_{GDi} (gm^{-3}), C_{GEi} (gm^{-3}), Q_L (Lh^{-1}), and τ (min) are correspondingly, 3.14, 1.9, 7.8, and 5.5 in (a), and 0.87, 2.23, 8.35, and 4.2 in (b).
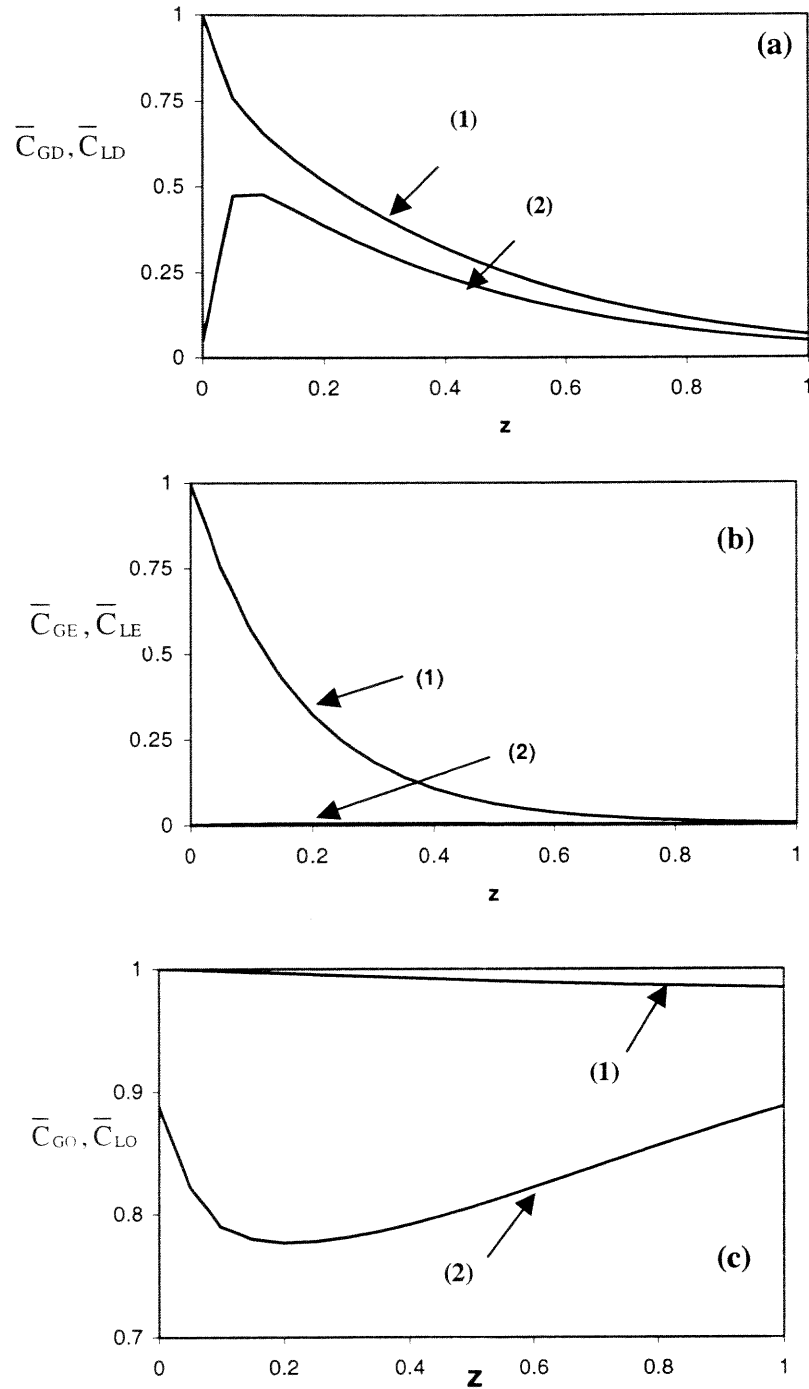
Figure 7.19 Model predicted dimensionless concentration profiles of (a) o-DCB, (b) ethanol and (c) oxygen along BTF-II when reaction is assumed to occur in the liquid phase and $C_{GDi} = 0.87$ gm^{-3}, $C_{GEi} = 2.23$ gm^{-3}, $Q_L = 8.35$ Lh^{-1} and $\tau = 4.2$ min. Curves 1 and 2 are for the gas and liquid phase, respectively.

Figure 7.20 shows two examples for the model-predicted variation of δ along the length of BTF-II, and can be compared with Figure 7.16. Curve 1 in Figure 7.20 corresponds to a case where oxygen is depleted before o-DCB and ethanol in the biofilm at any location along the length of the BTF. This can be also seen from Figure 7.21 where normalized concentrations of the three compounds have been plotted as a function of θ at the three locations along the BTF length. Curve 2 in Figure 7.20 corresponds to a rare case in which the ethanol concentration is so low towards the exit of BTF-II that ethanol instead of oxygen depletion determines the value of δ. This occurs at high z-values, i.e., to the right of the peak of curve 2. The presence of the peak is analogous to the case of curve 2 in Figure 7.16.
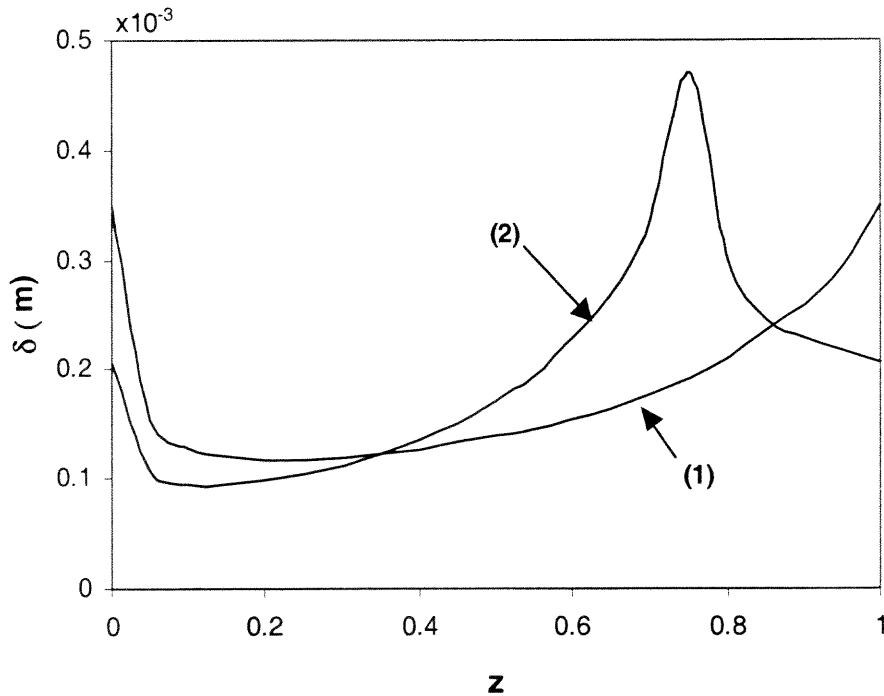
Figure 7.20 Model-predicted effective biofilm thickness δ along the length of unit BTF-II when reaction is assumed to occur in the liquid phase. The values for C_{GDi} (gm^{-3}), C_{GEi} (gm^{-3}), Q_L (Lh^{-1}), and τ (min) are correspondingly, 0.87, 2.23, 8.35, and 4.2 for curve 1, and 3.14, 1.9, 7.8, and 5.5 for curve 2.
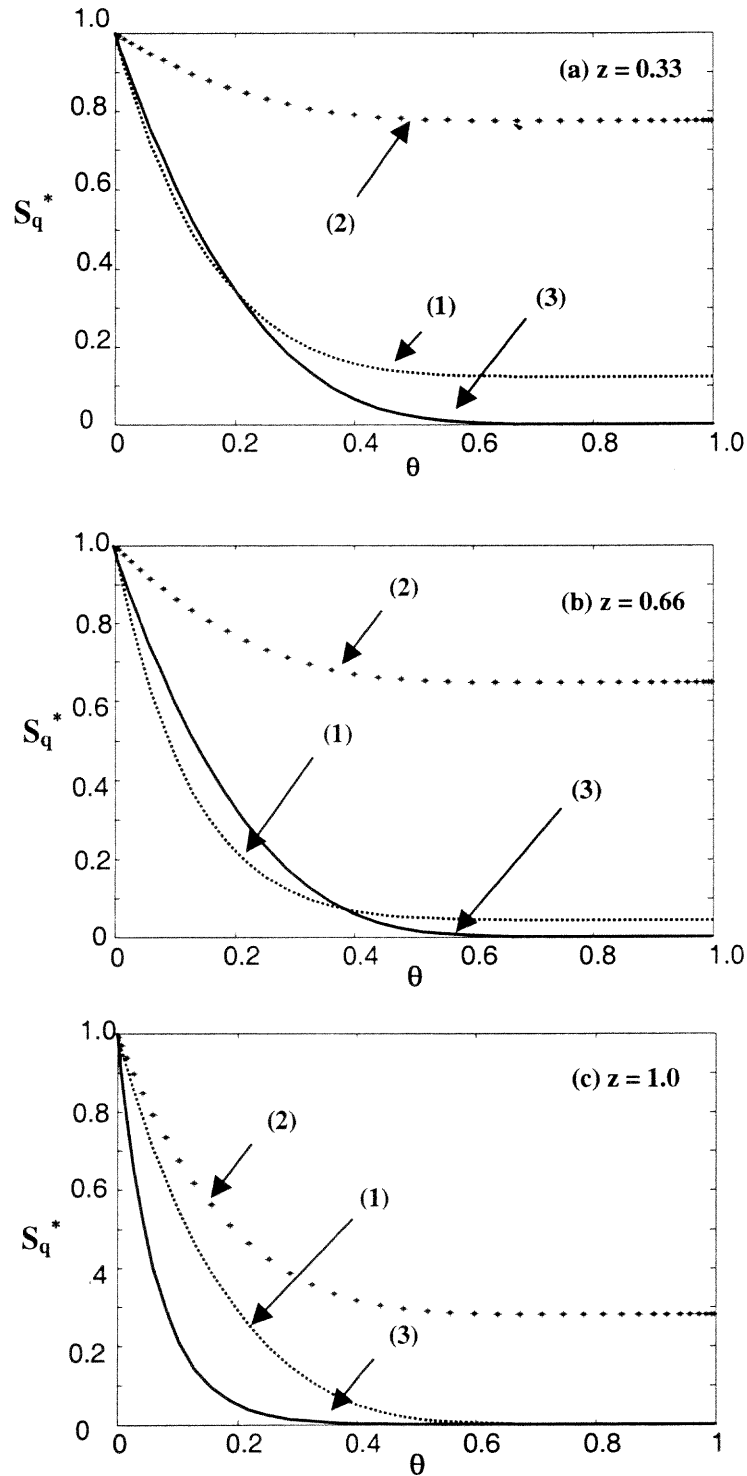
Figure 7.21 Model predicted normalized concentration profiles in the active biofilm for o-DCB (curves 1), ethanol (curves 2) and oxygen (curves 3) at three locations along BTF-II when $C_{GDi} = 0.87$ gm^{-3}, $C_{GEi} = 2.23$ gm^{-3}, $Q_L = 8.35$ Lh^{-1}, $\tau = 4.2$ min, and reaction is assumed to occur in the liquid phase.

7.4.2 Removal of o-DCB/ethanol Mixtures Without Reaction in the Liquid Phase

The data sets from removal of o-DCB and ethanol mixtures in BTF-II modeled in section 7.4.1 were also analyzed with the decoupled model under the assumption that reaction in the liquid phase does not occur. This assumption does not alter the solution to equations (6.16) through (6.20) for determination of $\varepsilon_D \delta$ and $\varepsilon_E \delta$, but affects the solution to equations (6.24) through (6.28) and (6.39) through (6.41) since it is now assumed that $\eta_{LD} = \eta_{LE} = 0$. The intent of this analysis was to investigate if a different value of ξ can, at the phenomenological level, substitute for VOC removal via reaction in the liquid phase.

The same five data sets used in determining the value of ξ in section 7.4.1 were used here as well. Following the methodology described in section 7.4.1 a ξ value of 3.4 was determined as best. As can be seen from Figure 7.22, which is exactly analogous to
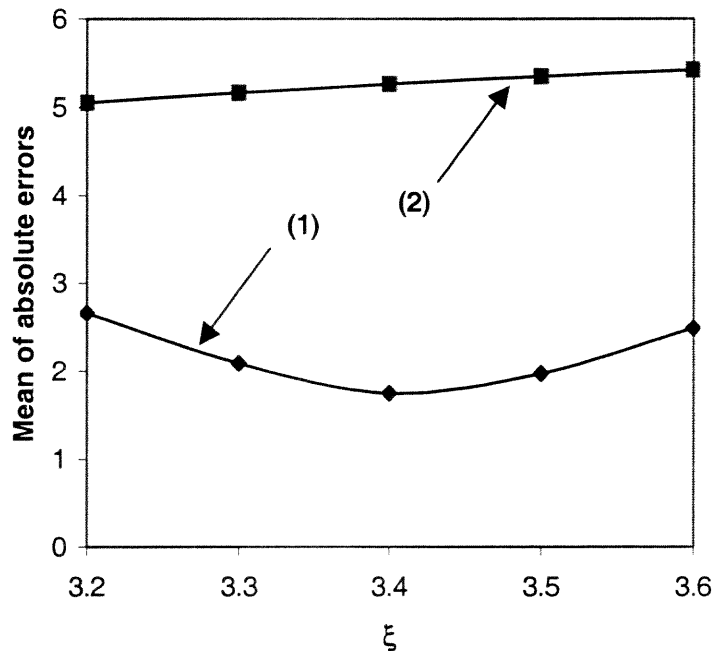
Figure 7.22 Determination of the optimal value of ξ for BTF-II when reaction in the liquid phase is neglected. Mean values of $\left| 100 \times (R_{pred} - R_{exp})/R_{exp} \right|$ for both o-DCB (curve 1) and ethanol (curve 2) from 5 data sets were used in determining the best value of ξ

Figure 7.17, $\xi = 3.4$ is in fact best for o-DCB but not for ethanol.

Model-predicted results, using a ξ-value of 3.4, and experimental data are shown in Table 7.10. Comparing the percent error shown in Table 7.9 and 7.10, one can conclude that both assumptions (reaction or lack of it in the liquid phase) yield almost identical results regarding predictions of removal rates for both o-DCB and ethanol. On the other hand, o-DCB and ethanol concentration profiles in the air along the length of BTF-II are much better predicted when reaction in the liquid is assumed to occur. This can be seen from Figures 7.18 and 7.23 where results predicted by the model under the two assumptions regarding reaction in the liquid phase are plotted against the same two sets of experimental data. In fact, the difference is much more pronounced for o-DCB. More specifically, when reaction in the liquid phase is neglected the model predicts the experimental o-DCB concentration values within 30% error at the middle point and within a 50% error at the exit of BTF-II. These errors when reaction is assumed to occur are, correspondingly, 5% and 10% as discussed in section 7.4.1. The errors in ethanol concentration predictions are almost identical to those reported in section 7.4.1.

As had been discussed in Chapter 5, some experiments were performed by varying the biomass concentration in the liquid phase and led to different removal rates. This experimental indication, along with the modeling results discussed in this section and section 7.4.1 have led to the conclusion that reaction must be happening in the liquid phase. On the other hand, for practical applications where removal rates are much more important than concentration values per se, both assumptions regarding the liquid phase can be used with no severe implications for predictions.

Table 7.10 Experimental data and model predictions for biofiltration of o-dichlorobenzene and ethanol in BTF-II when reaction in the liquid phase is neglected[1].

	Inlet Concentration (gm^{-3})	Percent Removal (%)		Removal Rate $(gm^{-3}\text{-reactor } h^{-1})$		Error %
		X_{exp}	X_{pred}	R_{exp}	R_{pred}	
			$\tau = 6.5$ min ; $Q_L = 3.6$ Lh^{-1}			
o-DCB	1.88	93.10	93.04	16.16	16.66	3.11
Ethanol	2.65	95.92	99.13	23.46	25.07	6.86
o-DCB	4.70	91.97	89.66	39.90	40.13	0.58
Ethanol	2.43	96.22	99.29	21.58	22.98	6.48
			$\tau = 5.5$ min ; $Q_L = 7.8$ Lh^{-1}			
o-DCB	3.44	95.2	35.87	96.69	36.96	3.02
Ethanol	1.39	95.43	14.56	99.81	15.42	5.88
			$\tau = 4.2$ min ; $Q_L = 8.35$ Lh^{-1}			
o-DCB	0.87	92.00	11.48	94.31	11.72	2.08
Ethanol	2.23	96.76	30.84	99.7	31.76	2.99
			$\tau = 4.2$ min ; $Q_L = 8.7$ Lh^{-1}			
o-DCB	3.35	90.25	91.88	43.19	43.97	1.81
Ethanol	2.35	97.35	99.61	32.68	33.44	2.33
o-DCB	2.11	95.24	93.47	28.71	28.17	-1.86
Ethanol	2.62	95.38	99.68	35.70	37.31	4.51
			$\tau = 4.00$ min ; $Q_L = 4.5$ Lh^{-1}			
o-DCB	2.20	85.88	84.29	26.99	26.49	-1.85
Ethanol	2.57	94.36	98.95	34.64	36.33	4.87
o-DCB	3.50	81.89	81.66	40.95	40.83	-0.30
Ethanol	2.51	92.76	98.88	33.26	35.46	6.60
			$\tau = 4.2$ min ; $Q_L = 7.8$ Lh^{-1}			
o-DCB	2.87	92.38	94.23	37.88	38.63	2.00
Ethanol	1.05	91.91	99.72	13.79	14.96	8.50
o-DCB	3.17	91.98	94.48	41.65	42.79	2.72
Ethanol	0.53	99.31	99.74	7.52	7.55	0.44

[1]All symbols as defined in Table 7.7; air and liquid in co-current flow.
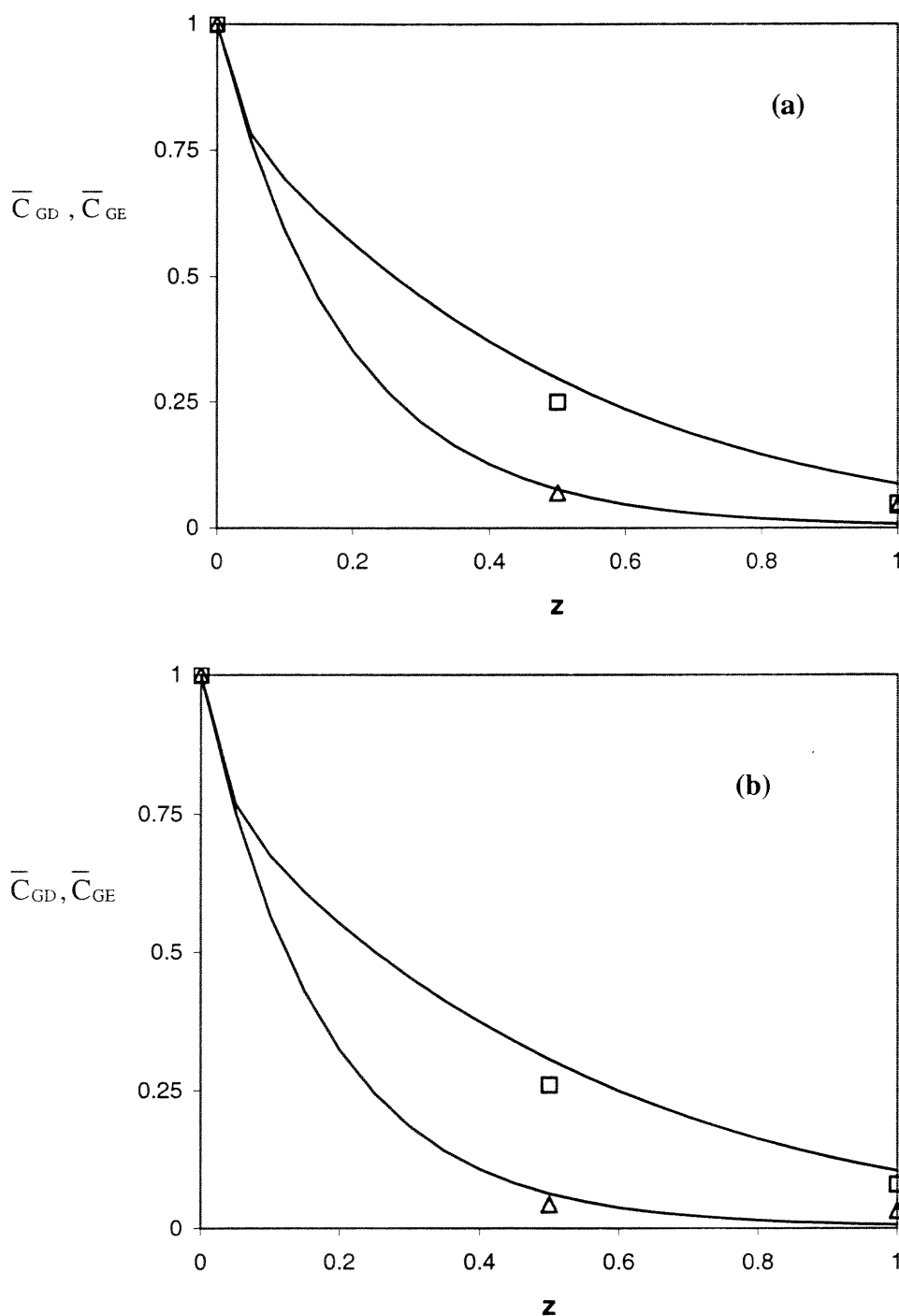
Figure 7.23 Model-predicted dimensionless concentration profiles of o-DCB(curves 1) and ethanol (curves 2) in BTF-II in the air along BTF-II when reaction in the liquid phase is neglected. Symbols represent experimental data. The values for C_{GDi} (gm^{-3}), C_{GEi} (gm^{-3}), Q_L (Lh^{-1}), and τ (min) are correspondingly, 3.14, 1.9, 7.8, and 5.5 in (a), and 0.87, 2,23, 8.35, and 4.2 in (b).

7.4.3 Removal of o-DCB in the absence of ethanol

Unit BTF-II has been also used in experiments with air streams carrying o-DCB only and the results (data) have been reported in Table 5.3 of Chapter 5. In principle, the data should be predicted by the model equations when all ethanol concentration values are set equal to zero. Since in the absence of ethanol the biomass concentration in the liquid phase is very low (see section 7.3) it was assumed that reaction does not occur in the liquid phase ($\eta_{LD} = 0$). The parameter values (except for ξ) used in solving the model equations were those used in sections 7.4.1 and 7.4.2. The model equations were solved by using $\xi = 3.0$. The model predicted removal rates failed to agree with the data. The model predicted a 3-7 % drop in o-DCB removal rates when compared to similar operating conditions but in the presence of ethanol. The experimentally determined drop in o-DCB removal rates (compare results in Table 5.2 and 5.3 in Chapter 5) is in order of 10-15%. For the model to predict the experiments a lower value of ξ should be used. Doing that, the physical implication would be that the wetted surface area in BTF-II decreases (a 10% decrease would be required) simply because of the absence of ethanol, something which is unrealistic. One way of explaining this paradox would be to redefine A_S; instead of A_S standing for the specific wetted surface area of biofilm it should stand for the specific wetted surface area of <u>active</u> biofilm. In the absence of ethanol, the carbon source is substantially less and this may lead to partial inactivation (non-viability) of part of the developed biofilm, thus, implying a need for a reduction in the value of ξ. The foregoing speculation needs further studies for confirmation (or rejection).

7.5 Parameter Sensitivity Studies

Since the model proposed here involves a very large number of parameters, some taken from the literature, others estimated, experimentally determined or fitted, sensitivity studies were performed with the intent of determining which parameters affect the model most and thus, their accurate determination is required.

The approach followed was first used by Shareefdeen (1993) and Mpanias (1998). The experiment performed with C_{GDi} = 1.88 gm^{-3}, C_{GEi} = 2.65 gm^{-3}, Q_L = 3.6 Lh^{-1}, and τ = 6.5 min was used as basis. The experimentally determined removal rate (R) was 16.2 and 23.46 gm^{-3}-reactor h^{-1} for o-DCB and ethanol, respectively (see Tables 5.2, 7.8, and 7.9).

Results of the sensitivity studies are shown in graphical form in Figures 7.24 through 7.28. On the x-axis of these plots, the relative value of the parameter under investigation is shown. The relative value of a parameter is the ratio of an assumed new value for a parameter under which the model equations were solved divided by the base value of that parameter reported in Tables 7.1 (culture BTF-II), 7.2 and 7.6. On the y-axis of the plots, the relative value of the removal rate is indicated. This is defined as the predicted removal rate under the assumed new value of a model parameter divided by the corresponding experimentally observed removal rate in the experiment used as basis (i.e., 16.2 for o-DCB and 23.46 for ethanol). In this approach, the more the relative value of R deviates from 1 the more sensitive the model is to the parameter investigated.

Figure 7.24 shows the sensitivity of removal rates on the value of the fitted parameter ξ. Figure 7.24a is for the case where reaction is assumed to occur in the liquid phase and thus, the base value for ξ is 3.0. Ethanol removal rates appear insensitive to the value of ξ whereas an underestimation of ξ (relative value of ξ less than 1) leads to

significant underestimation of the o-DCB removal rate. Figure 7.24b is for the case where

reaction in the liquid phase is neglected and thus, the base value for ξ is 3.4. The effect of ξ

on the removal rate of o-DCB is similar to that found in Figure 7.24a. Underestimating the

value of ξ leads to a significant underestimation of the ethanol removal rate, a trend

drastically different from that seen in Figure 7.24a.
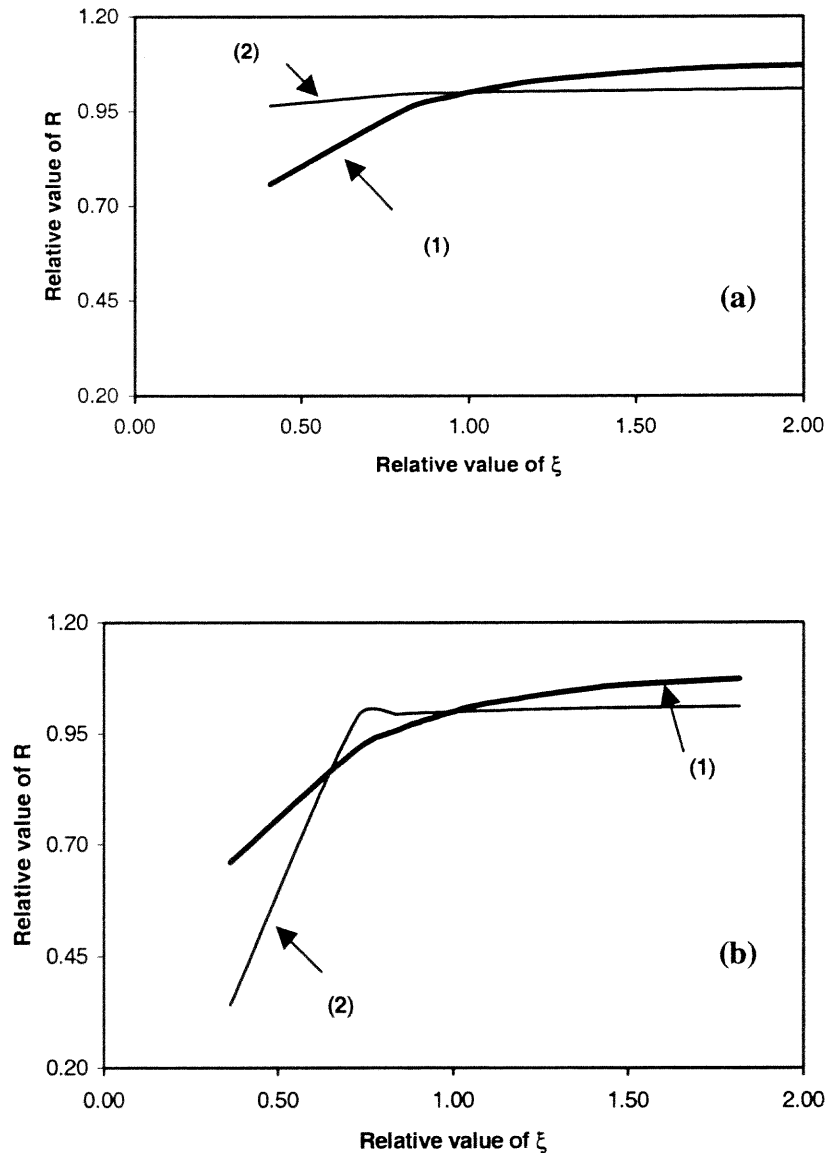
Figure 7.24 Sensitivity of the removal rates of o-DCB (curves 1) and ethanol (curves 2)
on the value of ξ. Basis: C_{GDi} = 1.88 gm^{-3}, C_{GEi} = 2.65 gm^{-3}, Q_L = 3.6 Lh^{-1} and τ = 6.5
min. Basis for ξ: 3.0 in (a) and 3.4 in (b).

The biomass concentration in the recirculating liquid (X_{VL}) does not need to be accurately known to fairly predict the ethanol removal rate, as can be seen from Figure 7.25 (curve 2). On the other hand, accurate knowledge of X_{VL} leads to better (although not by much) prediction of the o-DCB removal rate (curve 1 in Figure 7.25).
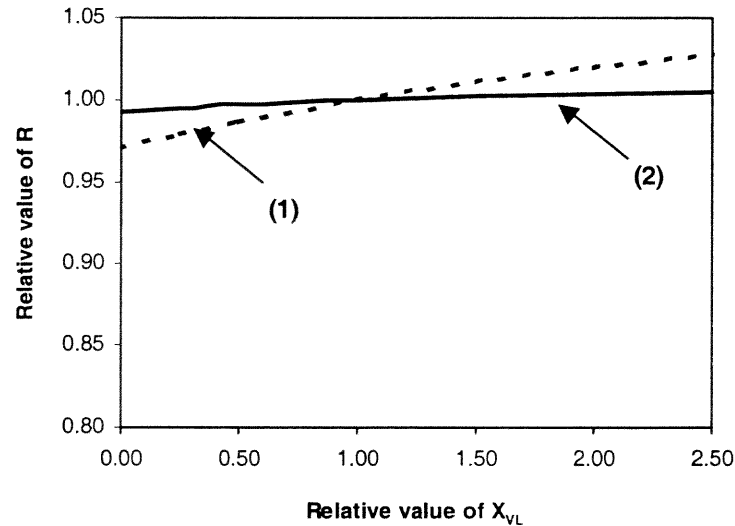
Figure 7.25 Sensitivity of the removal rates of o-DCB (curve 1) and ethanol (curve 2) on the value of X_{VL}. Basis same as in Figure 7.24a.

Use of air streams enriched (relative C_{GOi} values higher than 1) with oxygen do not seem to enhance ethanol removal, whereas o-DCB removal is enhanced very moderately as shown in Figure 7.26. This is a bit surprising since oxygen depletion in the biofilm determines the value of δ in most cases of o-DCB/ethanol mixtures and thus, one would had anticipated a stronger dependence of R-values on C_{GOi} values. On the other hand, use of air streams lean in oxygen, is predicted to very drastically reduce the removal rate of both ethanol and o-DCB.
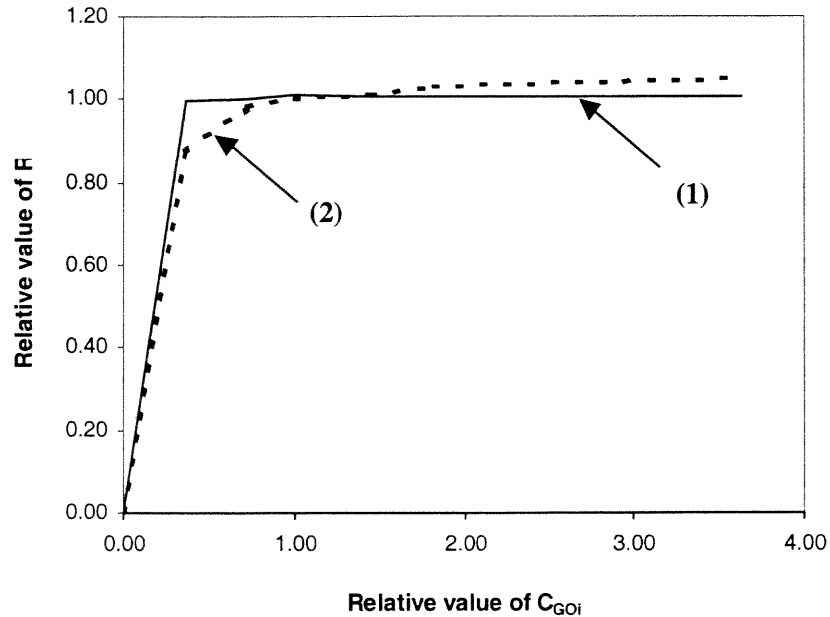
Figure 7.26 Sensitivity of the removal rates of o-DCB (curve 1) and ethanol (curve 2) on the value of C_{GOi}. Basis same as in Figure 7.24a.

Removal rates of both o-DCB and ethanol appear to be insensitive to the accurate knowledge of the inhibition constants (K_{ID} and K_{IE}) as seen in Figure 7.27. Ethanol removal rates appear to be insensitive to the K_E-value, thus implying that a first-order expression could be used for describing ethanol biodegradation. On the other hand, o-DCB removal rates appear to be sensitive to the K_D-value (Figure 7.27), thus implying that a Monod rather than an Andrews expression could be used for describing the biodegradation kinetics of o-DCB. Figure 7.27 suggests that the removal rate of both o-DCB and ethanol are sensitive to the value of μ^*_D and μ^*_E, respectively. Figure 7.27 has to be used with caution regarding conclusions on the effect of yield coefficients on removal rates. For the case of ethanol, even if all carbon was incorporated into new biomass the relative Y_E could not [based on stoichiometry analogous to that of equation (7.15)] exceed 2.4. One can then conclude from Figure 7.27b that the ethanol removal rate is insensitive to the Y_E-value. For

o-DCB, if all carbon was incorporated into new biomass the Y_D-value could not exceed 1
[based on a stoichiometry analogous to that of equation (7.14)]; hence, the relative Y_D –
value could not exceed 3.9. For o-DCB then, Figure 7.27a suggests that the removal rate is
very sensitive to the value of the yield coefficient, Y_D.
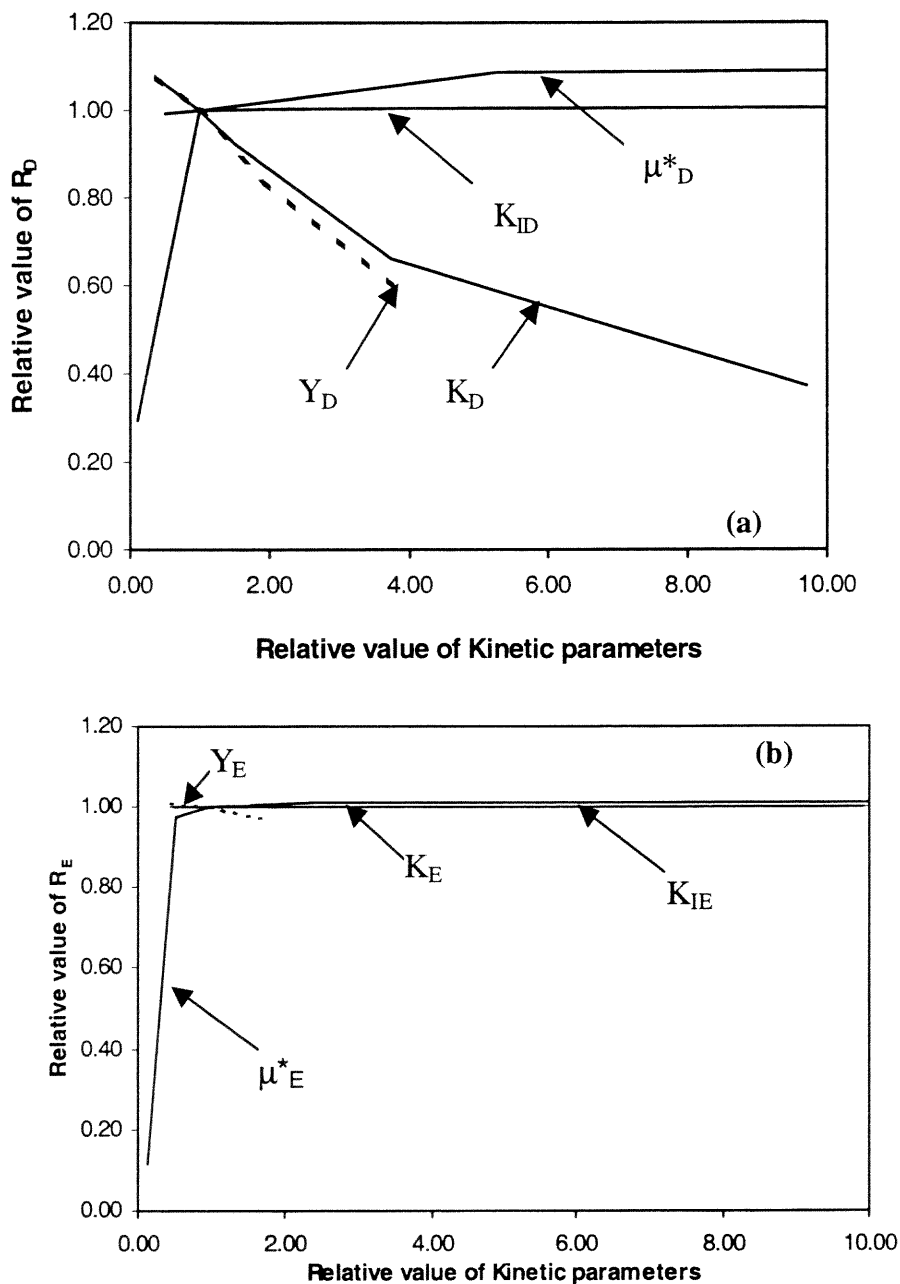
Figure 7.27 Sensitivity of the removal rates of o-DCB (a) and ethanol (b) on the values of
the kinetic parameters. Basis same as in Figure 7.24a.

Figure 7.28 suggests that accurate knowledge of the μ^*_E and Y_E kinetic parameters of ethanol does not impact the accurate prediction of the o-DCB removal rates unless μ^*_E is significantly over predicted or Y_E significantly under predicted.
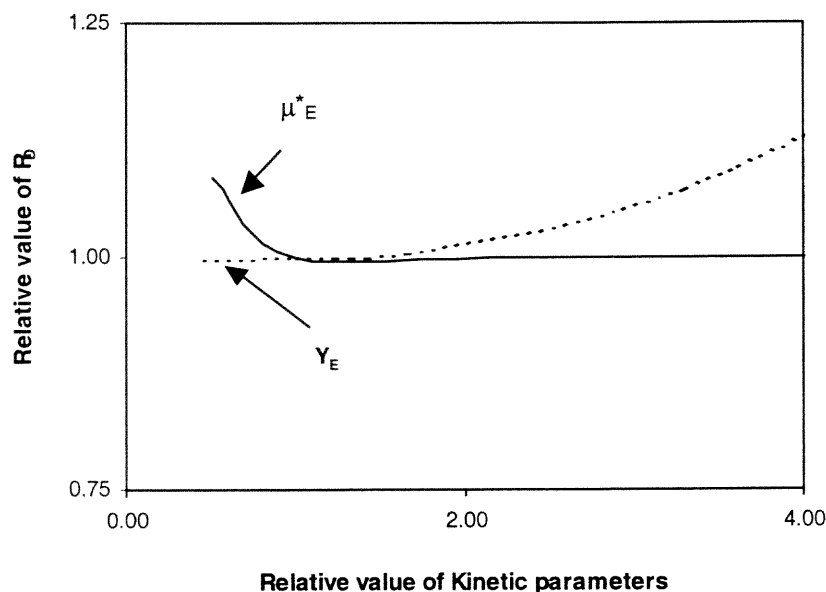
Figure 7.28 Sensitivity of the o-DCB removal rates on ethanol biodegradation kinetic parameters. Basis same as in Figure 7.24a.

The results of the sensitivity studies need to be used with extreme caution. To draw general conclusions, one would need to repeat the studies using a variety of experimental conditions as base cases. Furthermore, studies in which more than one parameter is varied would be needed before the results were generalized.

CHAPTER 8

CONCLUSIONS AND RECOMMENDATIONS

Perhaps the most important conclusion from this study is that, with proper biomass selection, it is possible to develop robust biotrickling filter units for treatment of air streams contaminated with vapors of widely dissimilar volatile organic compounds. Earlier studies had shown that the presence of a readily biodegradable compound can hamper, or even totally preclude, the removal of a hard to biodegrade compound. This study has shown that the presence of the readily biodegradable and highly soluble ethanol not only does not hamper but actually enhances the removal of the much less water soluble and much slower degrading o-DCB. In fact, in the absence of ethanol the percent removals of o-DCB was found to be between 41 and 70 %(in BTF-I). In the presence of ethanol and for similar operating conditions, o-DCB percent removals ranged from 72 to 96 %

The indirect indications that biomass differentiation did not occur in the BTF used for treating o-DCB/ethanol mixtures strongly suggests that selection of the original consortium and proper initial acclimation play a paramount role in the development of robust BTF units. Biomass differentiation has been suggested even in biofilters treating compounds as similar as ethanol and butanol. If such differentiation occurs, at best one can expect sequential removal of the different compounds, thus, leading to larger units (higher capital cost) due to lower removal rates per unit BTF packing material.

This study has shown that BTFs can be robustly (stably) operated over long periods of time. Occasionally, performance declines due to high biomass build-up. This occurs like

an unpredictable catastrophic event as deterioration in removal rates occurs abruptly (over 4-5 day periods). The interesting thing is that removal of excess biomass reverts operation to the usual high removal rate levels within very short periods of about 4 days. This is very significant as these occurrences are about 4 months apart, at least under the operating conditions tested, and the reversibility of the negative effect is another strong indication of the robustness of BTFs. The abrupt deterioration of BTF performance that was also found to be correlated with an abrupt increase in the pressure drop along the BTF unit, strongly suggests that there are at least two time scales for the events happening in a BTF. Development of models capable of predicting events at the two drastically different time scales should be undertaken in future studies. Results of the present study suggest that the daily partial replenishment of the liquid with fresh nutrient medium allowed for maintaining steady state conditions as far as the short time scale is concerned.

The second major finding of the present study is that biodegradation of VOCs in BTFs occurs not only in the biofilms immobilized on the packing material but in the liquid recirculating through the BTF as well. The contribution of the liquid phase to the removal of VOCs may be significant in cases where the biomass concentration in the liquid is high. This happens in cases where large concentrations of readily biodegradable compounds are present in the air streams fed to the BTFs. The present study managed to describe reaction in the liquid level through proper model development.

At the process modeling level, the present study introduced a significant simplification through the use of the notion of effectiveness factors. The resulting decoupling of the mass balance equations in the biofilm from the mass balances in the air and liquid transforms the original partial differential equation problem to an equivalent

problem of two ordinary differential equation systems. This transformation leads to reduced complexity during numerically solving the equations at, apparently, no expense to the accuracy of data prediction.

The proposed model was capable of predicting experimental removal rates within a less than 10% error in all cases, and oftentimes within a 5% error. This is indeed remarkable since the model involves a very large number of parameters and the value of only one parameter was determined through fitting of data. All other parameters were either taken from the literature or estimated from independent experiments. The model predicts that in the great majority of cases, removal of o-DCB/ethanol mixtures cannot be properly described if oxygen consumption in the biofilm is neglected. In fact, depletion of oxygen in the biofilm was found to determine the effective biofilm thickness in almost all cases involving ethanol and throughout the BTF length.

Kinetic experiments with suspended cultures have shown that, individually, o-DCB and ethanol get degraded following the self-inhibition kinetics of Andrews. Results from kinetic studies with o-DCB/ethanol mixtures have shown that, at least for the concentration ranges tested, ethanol does not affect the kinetics of o-DCB biodegradation but o-DCB may exert inhibition on the ethanol degradation. This uncompetitive cross-inhibition was unimportant to the ethanol removal in the BTF due to the concentrations tested. In fact, sensitivity studies show that self-inhibition was not important either, under the conditions of BTF experiments.

Results from the operation of unit BTF-I with o-DCB only have led to very interesting conclusions. Since this unit had been used in an earlier study as well (Mpanias, 1998), the results obtained strongly suggest that BTFs are extremely robust units and that

stability of biomass is maintained over long periods of time. Visual observations, which in future studies should be quantified, of BTF-I and BTF-II showed a much higher particle surface coverage with biofilm, in BTF-II. This probably explains why o-DCB removal was higher in BTF-II. This also suggests that in BTF development for treatment of a single VOC one may originally use the VOC of interest in mixtures with a readily biodegradable compound to ensure high surface coverage with biofilm. This proposition is very attractive, but one needs to ensure that usage of the auxiliary compound will not alter the biomass characteristics in ways that eventually will be negative for the removal of the VOC of interest.

The results obtained from this study have significantly contributed toward a better understanding of BTFs in general and removal of dissimilar VOCs in BTFs in particular. Future studies should consider even more complex mixtures, attempt direct measurement of parameters such as the active biofilm surface area, experiment with much higher air flow rates to better emulate conditions expected to be encountered in field applications, and model transient behavior to predict pressure drop build-up in BTF units.

APPENDIX A

MATLAB SCRIPTS AND FUNCTIONS FOR SOLVING THE CONCENTRATION PROFILES IN THE BIOFILM

The scripts and functions required to input the parameters, calculate the collocation matrices and calculate effectiveness factores are presented here. All scripts are written in MATLAB [©] 6.0.0.42a (R12)

```
%PCOM.M
%This script loads the parameters common to both BTF-I and BTF-II
%Yield is the variable which determines whether o-DCB consortium or
%mixed consortium parameters are used for o-DCB degradation
%
global Xv fXv mug rhog mul rhol sigl S Vp At dp sigp K ...
    m Dw Dg;
%
Xv=75000; % biofilm density in gm-3
% ratio of diffusivity in biofilm to water.
fXv=1-.43.*(Xv/1000).^0.92./(11.19+.27.*(Xv/1000).^.99);
mug=1.8E-05; % viscosity of air in kgm-1s-1
rhog=1.193; % density of air in kgm-3
mul=9.82E-04; % viscosity of water in kgm-1s-1
rhol=9.9785E02; % density of water in kgm-3
sigl=7.2E-02; %surface tension of water in Nm-1.
S=1.82E-2; % Cross sectional area of packed column.
Vp=1.3E-01; %Packed volume in m3
At=6.2336E02; % Specific surface area of packing in m-1
dp=1.27E-2; %Specific diameter of packing
sigp=6.1E-2; %surface tension of packing in Nm-1.
m(2)=34.4; %Henry's constant for Oxygen
Dw(2)=2.39E-09*3600; % diffusivity of O2 in water in m2h-1
Dg(2)=2.03E-05*3600; % diffusivity of O2 in air in m2h-1
Cgi(2)=275; % conc of O2 in inlet of col in gm-3
K(2)=0.26; %Kinetic constant for O2 in gm-3
%-----------------------end of line----------------------------------


PVOC.m
% This scripts loads data pertaining to properties of VOCs-oDCB and %Ethanol
%Yield is the variable which determines whether o-DCB consortium or
%mixed consortium parameters are used for o-DCB degradation
%
global m Dw Dg E E1 E2 E1O E2O mus GAMMA K KI Y YE;
m(1)=0.119; % Henry's constant for o-DCB
m(3)=0.00028; % Henry's constant for Ethanol
Dw(1)=7.8E-10*3600; % o-DCB Diffusivity in water in m2h-1
Dw(3)=1E-9*3600; % Ethanol Diffusivity in water in m2h-1
Dg(1)=6.9E-06*3600; % o-DCB Diffusivity in air in m2s-1
Dg(3)=1.01E-05*3600; % Ethanol Diffusivity in air in m2s-1
E(1)= 3.0;
E1(1)= 2.55;
E2(1)= 2.55;
E1O= 0;
E2O=7.12;
%
%Kinetic parameters for o-DCB
if yield=='new'
        mus(1)= 0.095; %Kinetic constant for biodeg in h-1
        Y(1)=0.258; Yield coefficient for o-DCB
        Y(2)=0.242;%Yield coefficient of O2 on o-DCB ingm-3
else
    mus(1)=0.146;
    Y(1)=0.398;
    Y(2)=0.457;
end
```

```
K(1)=13.389;% Growth factor in Andrews expression (gm-3)
KI(1)=19.657;% Inhibition factor in And expn (gm-3)
GAMMA(1)=K(1)/KI(1);
%
% From Kinetic experiments on ethanol
mus(3)=0.39;%Kinetic constant for biodeg in h-1
K(3)=570; % Growth factor in Andrews expression (gm-3)
KI(3)=1100; % Inhibition factor in And expn (gm-3)
YE(1)=0.444; % Yield coefficient
YE(2)=0.3; % Yield coefficient of oxygen based on Ethanol
GAMMA(3)=K(3)/KI(3);
%--------------------------------end of line--------------------------

%PARAMS.M: This script evaluates the parameters for the diffusion problem
% Also defines the matrices for solution by orthogonal collocation
% the subroutines for formation of collocation matrices are presented by Lin et al. (1999)
%
global LAMBDA LAMBDAe
pcom;
pvoc;
LAMBDA=(Dw(1)*Y(1)*K(1))/(Dw(2)*Y(2)*K(2));%to convert oDCB conc to oxy
LAMBDAe=(Dw(3)*YE(1)*K(3))/(Dw(2)*YE(2)*K(2));%to convert ethanol
%concentration  to oxygen concentration
%
% Set up physical domain and trial functions
ndisc = 40; % # of discretization points
N     = 10;  % # of interior points
%
[x w dx ddx] = pd('slab',ndisc);
tfcts                                        = gdf(x,'x.^(2*n)','x',{'n'[0:N]});
%
% Compute collocation points and discretization arrays
cpts                                         = colpts(tfcts,x,w.*(1-x.^2),[1],dx);
[Q W A B] = colmat(tfcts,cpts,x,w,dx,ddx);
BB=B(1:N,1:N);
%-------------------------------------------------------------------------
```

```
% GETCORELL.M
% This script determines the effective biofilm thickness
% and effectiveness factor on the basis concentrations of
% ethanol, o-DCB and oxygen at surface of biofilm.
%
%
global delta efirst ofirst cfirst
params;
% Entering the liquid phase concentrations
cval=[0.1:0.1:2]%non-dimensionalized o-DCB concentrations
oval=[15:1:30];  %non-dimensionalized oxygen concentrations
eval=[0.1:0.05:1]; %non-dimensionalized ethanol concentrations
%
ncval=length(cval);
noval=length(oval);
neval=length(eval);


% Initializing the solution matrices
%Effectiveness factor for reaction on o-DCB
DFAC=zeros(noval,ncval,neval);
%Effectiveness factor for reaction on ethanol
EFAC=zeros(noval,ncval,neval);


for ival=1:noval
    ofirst=oval(ival);
    for jval=1:ncval
                cfirst=cval(jval);
                for kval=1:neval
                        efirst=eval(kval);
                        delta=.00003;
                        checkc=.0001;
                        check=max([efirst ofirst cfirst]);
                        while check>checkc
                                biofilmtri;
% script which solves the diffusion-reaction in the biofilm
                                check=min([c(1) o(1) e(1)]);
                                delta=delta+.000001;
                        end
                        DFAC(ival,jval,kval)=delta.*A(end,:)*[u;1]/(rxn(
...1,ofirst));

                        EFAC(ival,jval,kval)= delta.*A(end,:)*[v;1]/(rxne(
...1,ofirst));
                end
    end
end
save reloDCB oval cval eval DFAC EFAC;
```

%---

%BIFILMTRI.M Solves the diffusion profile for o-DCB, ethanol and O2
%simultaneously in the biofilm under %steady state conditions (stoichiometric simplification of Mpanias
(1998) not used)
% called by getcorell
%

```
% Newton-Raphson method
u     = zeros(N,1);  % initial guess for o-DCB concentration variable
v     = zeros(N,1);  % initial guess for ethanol concentration variable
uo    = zeros(N,1);  % initial guess for oxygen concentration variable
update = 1;
inewt=1;
while norm(update) > sqrt(eps)
        f1 = BB*u -rxn(u,uo*ofirst)+B(1:N,N+1);
    f2 = BB*v -rxne(v,uo*ofirst)+B(1:N,N+1);
        f3=BB*uo-LAMBDA*rxno(u*cfirst,uo)- ...LAMBDAe*rxnoe(v*efirst,uo)+B(1:N,N+1);
    f=[f1;f2;f3];
        i=eye(N);
        h=0.0001;% update for Newrap.
        umat=repmat(u,1,N);
    vmat=repmat(v,1,N);
omat=repmat(uo,1,N);
        vnew=vmat+h*i;
        unew=umat+h*i;
        uonew=omat+h*i;
        upp=[rxn(unew,omat*ofirst)-rxn(umat,omat*ofirst)  zeros(N)...
    rxn(umat,uonew*ofirst)-rxn(umat,omat*ofirst)]./h;
mid=[zeros(N) rxne(vnew,omat*ofirst)-rxne(vmat,omat*ofirst) ...
    rxne(vmat,uonew*ofirst)-rxne(vmat,omat*ofirst)]./h;
low=[(rxno(unew*cfirst,omat)-rxno(umat*cfirst,omat)).*LAMBDA ...
    ...                                (rxnoe(vnew*efirst,omat)-rxnoe(vmat*efirst,omat)).*LAMBDAe ...
    ... (rxno(umat*cfirst,uonew)-rxno(umat*cfirst,omat)).*LAMBDA+ ...
    ... (rxnoe(vmat*efirst,uonew)-rxnoe(vmat*efirst,omat)).*LAMBDAe]./h;
        J = blkdiag(BB,BB,BB) -[upp;mid;low];
        update = -J\f;
        new = [u;v;uo] + update;
u=new(1:N);
        v=new(N+1:2*N);
uo=new(2*N+1:end);
        inewt=inewt+1;
        if inewt==1000
        exitflag=1;
        display('Maximum number of iterations exceeded')
        break
        end
        norm(update);
end
%
% The solution profile
b = Q\[u;1];
c = tfcts*b*cfirst;  %o-DCB concentration in biofilm
bo= Q\[uo;1];
o= tfcts*bo*ofirst;  %oxygen concentration in biofilm
be= Q\[v;1];
e= tfcts*be*efirst;  %ethanol concentration in biofilm
z=1-x;  %interpolation points along biofilm
%-------------------------------------------------------------------
```

APPENDIX B

MATLAB SCRIPTS AND FUNCTIONS FOR SOLVING THE STEADY STATE MODEL DESCRIBING REMOVAL OF A MIXTURE OF TWO VOCS IN A BIOTRICKLING FILTER

The scripts and functions required to calculate the concentration profiles in the BTF are

listed here. All scripts are written in MATLAB $^{©}$ 6.0.0.42a (R12)

```
%BIOREACTOR.M
%CALCULATES THE CONCENTRATION PROFILE FOR 2 VOCS AND OXYGEN
%ALONG THE LENGTH OF THE BTF
%
global  ALPHA PSI RHO EPS BETA EFAC  VV Cg1i Cg2i Cg3i DFAC As Ql  Qg ...OMEGA D_LIQ
DE_LIQ SIGMA CVAL OVAL EVAL
%
PCOM.M;
PVOC.M;
% DFAC and EFAC are the effectiveness factor terms for o-DCB and ethanol %calculated in
GETCORELL.M at points cval, oval and eval which are %vectors with the range of o-DCB, oxygen and
ethanol concentrations
load reloDCB oval cval eval DFAC EFAC
%
%Input the process parameters
Ql=0.0036; %liquid recirculation rate in m3/h
Qg=0.12; % Air flow rate in m3/h
XVL=1000; Biomass concentration in recirculating liquid in g/m3
%
%Obtaining the mass transfer coefficients and wetted area
[As, Kl]=intarea(Ql,Qg);
%
mvoc=[m(2); m(3)];
PSI=Kl(1).*Vp./Ql;
RHO=Kl(1).*Vp./(Qg.*m(1));
EPS=m(1).*Kl(2:3)./(mvoc.*Kl(1));
BETA=Kl(2:3)./Kl(1);
%Input the inlet concentrations
Cg1i=4.7;%Inlet o-DCB concentration in g/m3 in the gas phase
Cg2i=275; %Inlet  oxygen concentration in g/m3 in the gas phase
Cg3i=2.3;%Inlet EtoH concentration in g/m3 in the gas phase
%suffix=1 denotes odcb, 2 denotes O2 and 3 denotes EtOH
%
ALPHA(1)=Cg1i/K(1)/m(1);
ALPHA(3)=Cg3i/K(3)/m(3);
ALPHA(2)=Cg2i/K(2)/m(2);
OMEGA(1)=Y(1)*Cg1i*m(2)/Y(2)/Cg2i/m(1);
OMEGA(2)=YE(1)*Cg3i*m(2)/YE(2)/Cg2i/m(3);
%Calculating the liquid phase contribution factor
D_LIQ=m(1)*(23.891*Ql*1000+185.35)*.000001*XVL*mus(1)/Y(1)/Ql/Cg1i;
DE_LIQ=m(3)*(23.891*Ql*1000+185.35)*.000001*XVL*mus(3)/YE(1)/Ql/Cg3i;
%Initial guesses for liquid phase concentrations at BTF inlet, h=0
CL01=0.22;
CL02=1.0;
CL03=0.1;
%Initializing the correction for each iteration
dif1=1;
dif2=1;
dif3=1;
inter=1;
while ((abs(dif1)>.0001) | (abs(dif2)>.0001)|(abs(dif3)>.0001))
%Solving the liquid and gas phase mass balance equation using the Runge-%Kutta method
%RLN.M defines the mass balance equations
  [h,U]=ode23s('rln',[0:0.05:1],[1 1 1 CL01 CL02 CL03]);
  dif1=U(end,4)-CL01;
  dif2=U(end,5)-CL02;
```

```
    dif3=U(end,6)-CL03;
    CL01=CL01+dif1/2;
    CL02=min (CL02+dif2/2,1);
    CL03=CL03+dif3/2;
    inter=inter+1  ;
    end
inter
%
%Output of results obtained L=VOC loading in g/m3 reactor/h
%R = VOC removal rate in g/m3 reactor/h
%X = Percent removal
L=zeros(2,1);
R=zeros(2,1);
X=zeros(2,1);
 L(1)=Cg1i*Qg/VV;
 L(2)=Cg3i*Qg/VV;
 X(1)=(U(1,1)-U(end,1))*100;
 X(2)=(U(1,3)-U(end,3))*100;
 R=X.*L/100;
%------------------------------------------------------------------------


function [As, Kld]=intarea(l,g)
%INTAREA.M
%This function calculates the Mass transfer coefficients and interfacial area
%for both VOCs and Oxygen for a particullar
% Volumetric flow rate of the liquid to be called after pcom.m
%Kld(1)=effective mass transfer coefficient for o-DCB
%Kld(2)=effective mass transfer coefficient for Oxygen
%Kld(3)=effective mass transfer coefficient for Ethanol
global mug rhog mul rhol sigl S Vp At dp sigp E E1 E2 E1O E2O Dw Dg m VV
Kld=zeros(3,1);
Ql=l/3600;
Qg=g/3600;


% Finding the interfacial area As
As=E(1)*At*(1-exp(-...1.45*((sigp/sigl)^.75)*((Ql*rhol/(S*At*mul))^.1)*((Ql/S)^2*At/9.8)^-... .05
*(((Ql*rhol/S)^2)*((rhol*sigl*At)^-1))^.2));
%
kgq(1)=At*Dg(1)/E1(1))*5.23*(Qg*rhog/(S*At*mug))^.7*(mug*3600/(rhog*Dg(... 1)))^(1/3)*(At*dp)^-2;
%
klq(1)= (rhol/mul/9.81)^(-...1/3)/E2(1)*0.0051*(Ql*rhol/(S*As*mul))^(2/3)*(mul*3600/(rhol*Dw(1)))^(... -
.5)*(At*dp)^-0.4;
%
kgq(2)=At*Dg(3)/E1)*5.23*(Qg*rhog/(S*At*mug))^.7*(mug*3600/(rhog*Dg(3))... )^(1/3)...*(At*dp)^-2;
%
klq(2)=rhol/mul/9.81)^(-.../3)/E2*0.0051*(Ql*rhol/(S*As*mul))^(2/3)*(mul*3600/(rhol*Dw(3)))^(-.5)
...  *(At*dp)^-0.4;
mm=[m(1) m(3)];
Kl=As./(1./(mm.*kgq) +1./(klq));
Klo=3600*As*(rhol/(mul*9.81))^(-
...1/3)/E2O*0.0051*(Ql*rhol/(S*As*mul))^(2/3)*(mul*3600/(rhol*Dw(2)))^(-.5)*(At*dp)^-0.4;
 Kld=[Kl(1); Klo; Kl(2)];
%------------------------end of line----------------------------


function du=rln(x,y)
```

```matlab
%RLN.M
% This functyion sets up the equation for the RK method to solve for
%VOC concentrations in the biotrickling filter for mixtures of VOcs
%y(1)= Cgd(normalised)
%y(2)= Cgo(nondimensional normalised)
%y(3)= Cge(nondimensional normalised)
%y(4)= Cld(nondimensional normalised)
%y(5)= Clo(nondimensional normalised)
%y(6)= Cle(nondimensional normalised)

global ALPHA RHO EPS PSI  GAMMA BETA OMEGA
du=zeros(6,1);
du(1)=RHO*(y(4)-y(1));
du(2)=RHO*EPS(1)*(y(5)-y(2));
du(3)=RHO*EPS(2)*(y(6)-y(3));


%Determining non-dimensionalised liquid phase concentrations
sd=ALPHA(1)*y(4);
so=ALPHA(2)*y(5);
se=ALPHA(3)*y(6);
%Obtaining the effectiveness factor terms
ETA=zeros(2,1);
[ETA(1), ETA(2)]= geteta(sd,so,se);
%
du(4)=PSI*(y(1)-y(4))-ETA(1)*sd*so/(1+sd+GAMMA(1)*sd^2)/(1+so);
du(6)=PSI*BETA(2)*(y(3)-y(6))-ETA(2)*se*so/(1+se+GAMMA(3)*se^2)/(1+so);
du(5)=PSI*BETA(1)*(y(2)-y(5))-...ETA(1)*OMEGA(1)*sd*so/(1+sd+GAMMA(1)*sd^2)/(1+so)...
... -ETA(2)*OMEGA(2)*se*so/(1+se+GAMMA(3)*se^2)/(1+so);
%----------------------------end of line----------------------------




function [a, b]=geteta(c,o,e)
%GETETA.M
%this function determines the effectiveness factors terms for a %particular concentration of VOCs and O2 at
the liquid biofilm %interface
%a for o-DCB
%b for Ethanol
%
global EFAC As Xv VV mus YE Ql Cg1i Cg2i m Cg3i DFAC Y D_LIQ DE_LIQ...
...cval oval eval
[X Y Z]=meshgrid(oval,cval,eval);
if o<.0001
  b=0;
   a=0;
   return
end
%
if c<0.0001
  a=0.0;
else

  ed=interpn(X,Y,Z,DFAC,o,c,e)
   a=m(1)*ed*As*Xv*VV*mus(1)/(Y(1)*Ql*Cg1i)+D_LIQ;
end
```

```
if e<.0001
  b=0.0;
else
    z=interpn(X,Y,Z,EFAC,o,c,e)
  b=m(3)*z*As*Xv*VV*mus(3)/(YE(1)*Ql*Cg3i)+DE_LIQ;
end
%-----------------------------------------------------------------------
```

REFERENCES

1. Alonso, C., M. T. Suidan, G.A. Sorial, F.L. Smith, P. Biswas, P.J. Smith, and R. C. Brenner (1997). "Gas Treatment in Trickle-Bed Biofilters: Biomass, How much is enough?" *Biotechnology and Bioengineering,* **54**(6): 583-594.

2. Alonso, C., M. T. Suidan, B. R. Kim, and B. J. Kim (1998). "Dynamic mathematical model for the biodegradation of VOCs in a Biofilter: Biomass Accumulation Study." *Environmental Science & Technology,* **32**(20): 3118-3123.

3. Alonso, C., X. Zhu, M.T. Suidan, B.R. Kim, and B. J. Kim (1999). "Mathematical model for the biodegradation of VOCs in a Trickle Bed Biofilters." *Water Science and Technology,* **39**(7): 139-146.

4. Alonso, C., X. Zhu, M.T. Suidan, B.R. Kim, and B. J. Kim (2000). "Parameter estimation in biofilter systems." *Environmental Science and Technology,* **34**(11): 2318-2323.

5. Alonso, C., X. Zhu, M.T. Suidan, B.R. Kim, and B.J. Kim (2001). "Mathematical model of biofiltration of VOCs: Effect of nitrate concentration and backwashing." *Journal of Environmental Engineering,* **127**(7): 55-66.

6. Amanullah, M., S. Farooq, and S. Viswanathan, (1999). "Modeling and Simulation of a Biofilter." *Ind. Eng. Chem. Res.,* **37**(7): 2765-2774.

7. Baltzis, B.C. (1998). "Biofiltration of VOC vapors." *Biological Treatment of Hazardous Wastes,* G.A. Lewandowski and L.J. DeFilippi, Eds., John Wiley & Sons, 119-150.

8. Baltzis, B.C., C.J. Mpanias, and S. Bhattacharya (2001). "Modeling the removal of VOC mixtures biotrickling filters." *Biotechnology and Bioengineering,* **72**(4): 389-401.

9. Barton, J. W., B. H. Davison, K. T. Klasson and C.C. Gable (1999). "Estimation of mass transfer and kinetics in operating trickle-bed bioreactors for removal of VOCs." *Environmental Progress,* **18**(2): 87-92.

10. Chou, M.-S. and C.-C. Hsiao (1998). "Treatment of styrene-contaminated airstream in biotrickling filter packed with slags." *Journal of Environmental Engineering,* **124**(9): 844-850.

11. Chou, M.-S. and J.-J. Huang (1997). "Treatment of methylethylketone in air stream by biotrickling filters." *Journal of Environmental Engineering,* **123**(6): 569-576.

12. Chou, M.-S. and S.-L. Lu (1998.). "Treatment of 1,3-Butadiene in an Air Stream by a Biotrickling Filter and a Biofilter." *Journal of the Air and Waste Management Association,* **48**: 711-720.

13. Chou, M.-S. and J.-H. Lin (2000). "Biotrickling filtration of nitric oxide." *Journal of the Air and Waste Management Association*, **50**(4): 502-508.

14. Cox, H. H. J. and M. A. Deshusses (1999a). "Biomass control in waste air biotrickling filters by protozoan predation." *Biotechnology and Bioengineering*, **62**(2): 216-224.

15. Cox, H. H. J. and M. A. Deshusses (1999b). "Chemical removal of biomass from waste air biotrickling filters: screening of chemicals of potential interest." *Water Research*, **33**(10): 2383-2391.

16. Cox, H. H. J., T. T. Nguyen, and M. A. Deshusses (2000). "Toluene degradation in the recycle liquid of biotrickling filters for air pollution control." *Applied Microbiology and Biotechnology*, **54**(1): 133-137.

17. Deront M, F.M. Samb, N. Adler and P. Peringer (1998). " Biomass gowth monitoring using pressure drop in a cocurrent biofilter." *Biotechnology and Bioengineering*, **60**(1): 97-104.

18. Deshusses, M.A. and H. H. J. Cox (1999). "A cost benifit approach to reactor sizing and nutrient supply for biotrckling filters for air pollution control." *Environmental Progress*, **18**(3): 188-196.

19. Deshusses, M. A. and T. S. Webster (2000). "Construction and economics of a pilot/full-scale biological trickling filter reactor for the removal of volatile organic compounds from polluted air." *Journal of the Air and Waste Management Association*, **50**(11): 1947-1956.

20. Devinny, J. S., M. A. Deshusses and T. S. Webster (1998). *Biofiltration for Air Pollution Control*, Lewis Publishers, Boca Raton, Fl.

21. Diks, R.M.M. and S.P.P. Ottengraf (1991a) "Verification Studies of a Simplified Model for Removal of dichloromethane from waste gases using a biological trickling filter (Part I)." *Bioprocess Eng.* **6**: 93-99.

22. Diks, R.M.M. and S.P.P. Ottengraf (1991b) "Verification Studies of a Simplified Model for Removal of dichloromethane from waste gases using a biological trickling filter (Part II)." *Bioprocess Eng.* **6**: 131-140.

23. Finlayson, B.A. (1980). *Nonlinear Analysis in Chemical Engineering*, McGraw-Hill Inc, New York.

24. Fortin, N. Y. and M. A. Deshusses (1999a). "Treatment of methyl tert-butyl ether vapors in biotrickling filters. 1. Reactor startup, steady-state performance, and culture characteristics." *Environmental Science and Technology*, **33**(17): 2980-2986.

25. Fortin, N. Y. and M. A. Deshusses (1999b). "Treatment of methyl tert-butyl ether vapors in biotrickling filters. 2. Analysis of the rate-limiting step and behavior under transient conditions." *Environmental Science and Technology*, **33**(17): 2987-2991.

26. Hekmat, D. and D. Vortmeyer (1994). "Modelling of biodegradation processes in trickle-bed bioreactors." *Chemical Engineering Science,* **49**(24A): 4327-4345.

27. Hwang S-J. and H-M. Tang (1997). "Kinetic behavior of toluene biofiltration process." *Journal of the Air and Waste Management Association*, **47**: 664-673.

28. Kirchner, K., S. Wagner and H.-J. Rehm (1996). "Removal of organic air pollutants from exhaust gases in the trickle-bed bioreactor. Effect of oxygen." *Applied Microbiology and Biotechnology,* **45**(3): 415-419.

29. Lin, Y., H-Y Chang and R.A. Adomaitis (1999). "MWRtools: a library for weighted residual method calculations." *Computers and Chemical Engineering*, **23**: 1041-1061.

30. Lobo, R., S. Revah and T. Viveros-Garcia (1999). "An analysis of a trickle-bed bioreactor: Carbon disulfide removal." *Biotechnology and Bioengineering*, **63**(1): 98-109.

31. Lu, C., W. Chu, and M.-R. Lin (2000a). "Removal of BTEX vapor from waste gases by a trickle bed biofilter." *Journal of the Air and Waste Management Association*, **50**(3): 411-417.

32. Lu, C., M.-R. Lin, and J. Lin (2000b). "Removal of acrylonitrile vapor from waste gases by a trickle-bed air biofilter." *Bioresource Technology*, **75**(1): 35-41.

33. Lu, C., M.-R. Lin, and J. Lin (2001a). "Removal of styrene vapor from waste gases by a trickle-bed air biofilter." *Journal of Hazardous Materials*, **82**(3): 233-245.

34. Lu, C., M.-R. Lin, and J. Lin (2001b). "Treatment of methylacetate waste gas using a trickle-bed air biofilter." *Waste Management*, **21**(6): 489-498.

35. Lu, C., M.-R. Lin, and J. Lin (2001c). "Treatment of N, N-dimethylacetamide waste gas by a trickle-bed air biofilter." *Chemosphere*, **44**(2): 173-180.

36. Lu, C., M.-R. Lin, J. Lin, and K. Chang (2001d). "Removal of ethylacetate vapor from waste gases by a trickle-bed air biofilter." *Journal of Biotechnology*, **87**(2): 123-130.

37. Lu, C., M.-R. Lin, and I. Wey (2001e). "Removal of pentane and styrene mixtures from waste gases by a trickle-bed air biofilter." *Journal of Chemical Technology and Biotechnology*, **76**(8): 820-826.

38. Mohseni, M. and D.G. Allen (2000). "Biofiltration of mixtures of hydrophilic and hydrophobic volatile organic compounds." *Chemical Engineering Science*, **55**: 1545-1558.

39. Mpanias, C.J. (1998). "Removal of volatile organic compound (VOC) vapors in biotrickling filters: process modelling and validation with chlorinated aromatic compounds." *PhD Dissertation*, New Jersey Institute of Technology, Newark.

40. Mpanias, C.J. and B.C. Baltzis (1998). "Experimental and modeling study on the removal of mono-chlorobenzene vapor in biotrickling filters." *Biotechnology and Bioengineering*, **59**(3): 328-343.

41. Mukhopadhyay, N. and E.C. Moretti (1993). "Current and Potential Future Industrial Practices for Reducing and Controlling Volatile Organic Compounds." AIChE Center for Waster Reduction Technologies, New York, NY (1993).

42. Okkerse, W. J. H., R. M. M. Ottengraf, R.M.M. Diks, B. Osinga-Kuipers and P. Jacobs (1999a). "Long term performance of biotrickling filters removing a mixture of volatile compounds from an artificial waste gas: dichloromethane and methylmethacrylate." *Bioprocess Engineering,* **20**(1): 49-57.

43. Okkerse., W. J. H., S. P. P. Ottengraf, R.M.M. Diks, B. Osinga-Kuipers, P. Jacobs (1999b). "Biomass accumulation and clogging in biotrickling filters for waste gas treatment. Evaluation of a dynamic model using dichloromethane as a model pollutant." *Biotechnology and Bioengineering,* **63**(4): 418-430.

44. Perry, R.H., D. Green, and J.O. Maloney (eds), (1997). *Perry's Chemical Engineer's Handbook,* Seventh Edition, McGraw-Hill Inc., New York.

45. Piexoto, J. and M. Mota (1998). "Biodegradation of toluene in a trickling filter." *Bioprocess Engineering,* **19**: 393-397.

46. Ruokojarvi, A., J. Ruuskanen, P.J. Martikainen, and M. Olkkonen (2001). "Oxidation of gas mixtures containing dimethyl sulfide, hydrogen sulfide, and methanethiol using a two-stage biotrickling filter." *Journal of the Air and Waste Management Association,* **51**(1): 11-16.

47. Sander, R. (1999) "Modeling atmospheric chemistry: Interactions between gas-phase species and liquid cloud/ aerosol particles." *Surv. Geophys.,* **20** : 1-31.

48. Shareefdeen, Z. and B.C. Baltzis (1994). "Biofiltration of toluene vapor under steady-state and transient conditions: theory and experimental results." *Chem. Eng. Sci.* **49**: 4347-4360.

49. Smith, F. L., G. A. Sorial, M.T. Suidan, A. Pandit, P. Biswas, and R. C. Brenner. (1998). "Evaluation of trickle-bed air biofilter performance as a function of inlet VOC concentration and loading and biomass control." *Journal of the Air & Waste Management Association,* **48**: 627-636.

50. Smith, F. L., G. A. Sorial, M.T. Suidan, A. W. Breen, P. Biswas and R. C. Brenner. (1996). "Development of two biomass control strategies for extended, stable operation of highly efficient biofilters with high toluene loadings." *Environmental Science and Technology,* **30**(5): 1744-1751.

51. Sorial, G. A., F. L. Smith, M.T. Suidan, A. Pandit, P. Biswas, and R. C. Brenner. (1997). "Evaluation of trickle bed air biofilter performance for BTEX removal." *Journal of Environmental Engineering,* **123**(6): 530-537.

52. Togna, P. A. and M. Singh (1994). "Biological Vapor-Phase Treatment using Biofilter and Biotrickling filter Reactors: Practical Operating regimes." *Environmental Progress,* **13**(2): 94-97.

53. Villadsen, J.V. and W.E. Stewart (1967). "Solution of Boundary-Value Problems by Orthogonal Collocation." *Chem. Engng. Sci.,* **22**: 1483-1501.

54. Wang, K.-W., B.C. Baltzis, and G.A. Lewandowski (1996). "Kinetics of phenol biodegradation in the presence of glucose." *Biotechnology and Bioengineering,* **51**(1) : 87 :94.

55. Yaws, C.L., J.R. Hopper, S.D. Sheth, M. Han and R. W. Pike (1997). "Solubility and Henry's law for alcohols in water." *Waste Management,* **17**(8): 541-547.

56. Zhu, X., C. Alonso, M.T. Suidan, H. Cao, B.J. Kim and B. R. Kim (1998). "The effect of liquid phase on VOC removal in trickle-bed biofilters." *Water Science Technology,* **38**(3): 315-322.

57. Zuber, L., I. J. Dunn, and M. A. Deshusses (1997). "Comparative Scale-up and cost estimation of a biological trickling filter and a three phase airlift bioreactor for the removal of methylene chloride from polluted air." *Journal of the Air and Waste Management Association,* **47**: 969-975.